THE RHO FAMILY GEF ASEF2 REGULATES CANCER CELL MIGRATION BY MODULATING RAC ACTIVATION AND ACTOMYOSIN CONTRACTILITY

By

Léolène Jean Carrington

Dissertation
Submitted to the Faculty of the
Graduate School of Vanderbilt University
in partial fulfillment of the requirements
for the degree of

DOCTOR OF PHILOSOPHY
in

Biological Sciences
May, 2016
Nashville, Tennessee

Approved:

Katherine L. Friedman, Ph.D.

Todd R. Graham, Ph.D.

Charles K. Singleton, Ph.D.

Alissa M. Weaver, M.D., Ph.D.

Donna J. Webb, Ph.D

To my extraordinary parents, Léonel and Sonia- your lifelong sacrifices to give me a good education has made all this possible. Thank you for instilling in me confidence and a drive for pursuing higher education. Thank you for your loving encouragements, stern support, and unconditional love. Because you always thought I was the best, I always strived to do the best I can.

To my patient and utmost loving husband, Sheridan- it would not have been possible for me to get to this point without you by my side. Thank you for being my champion and my anchor as I sketch my life journey. You are truly the best husband that any wife could ask for.

ACKNOWLEDGEMENTS

I would like to express my gratitude to my research advisor, Dr. Donna J. Webb for all of the time and effort she has put into my success as a scientist. I am truly appreciative of the guidance and support that she has provided me to complete this project. I have learned so much from observing how she approaches science- her expertise, understanding, and patience, added considerably to my graduate experience.

I also would like to thank my committee members: Dr. Katherine L. Friedman, Dr. Todd. R. Graham, Dr. Charles K. Singleton and Dr. Alissa M. Weaver- for their thoughtful questions, their invaluable suggestions and their continued guidance. Their helpful comments on all parts of the draft process have contributed to the success of this thesis.

I would like to thank all of the members of the Webb lab, past and present, who have provided technical and emotional support. I would especially like to thank Devi Majumdar, who was my mentor as a rotation student in Donna's lab. Devi was a good friend and an excellent scientist. Her approach to research has contributed to my success in graduate school, and for that I will forever be grateful. Special thanks to Louis Hinkle, who is hands down the best undergrad ever. I would also like to thank Claire Brown and Erika Wee for their assistance in learning FRET. FRET imaging was conducted at the McGill University Life Sciences Complex Imaging Facility on equipment purchased with funding from the Ministère du Développement économique, Innovation et Exportation - Québec (MDEIE).

To all my friends and adopted families, I am so thankful for the invaluable friendship and support you have provided. Truly, you all have been with me through the good and the bad times and I cannot say thank you enough. And for all the celebrations you have put together, many thanks. I am appreciative of the helpful comments on the draft process, the shoulders to cry on,

and the confidence boost.

Special thanks to the Fisk-Vanderbilt MS-PhD Bridge Program for providing me a way to reach my career goals. I thank all the directors, coordinators for putting their efforts into such an excellent program. Thank you for the trust in my academic abilities, the financial and the social support. I would especially like to thank Dr. Dina Stroud for her continuous mentoring and for always championing for me. Also, many thanks to Dr. Jedidah Isler for all the advice and support.

In conclusion, I recognize that this research would not have been possible without the financial assistance from the National Institutes of Health: a Ruth L. Kirschstein National Research Service Award (NRSA) 1F31-GM108407 and a R01-GM092914 and S10RR025524, awarded to me and my mentor, respectively. This work was also supported by the Gisela Mosig Graduate Student Travel Fund, which enabled me to attend several national meetings, including a Gordon research conference. I am grateful to the graduate school for awarding me a dissertation enhancement grant.

TABLE OF CONTENTS

Page

LIST OF FIGURES

LIST OF ABREVIATIONS

ABR	APC binding region
APC	Adenomatous polyposis coli
Arp	Actin related protein
Asef1	APC-stimulated exchange factor 1
Asef2	APC-stimulated exchange factor 2
CA	Constitutively active
Cdc42	Cell division cycle 42
Col I	Type I collagen
Dbl	Diffuse B cell lymphoma
DH	Dbl homology
DMEM	Dulbecco's modified Eagle's media
DN	Dominant negative
DNA	Deoxyribonucleic acid
ECM	Extracellular matrix
F-actin	Filamentous actin
FACS	Fluorescence-activated cell sorting
FAK	Focal adhesion kinase
FBS	Fetal bovine serum
Fn	Fibronectin
FRET	Fluorescence resonance energy transfer
GAP	GTPase activating protein
GDP	Guanosine diphosphate
GEF	Guanine nucleotide exchange factor
GFP	Green fluorescent protein
GSK-3	Glycogen synthase kinase-3
GST	Glutathione-S-transferase

GTP	Guanosine triphosphate
h	Hour(s)
KD	Kinase dead
Min	Minute(s)
µM	micromolar
MMP	Matrix metalloprotienase
MyoII	Myosin II motor proteins
nM	nanomolar
PAK	p21 activated protein
PBS	Phosphate buffered saline
PCR	Polymerase chain reaction
PH	Pleckstrin homology
Rac	Ras-related C3 botulinum toxin substrate
Rho	Ras homolog
Scr	Scrambled
SDS	Sodium dodecyl sulfate
SDS-PAGE	SDS-polyacrylamide gel electrophoresis
SEM	Standard error of the mean
SH3	Src homology 3
shRNA	Small hairpin RNA
Src	Sarcoma
Tiam1	T lymphoma invasion and metastasis 1
TIRF	Total internal reflection microscopy
WASP	Wiskott-Aldrich syndrome protein
WAVE	WASP verprolin homologous protein

CHAPTER I

INTRODUCTION

Overview of Thesis

Cell migration is a highly integrated multistep process that is vital for embryonic development, the inflammatory response, tissue repair and regeneration, maintaining homeostasis in the adult, and many other important cellular processes (Lauffenburger and Horwitz, 1996). Aberrant cell migration, on the other hand, contributes to many pathological disorders such as atherosclerosis, arthritis, and tumor cell metastasis. Indeed, an essential first step in forming deadly metastases is the migration of cancer cells away from the primary tumor into the surrounding tissue. Because of the many functions that cell migration serves, it is important to understand how cells migrate, which molecules are involved, and how their interactions elicit biological responses.

The process of cell movement is highly coordinated and is dependent on proper regulation of the actin cytoskeleton. Therefore, reorganization of actin must be tightly controlled. Such remodeling of the actin cytoskeleton is regulated by proteins of the Rho family of GTPases, including Rac and Rho. Once activated, these GTPases then interact with downstream effector proteins to modulate actin and thereby regulate cell migration. Various Rho GTPases have been shown to be upregulated in human tumors, including breast and prostate cancer. Therefore, identifying and characterizing regulators of Rho GTPases, such as the guanine nucleotide exchange factors (GEFs), and determining their role in cancer cells is greatly needed.

Asef2 is a recently identified GEF known to activate both Rac and Cdc42, but its role in regulating cancer cell migration is not well understood. Data from this thesis suggest a novel role

for Rac in regulating actomyosin contractility and cell migration (Jean et al., 2013). Activation of Rac by Asef2 inhibits cell migration by increasing Myosin II-dependent cell contractility, which has classically been thought to be mediated by Rho (Chrzanowska-Wodnicka and Burridge, 1996; Wheeler and Ridley, 2004). Using high-end optical imaging techniques, this thesis investigates the mechanisms by which Rac signaling regulates Myosin II-dependent contractility and the force-generating mechanical signals that modulate cell migration. Since little is known about Rac-mediated force generation through Myosin II, this body of work provides novel insight into how the Rac-Myosin II pathway regulates cell migration and its underlying processes.

The Extracellular Matrix

Cells migrate on an extracellular matrix (ECM), which is essentially the non-cellular component present within all tissues and organs that provide essential physical scaffolding for the cellular constituents and also critical biochemical and biomechanical cues to direct cell growth, survival and migration among others (Frantz et al., 2010). The ECM can exist either as complex three-dimensional (3D) networks of macromolecules in which cells are embedded, or as basement membranes laid down by cells to form a structural framework for tissue organization (Frantz et al., 2010; Hynes, 2009; Lawson and Burridge, 2014).

The ECM is comprised of an interweaving mesh of fibrous proteins such as collagen and fibronectin, and various proteoglycans (Fig. 1) (Frantz et al., 2010). Collagen is the most abundant fibrous protein within the ECM architecture and constitutes up to 30% of the total protein mass of a multicellular organism (Frantz et al., 2010). Collagen is predominantly transcribed and secreted by fibroblasts that either reside in the stroma or are recruited to it from neighboring tissues (De Wever et al., 2008). By exerting tension on the matrix, fibroblasts are

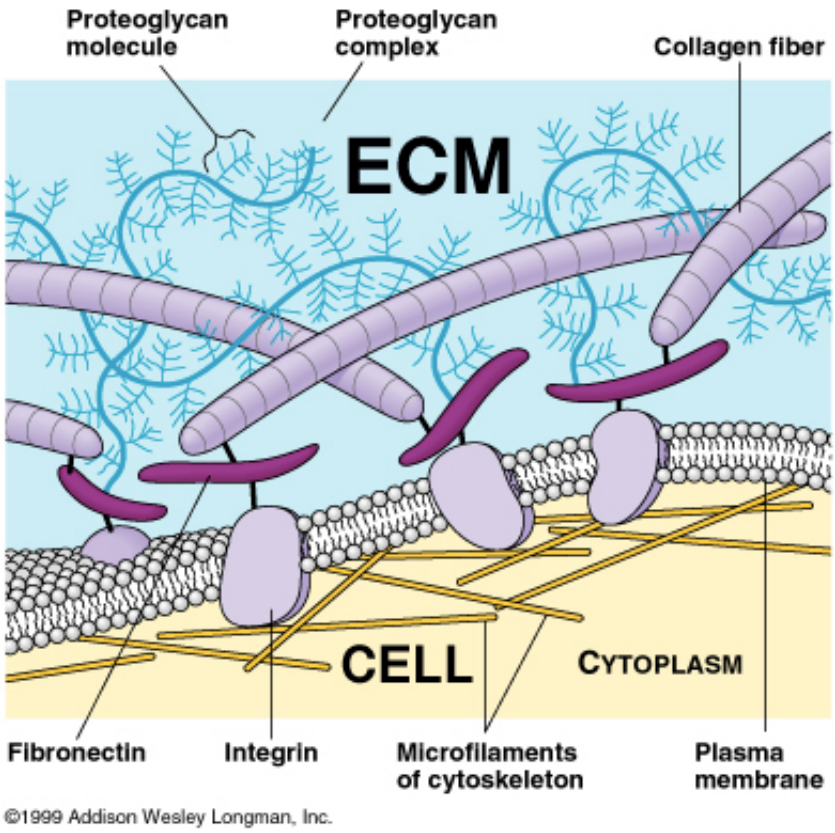

Figure 1. Schematic of the extracellular matrix. The ECM is composed of three major classes of molecules: 1) structural proteins, such as collagen, 2) specialized proteins, such as: fibronectin and 3) proteoglycans, which are complex proteins that are covalently bonded at multiple sites along the protein chain to a class of polysaccharides, known as glycosaminoglycans.

able to organize collagen fibrils into sheets and cables and, thus, can dramatically influence the alignment of collagen fibers within tissues (Frantz et al., 2010). As the main structural element of the ECM, collagen provides tensile strength, regulate cell adhesion and direct tissue development (Rozario and DeSimone, 2010). Fibronectin, which is produced by a wide variety of epithelial and mesenchymal cells, also play a crucial role in cell adhesion, migration, growth and differentiation. Fibronectin is also found in basement membranes and in loose connective tissue stroma. Active fibronectin fibrillogenesis (i.e. development of fine fibrils) by cells is usually required for Collagen I matrix assembly *in vivo*.

ECM proteins typically include multiple independently folded domains whose sequences and arrangement are highly conserved. Some of these domains bind adhesion receptors, such as integrins to mediate cell-matrix adhesion and also transduce signals into cells (Hynes, 2009). Because of its diverse nature and composition, the ECM can have many functions, such as providing support, segregating tissues, and regulating intercellular communication.

The actin cytoskeleton

Cell migration consists of several critical steps that are highly dependent on the continuous reorganization and turnover of the actin cytoskeleton (Ridley, 2011). The actin cytoskeleton, which consists of arrays of functionally different subsets of intracellular actin filament, provides the structural framework that define cell shape and polarity. At the front or leading edge of migrating cells, actin is organized into several distinct structures and its polymerization in these cellular protrusions drives cell migration. Protrusions generally contain two actin-based structures (Fig. 2), the lamellipodium and the lamellum, with the lamellipodium spatially anterior to the lamellum (Heath and Holifield, 1991; Vicente-Manzanares et al., 2009b).

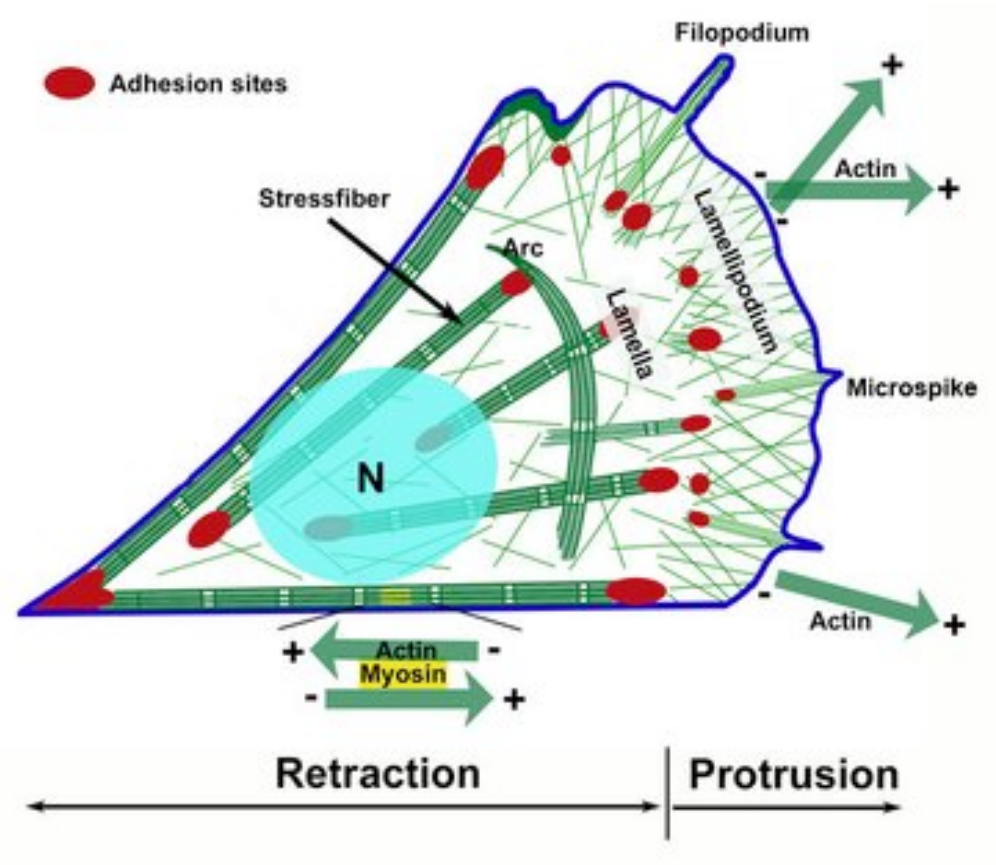

Figure 2. Schematic of the actin cytoskeleton of a migrating fibroblast. At the cell front, the lamellipodium contain polarized branched F-actin networks that drive membrane extension. The flat region behind the lamellipodium and in front of the nucleus (N) is termed the lamella. The cell attaches to the substrate at adhesion sites. At the center of the cell, actin filaments form bipolar assemblies with myosin to form contractile arrays (for retracting).

Figure taken from the web page of the Vic Small lab of the Austrian Academy of Sciences in Salzburg and Vienna. http://cellix.imba.oeaw.ac.at/cytoskeleton/actin

The lamellipodium is rich in cross-linked dendritic F-actin arrays facilitated primarily by the actin nucleator Arp2/3 and cofilin (Pollard and Borisy, 2003; Small, 1988). Extending from the lamellipodium are thinner protrusions called filopodia, which are composed of thin bundled actin filaments that actively search the environment and promote directional cell migration (Mattila and Lappalainen, 2008). The actin filament network of the lamellum consist primarily of condensed linear actin bundles, and thus is more stable and less dynamic than that of lamellipodia (Ponti et al., 2004). Furthermore, the lamellipodium and the lamellum are kinetically different. Whereas the lamellipodium is characterized by a fast retrograde flow of actin, the lamellum exhibits slower retrograde flow (Ponti et al., 2004). The convergent zone between the two is characterized by active depolymerization of the branched dendritic network and the reorganization of actin (Vicente-Manzanares et al., 2009b). Essentially, the dynamic properties of actin filaments provide the driving force for cells to move by giving them the ability to 1) push via polymerization and 2) contract via interaction with motor proteins.

The Migration Cycle

Migration may be viewed as a repetitive, multistep cycle (Fig. 3) which includes extension of a protrusion, usually induced by an exogenous agent, formation of stable attachments (adhesions) near the leading edge of the protrusion, translocation of the cell body forward, and release of adhesions along with retraction at the cell rear (Lauffenburger and Horwitz, 1996; Lee et al., 1993; Sheetz, 1994). Polymerization of the actin cytoskeletal network is thought to drive the initial extension of the membrane protrusion at the cell front, termed lamellipodia (Borisy and Svitkina, 2000; Carson et al., 1986; Wang, 1985). The interaction of the integrin family of transmembrane receptors with the ECM initiates the formation of adhesions by recruiting signaling and structural proteins, such as paxillin and vinculin, to these sites (Burridge

and Chrzanowska-Wodnicka, 1996; Miyamoto et al., 1995a; Miyamoto et al., 1995b; Schoenwaelder and Burridge, 1999; Yamada and Miyamoto, 1995; Zaidel-Bar et al., 2003). In turn, these small nascent adhesions stabilize the protrusion and transmit strong forces, which serve as traction points for the forces that move the cell body forward (Beningo et al., 2001; Galbraith and Sheetz, 1997; Lee et al., 1994). These nascent adhesions can continue to grow and mature into large focal adhesions. Alternatively, after assembly, the adhesions at the leading edge of the cell must disassemble for migration to continue (Laukaitis et al., 2001; Webb et al., 2004). The process of adhesion assembly and disassembly at the leading edge is termed adhesion turnover (Webb et al., 2002).

Cell body translocation is independent of actin polymerization (Anderson et al., 1996). Myosin II motor proteins, which bind and slide anti-parallel actin filaments that are anchored to adhesions, generate traction force on the substratum and provide the contractile force needed for translocation (Parsons et al., 2010; Svitkina et al., 1997). The actomyosin cytoskeleton also promotes adhesion disassembly and retraction of the rear of migrating cells to allow the cell to move forward (Chrzanowska-Wodnicka and Burridge, 1996; Crowley and Horwitz, 1995; Worthylake et al., 2001). Release of adhesions and retraction at the rear completes the migratory cycle (Lauffenburger and Horwitz, 1996; Lee et al., 1993; Sheetz, 1994). While some progress has been made over the last few years, many of the signaling pathways that regulate these processes still remain to be identified.

It is crucial that each step of the migration process be tightly controlled for proper function. For instance, a cell's failure to rapidly disassemble its adhesions prevents its disengagement from the ECM, and thus delay or disrupt its migration process. All of these migratory steps form a cyclic process that is dependent on the coordination of cell adhesion to

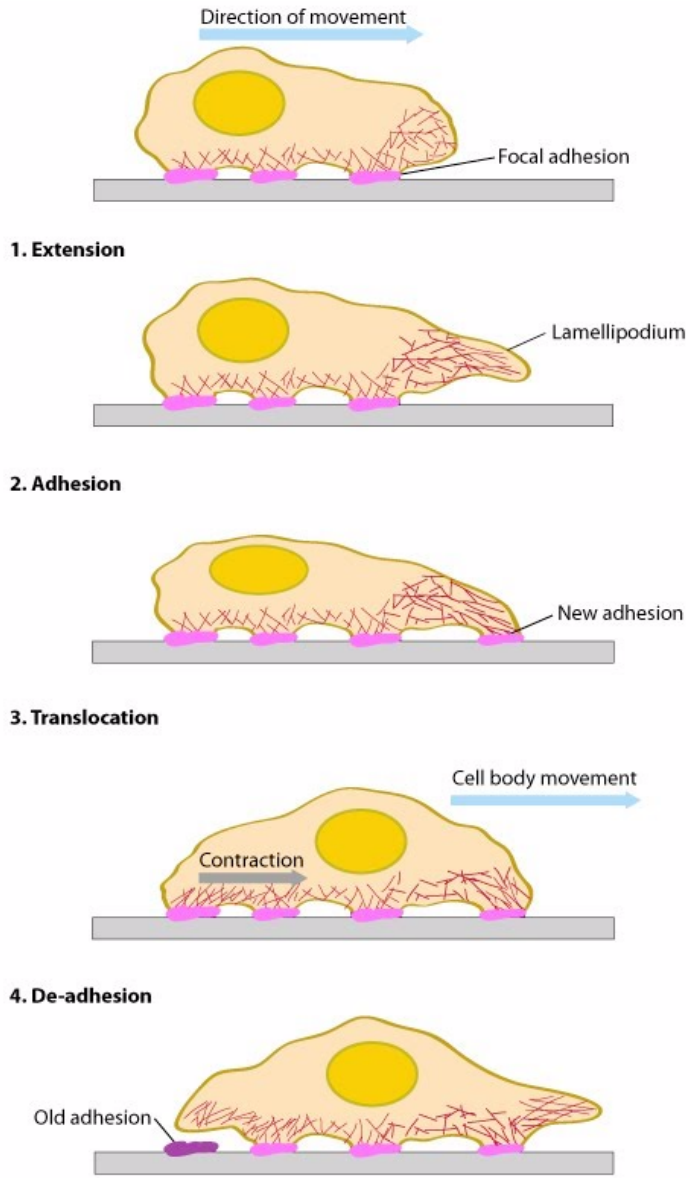

Figure 3. The migration cycle. 1) Polymerization of actin filaments at the leading edge is translated into a protrusive force to initiate cell migration. This begins with the extension of an actin-rich protrusion. 2) Membrane protrusion facilitates the binding of transmembrane cell surface receptors to the substratum components. New adhesions are rapidly linked to the network of actin filaments. This protrusion is then stabilized by the formation of cell-matrix adhesions. 3) The combined activity of retrograde actin flow and contraction forces generates tensions that allow the cell body to translocate in the direction of the migration. 4) The forces produced by the contractile network combined with actin filament and FA disassembly help to retract the trailing cell edge.

Used by permission from MBInfo: www.mechanobio.info; Mechanobiology Institute, National University of Singapore.

the ECM and the cell's ability to contract its body in order to move in a sustained migration (Fig. 2). Since adhesion dynamics and cell contractility play such an important role in regulating cell migration, these two aspects of migration will be the main focus of this dissertation.

Cell Adhesion - Composition

The adhesion of cells to the ECM is mainly mediated by heterodimeric transmembrane receptors, named integrins that are composed of one α-chain in non-covalent association with one β-chain. Both subunits typically have large extracellular but short intracellular domains. The extracellular domains of integrins bind directly to specific sequence motifs within ECM proteins, such as collagen, while the short intracellular tail domains interact directly or indirectly with various intracellular adhesion proteins (Hynes, 2002). The binding of integrins to their ECM ligands induces a conformational change that unmasks their short cytoplasmic tails. The exposed cytoplasmic tail promote the recruitment and formation of multiprotein complexes that connects the integrins-ECM complex to the actin cytoskeleton (Hynes, 2002; Vicente-Manzanares et al., 2009a). For instance, ligand binding induces the recruitment of scaffold and signaling proteins such as paxillin and the protein Tyr kinase focal adhesion kinase (FAK), respectively (Parsons, 2003). In turn, these proteins associate with additional molecules that regulate signaling to Rho GTPases, which are regulatory proteins that serve as a convergence point between actin re-organization and adhesion dynamics (Brown and Turner, 2004; Parsons et al., 2010).

In addition to their role in biochemical signaling pathways, integrins are also mechanotransducers in that they convert a mechanical stimulus into a biochemical signal. Cells use their integrins to detect the varying changes in their environment and the architecture of the ECM (i.e. such as ECM stiffness). The cell's response to these changes can vary from strengthening the associated adhesions, re-organizing the cytoskeleton and remodeling the ECM

(Roca-Cusachs et al., 2012; Schwartz and DeSimone, 2008). Integrin α5β1 is a major cellular receptor for the ECM protein fibronectin and plays a fundamental role during mammalian development. Binding of α5β1 integrin to Fn molecules results in integrin clustering and stimulates an intracellular signaling cascade which recruits adhesion proteins to the actin cytoskeleton (To and Midwood, 2011).

Integrin-based adhesions are highly complex structures and are composed of over 150 different protein-protein interactions (Geiger et al., 2009; Geiger and Yamada, 2011; Huttenlocher and Horwitz, 2011). As such, they appear in a variety of sizes, morphologies, and locations depending on the cell and its environment. Although a robust categorization of adhesions has not been described, definite subclasses have now been identified, e.g., nascent adhesions, focal complexes (FCs), focal adhesions (FAs), and fibrillar adhesions (Geiger and Yamada, 2011; Vicente-Manzanares et al., 2009b; Zaidel-Bar et al., 2004). Fibrillar adhesions, which are characterized by long lifetimes and a highly elongated structure, are specialized adhesions involved in ECM modification (Broussard et al., 2008; Brown and Turner, 2004; Parsons et al., 2010; Rid et al., 2005; Zamir et al., 2000). Fibrillar adhesions are not the focus of this dissertation since previous studies demonstrated that they are not typically present in rapidly migrating cells (Huttenlocher and Horwitz, 2011).

Nascent adhesions and focal complexes are small, dynamic, and dot-like adhesions that are found near the leading edge in protrusions and they have been shown to mediate signals that promote actin polymerization (Alexandrova et al., 2008) (Choi et al., 2008). Nascent adhesions form concurrently with lamellipodial protrusion and are less than the 0.25 μm resolution of most light microscopy techniques (Choi et al., 2008). Some of these nascent adhesions will further mature into FCs (0.5 μm)- adhesion contacts found at the tip of extending protrusions, and then

to FAs (1-5 μm) (Choi et al., 2008), which are more stable, and more highly organized at the rear and sides of the cell (Zaidel-Bar et al., 2003). Focal adhesions, which are the best characterized of the cell-matrix adhesions, are the resulting transmembrane junctions between the ECM and the cell cytoskeleton (Burridge et al., 1988). Interestingly, an inverse correlation between the size and organization of focal adhesions and cell migration speed has been observed (Lauffenburger and Horwitz, 1996). Indeed, migration rates have been shown to be highly sensitive to adhesive strength (Palecek et al., 1997). Whereas an optimal adhesive environment supports maximal migration, too weak or too strong adhesive environments prevent formation of new adhesions or retraction of trailing adhesions, respectively. Therefore, this suggests that the rates of cell migration are not fixed, but rather are modulated by physical cues in the extracellular environment.

The proteins in FAs (Fig. 4) vary widely in function as they can either link integrins to the actin cytoskeleton and/or recruit other molecules to adhesions. The best studied scaffolding and signaling proteins in FAs are paxillin, talin, vinculin and zyxin. Whereas talin transitions integrins to an active state by linking their cytoplasmic tail to actin and to vinculin (Campbell and Ginsberg, 2004), vinculin directly binds F-actin and the actin cross-linking protein, α-actinin (Otey and Carpen, 2004; Ziegler et al., 2006). Several protein kinases have also been shown to be part of the plethora of signaling molecules that associate with integrin-containing adhesions. Kinases, such as FAK, Abelson kinase (Abl) and Src kinase, regulate adhesion signaling by phosphorylating many early adhesion proteins, such as paxillin and Cas, to recruit additional molecules (Parsons, 2003). Paxillin and Cas bind the additional regulatory proteins that control

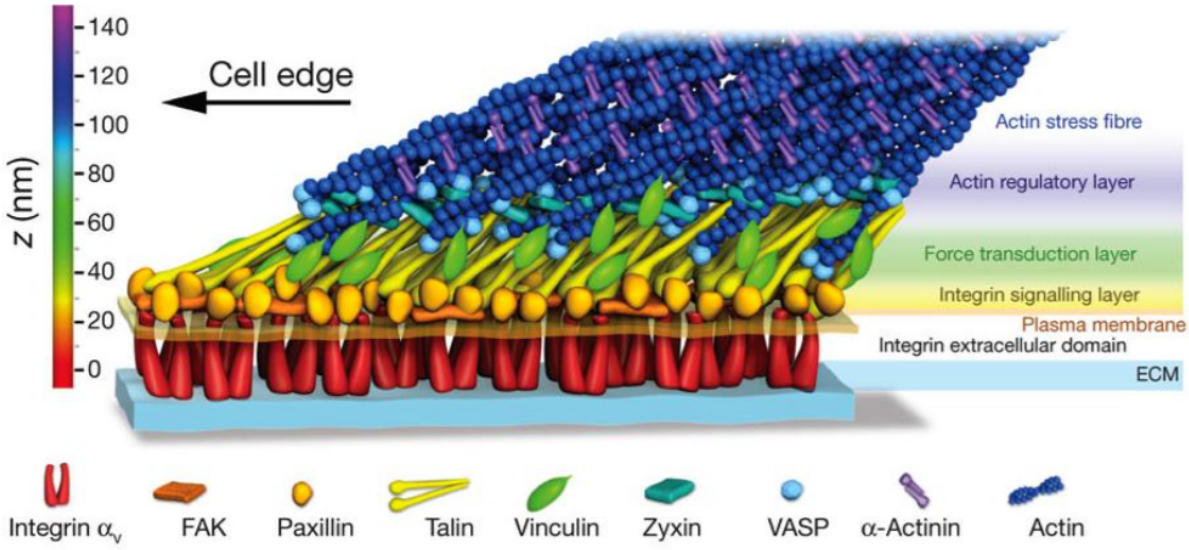

Figure 4. Schematic of focal adhesion nanoscale architecture and composition. The extracellular domains of integrins bind the ECM, while their cytoplasmic tails interact with the integrin signaling layer, such as FAK and paxillin. The force transduction layer contains the tension sensitive proteins such as talin and vinculin. Finally, the actin regulatory layer, which includes zyxin, VASP and α-actinin, link the adhesion to an actin stress fiber (contractile machinery).

Reprinted from (Kanchanawong, Shtengel et al. 2010)

the activity of the Rho GTPases, which then modulate actin remodeling and adhesion dynamics (Defilippi et al., 2006; Mitra and Schlaepfer, 2006; Peacock et al., 2007; Tomar and Schlaepfer, 2009).

Cell Adhesion - Turnover

Polarized cell migration requires continuous assembly and disassembly of cell-matrix adhesions (Fig. 5) and the constant remodeling of the associated actin cytoskeleton. The constant assembly and disassembly of leading edge adhesions, termed adhesion turnover, is crucial for efficient cell migration (Webb et al., 2002).

The earliest detectable adhesions, or nascent adhesions, form in the lamellipodium just behind the leading edge. These adhesions contain integrins, talin, vinculin, α-actinin, paxillin and FAK, among other proteins, and are enriched in phosphotyrosine (Choi et al., 2008). Protein phosphorylation, which is carried out by kinases, is the most common mechanism of regulating protein function and transmitting signals throughout the cell. Therefore, an enrichment of phosphotyrosine residues is indicative that these adhesions are active signaling complexes.

Once formed, nascent adhesions at the leading edge exert traction forces on the ECM (Beningo et al., 2001). High traction forces are typically observed at the cell front. As the leading edge of a migrating cell moves forward, nascent adhesions can either mature into larger stabilized adhesions; or they can undergo rapid turnover such that their components can be incorporated into newly formed adhesion sites (Bershadsky et al., 2003). Paxillin-containing adhesions near the leading edge have been shown to be highly dynamic, and to rapidly form and turn over (Choi et al., 2008; Webb et al., 2004). The formation and life cycle of nascent adhesions appear to be intimately linked to actin polymerization and organization (Alexandrova et al., 2008; Choi et al., 2008). Whereas actin polymerizes rapidly near the front of the

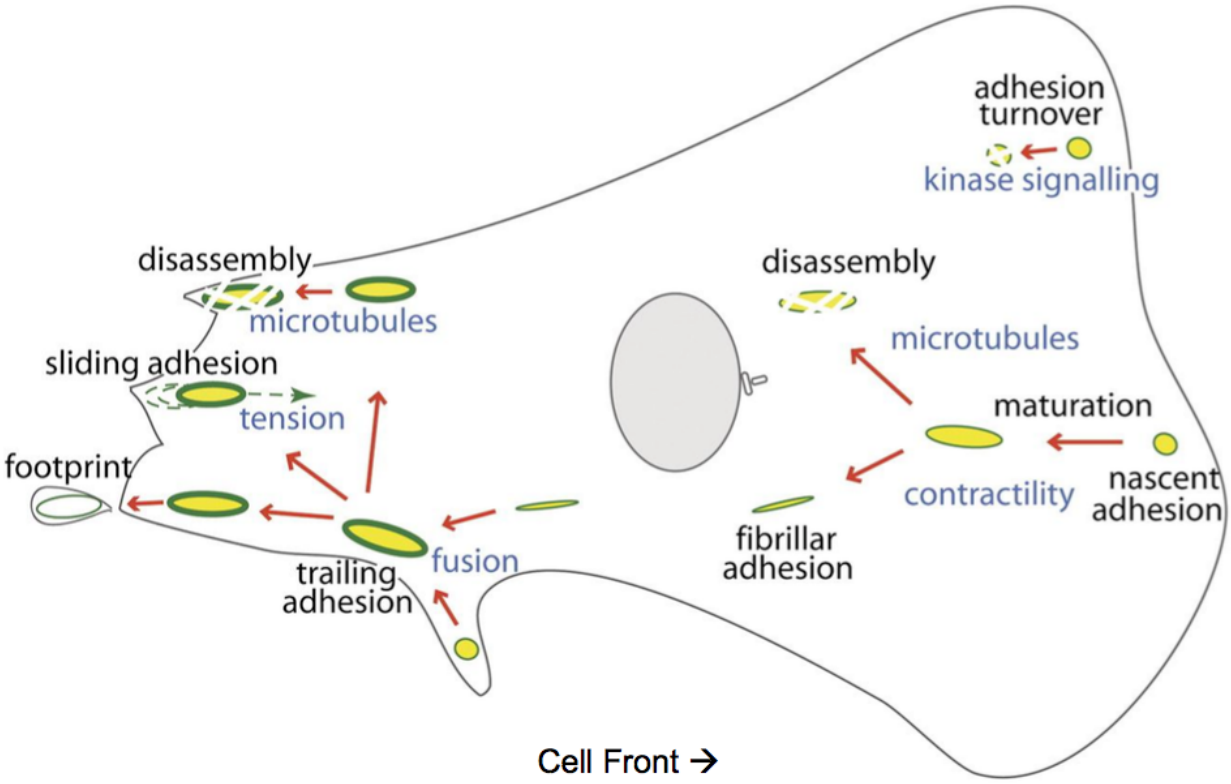

Figure 5. Model of adhesion dynamics. Nascent adhesions formed at the front either undergo turnover, which is predominantly controlled by kinase signaling, or mature in response to contractile forces. Mature adhesions can either disassemble or be transformed into fibrillar adhesions. Trailing adhesions arise as a result of fusion of additional nascent adhesions and remaining fibrillar adhesions. Once formed, trailing adhesions slide because of tension from attached stress fibers and either eventually disassemble or detach and leave integrin trails behind.

Reprinted from (Broussard, Webb et al. 2008)

lamellipodium as a branched array of filaments, it depolymerizes at locations more distal to the leading edge and tends to be more bundled (Pollard and Borisy, 2003). Therefore, as nascent adhesions approached the end of the lamellipodium, which is an area of actin disassembly, they either disassemble or begin to elongate and grow (i.e. mature). Inhibitors of actin polymerization have been shown to impair the formation of nascent adhesions (Alexandrova et al., 2008; Choi et al., 2008). Essentially, while branched actin in the lamellipodium provides a physical scaffold for nascent adhesions, actin depolymerization by cofilin can decouple these nascent adhesions from actin that then leads to adhesion disassembly (Oser and Condeelis, 2009).

While the majority of nascent adhesions undergo rapid turnover, a few undergo maturation behind the leading edge in response to tensile stress (Bershadsky et al., 2003). Nascent adhesions grow larger at the border of the lamellipodium and lamellum, and they show a differential increase in certain adhesion components like vinculin and α-actinin as they become focal complexes (FCs). This occurs when the protrusion experiences periodic or occasional pauses in forward movement in response to myosin II-dependent contractile events (Alexandrova et al., 2008; Choi et al., 2008; Vicente-Manzanares et al., 2008). The actin cross-linking protein, α-actinin, is suggested to play a crucial role in adhesion maturation. As one of the initial components detected in maturing adhesions, it has been shown to accumulate with actin filaments before other adhesion components (Choi et al., 2008; Parsons et al., 2010).

Adhesions mature along thin actin bundles that originate near the transition zone at the lamellipodium-lamellum interface. FCs, located at the lamellipodium-lamellum interface, represent an initial step in the maturation process (Ridley and Hall, 1992a; Rottner et al., 1999). Although their molecular constituents are similar to those found in nascent adhesions, they are highly dependent on myosin II activity (Choi et al., 2008; Ridley and Hall, 1992a; Rottner et al.,

1999). They are also a transient entity and thus as the lamellipodium moves forward, they mature into larger, elongated focal adhesions (FAs) (Choi et al., 2008). The addition of components during this elongation and growth process is sequential. Paxillin, for example, enters early, whereas vinculin enters later. Studies using GFP-tagged proteins have shown that paxillin and α-actinin join the adhesion sequentially (Webb et al., 2002). The maturation process of FAs can continue to occur over a long period of time, as the adhesions remain fixed when the forward movement of the protrusion (and cell) moves over them. As traction forces move the cell forward, FAs that are underneath the incoming cell body either disassemble or become fibrillar adhesions, which essentially represent the endpoint in terms of adhesion maturation (Broussard et al., 2008; Brown and Turner, 2004; Parsons et al., 2010). Maturation of focal adhesions is mediated by increased tension force and local actin polymerization (Bershadsky et al., 2006; Geiger et al., 2001).

FAs are elongated in morphology and reside at the ends of large actin bundles or stress fibers (Zimerman et al., 2004) that extend from near the front of the cell along the peripheral sides to the cell center or the rear. Being larger and more stable, FAs are composed of a heterogeneous class of adhesions with a spectrum of sizes that reflects the continuous process of adhesion maturation (Geiger and Yamada, 2011; Kanchanawong et al., 2010; Vicente-Manzanares et al., 2011). By contrast with FCs, FAs are enriched in the associated proteins including paxillin, talin, α-actinin and vinculin. The mechanisms that regulate the decision to disassemble or to elongate and grow are not well understood. However, the general notion is that myosin II-dependent contraction puts tension on adhesion molecules and induces changes in their conformation, thus opening new sites for binding or post-translational modification (Sawada et al., 2006).

Protein phosphorylation plays important roles in regulation of FAs formation and turnover (Webb et al., 2004). In protrusions, FAK and Src tyrosine kinases are the regulators of adhesion turnover. For instance, fibroblasts or cancer cells from FAK null mice have an increased number of large peripheral adhesions with impaired turnover leading to slower migration (Ilic et al., 1995). Fibroblasts from mice either lacking Src kinases or ectopically expressing kinase-dead c-Src also show large peripheral adhesions with reduced turnover, and impaired migration (Fincham and Frame, 1998; Klinghoffer et al., 1999; Webb et al., 2004). But in contrast, FA disassembly was induced when these cells were infected with the Rous sarcoma virus, which promotes activation of Src. FAK has also been shown to be required for adhesion disassembly (Tilghman et al., 2005). The scaffold functions of FAK seem to be important in the recruitment of regulators of Rho GTPases, which can mediate local myosin contractility and thereby adhesion maturation and disassembly (Tomar and Schlaepfer, 2009; Webb et al., 2004). These studies indicate an essential role for FAK/Src signaling in adhesion turnover.

Besides phosphorylation-dependent regulation, several other mechanisms can also contribute to the turnover process (Fig. 5). These mechanisms include microtubule targeting (Kaverina et al., 1999), proteolysis of adhesion proteins (Chan et al., 2010; Cortesio et al., 2011; Franco et al., 2004), and non-muscle myosin II-based cell contraction (Chrzanowska-Wodnicka and Burridge, 1996). Mature adhesions in the central region of the cell undergo microtubule and FAK-mediated mechanism of disassembly (Ezratty et al., 2005). This microtubule-induced disassembly is characterized by integrin endocytosis at adhesion sites regulated by clathrin and specific clathrin adaptor proteins (Ezratty et al., 2009). Microtubule-mediated turnover of FAs is thought to be through the modulation of Rho GTPase signaling (Broussard et al., 2008).

The Ca^{2+}-activated protease calpain also mediates adhesion disassembly in retracting

regions (Franco and Huttenlocher, 2005). Calpain cleavage of several proteins found in FAs, including FAK, paxillin and talin mediate adhesion disassembly and destabilize focal adhesions downstream from microtubules (Bhatt et al., 2002). Specifically, calpain-mediated proteolysis has been shown to stimulate the dissociation of major adhesion components such as paxillin, vinculin and zyxin (Franco et al., 2004). Calpain inhibition by chemical inhibitors, biological agents (such as calpastatin) and genetic deletion block disassembly (Franco and Huttenlocher, 2005). Calpain-based mechanisms appear to be particularly important for disassembly of adhesions that are found at the rear of the cell (Huttenlocher et al., 1997).

In addition to regulating adhesion turnover at the leading edge, FAK, Src, and other regulators of phosphorylation likely play a key role in adhesion disassembly at the rear (Huttenlocher and Horwitz, 2011). For example, adhesion disassembly can occur through FAK-Src signaling via regulation of myosin-light chain kinase (MLCK) and ERK (Webb et al., 2004). Myosin II activity, and thereby cell contractility, is involved in FA disassembly at the trailing edge. Furthermore, fibroblasts deficient in myosin IIA show impaired adhesion disassembly and rear detachment (Vicente-Manzanares et al., 2007). Lastly, FAK may regulate adhesion disassembly through its association with calpain and ERK at focal adhesions (Carragher et al., 2003).

For adhesion disassembly during retraction of the trailing edge, the adhesions at the rear often move centripetally and then disassemble, leaving integrin trails on the substratum (Ezratty et al., 2005; Laukaitis et al., 2001; Regen and Horwitz, 1992). Although not fully understood, adhesion sliding seems to be a Rho GTPase- and myosin II-dependent form of treadmilling, during which components are released at the rear of the adhesion and enter new adhesions in the proximal region (Ballestrem et al., 2001; Digman et al., 2008). Thus, though the whole adhesion

moves, individual components exchange in and out of it but otherwise remain stationary. As a result, integrins, instead of the cytoplasmic components of adhesions, remain associated with the substratum while the cytoskeleton-associated components translocate toward the cell body and disperse as the adhesion disassembles (Regen and Horwitz, 1992; Smilenov et al., 1999). This indicates a severing between integrin and the cytoplasmic components of the adhesion during release (Palecek et al., 1998). Post-translational modifications such as change in phosphorylation or proteolysis can contribute to the severing of linkages at the cell's rear. However, this effect is blocked by a myosin II inhibitor (Crowley and Horwitz, 1995), suggesting that it may also be tension-dependent. Thus, contractile forces at the cell's rear are likely key regulators of adhesive release by weakening integrin-substrate or integrin-cytoskeletal interactions (Huttenlocher and Horwitz, 2011; Worthylake et al., 2001).

Myosin II and migration

The interaction of myosin II motor proteins with actin filaments has recently emerged as a major force-generating apparatus in cell migration. Contraction of actin filaments is mediated by MyoII, which moves antiparallel actin filaments past each other and thereby provides the force that rearranges the actin cytoskeleton (Parsons et al., 2010). MyoII is also able to bundle actin filaments due to its oligomeric nature and actin-binding properties (Fig. 6). Actin filaments in the central and rear regions of migrating cells are often organized into thick bundles called stress fibers (Amano et al., 1997).

Myosin II is a bipolar actin motor composed of two heavy chains (MHCII), two regulatory light chains (RLCs) and two essential light chains (ELCs). While the RLCs regulate NM II activity, the ELC pair stabilize the heavy chains and there is no evidence that they undergo reversible phosphorylation (Vicente-Manzanares et al., 2009b). Each MHCII contains

an N-terminal head domain, a neck region, and a C-terminal α-helical rod domain (Wang et al., 2011). The head domains, which contain the ATPase motor region, bind to actin and allow MyoII to move along actin filaments by coupling the hydrolysis of ATP to conformational changes. The rod domains can associate with other MyoII rod domains to form bipolar filaments. These bipolar filaments generate contraction by sliding actin filaments relative to one another, which is a major cellular function of MyoII.

There are three major variants of myosin II: muscle, smooth muscle and non-muscle. While muscle myosin II is responsible for the contraction of the sarcomeres, smooth muscle and non-muscle myosin II are implicated in force generation and actin crosslinking that regulates cell migration (Aguilar-Cuenca et al., 2014; Vicente-Manzanares et al., 2009b). In mammals, MyoII has three isoforms, MyoIIA, MyoIIB and MyoIIC that are specified by the difference in their heavy chains. These three isoforms also have distinct intracellular localization and functions (Vicente-Manzanares et al., 2009b). The studies included in this dissertation focus on the non-muscle form of MyoII.

The activity and function of MyoII is regulated by phosphorylation of threonine 18 (T18) and serine 19 (S19) within the regulatory chain (Adelstein and Conti, 1975; Scholey et al., 1980). Whereas phosphorylation of S19 activates the motor domain of MyoII and drives actomyosin contractility (Adelstein and Conti, 1975; Ikebe, 1989), subsequent phosphorylation of T18 has an additive effect that further augments the ATPase activity of the motor (Ikebe, 1989; Umemoto et al., 1989). Moreover, phosphorylation of MyoII RLCs increases myosin II's assembly into bipolar myosin filaments, which bundle actin (Parsons et al., 2010).

These phosphorylation events are controlled by several protein kinases and phosphatases, many of which are regulated by Rho GTPases. The active ATPase allows MyoII to move along

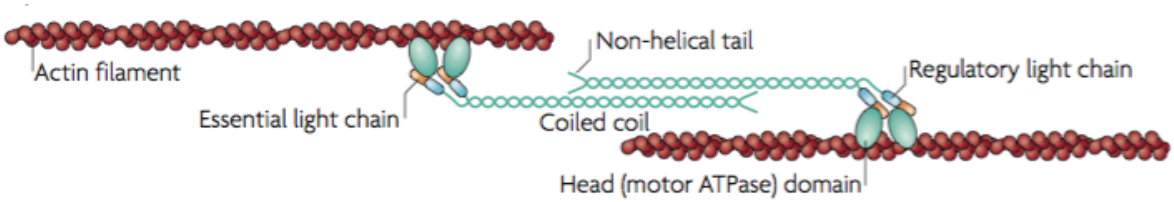

Figure 6. Schematic of the actomyosin. The subunit and domain structure of non-muscle myosin II, forms a dimer through interactions between the α-helical coiled-coil rod domains. MyoII molecules assemble into bipolar filaments through interactions between their rod domains. These filaments then bind actin through their head domains. Once the ATPase is activated at the head, there is a conformational change that moves actin filaments in an anti-parallel manner. Bipolar myosin filaments link actin filaments together in thick bundles that form cellular structures such as stress fibers.

Reprinted from Parsons et al. 2010

actin filaments by coupling the hydrolysis of ATP to conformational change (Fig. 6). The sliding of actin filaments relative to each other by MyoII generates the contractile forces seen in cells. Major insights on the function of the ATPase domain in actin motility have resulted from the use of synthetic drugs, most notably blebbistatin. Blebbistatin, which was identified in a small molecule screening, was first reported to impair cytokinesis and cell migration (Straight et al., 2003). The molecular mechanism behind blebbistatin activity revealed that it does not block the ATPase activity of MyoII, but instead slows down the phosphate release from the active pocket, lowering its affinity for actin (Kovacs et al., 2004).

MyoII is important for stabilizing leading edge protrusions and maintaining polarity (Lo et al., 2004). Although myosin II is not present in the lamellipodium, its activity influences the net rate of cellular protrusion at the leading edge (Ponti et al., 2004; Vicente-Manzanares et al., 2007). Knockdown of MyoII with small interfering RNAs or treatment of cells with blebbistatin reduces actin bundling in the lamellum, whereas the lamellipodium remains intact (Ponti et al., 2004). When MyoII is inhibited or deleted, a decrease in actin retrograde flow and in the size of adhesions was observed (Ponti et al., 2004; Rottner et al., 1999; Vicente-Manzanares et al., 2008), highlighting the requirement for MyoII activity in maintaining these structures.

While MyoII is dispensable for the assembly and disassembly of nascent adhesions inside the lamellipodium, MyoII-mediated tension is essential for the maturation of adhesions as well as retraction of the cell rear (Choi et al., 2008; Vicente-Manzanares et al., 2007). The contractile actomyosin forces on adhesions enable the recruitment of structural and signaling proteins that regulate adhesion maturation as well as disassembly (Gardel et al., 2010; Ponti et al., 2004; Wang, 1985). One way that MyoII promote adhesion maturation is through the generation of tension, which would induce conformational changes and expose cryptic binding or activation

sites in key adhesion components (del Rio et al., 2009; Friedland et al., 2009; Sawada et al., 2006). Talin binds vinculin when mechanically stretched (del Rio et al., 2009), and is required to transmit MyoII-generated forces to the substratum (Jiang et al., 2003). Because talin's head domain interacts with integrins while its tail binds actin filaments, talin bears the force transmitted from the actin cytoskeleton to the matrix. Thus, actomyosin contraction would trigger tension-sensitive talin to unfold and increase its binding to vinculin to reinforce the adhesion complex (del Rio et al., 2009; Parsons et al., 2010). Adhesion scaffold proteins, paxillin and CAS, can also change conformation to reveal new protein-binding and/or phosphorylation sites (Sawada et al., 2006; Zaidel-Bar et al., 2007). Thus, the resulting protein–protein interactions and/or phosphorylation would activate these scaffold proteins to recruit additional signaling proteins.

Another way that MyoII promote adhesion maturation is through the bundling of actin filaments, which would result in adhesion proteins at the ends of these actin filaments being brought together and being clustered. In turn, this would increase the molecular interactions between adhesion proteins and would result in increased integrin avidity (the combined strength of multiple integrin–ligand interactions) and signaling (Vicente-Manzanares et al., 2009b). For example, actomyosin-driven binding of vinculin to talin induces the clustering of integrins (Humphries et al., 2007).

By organizing the actomyosin cytoskeleton and generating contractile forces, MyoII is an important regulator of cell migration and its underlying processes. However, the upstream molecular signals that mediate actomyosin contractility are not well understood.

Traction and the clutch mechanism

As previously mentioned, adhesions generate traction by linking the ECM to actomyosin

filaments. In the absence of an adhesion, actin polymerizing at the leading edge flows backward because of the resistance from the plasma membrane (Mitchison and Cramer, 1996). Similarly, myosin-generated contraction in the lamellum pulls on the actin filaments and contributes to rearward movement. Therefore, the net rate of forward protrusion of the leading edge is determined by the rate of actin polymerization minus these rearward forces (Parsons et al., 2010). As actin retrograde flow moves over the adhesions, the latter function as traction points that resist the force arising from the rearward flow and shunt the force to the ECM, causing more force to be applied to the plasma membrane and leading to forward protrusion. These observations have led to the idea that the link between adhesions and actin is regulated by a clutch-like mechanism (Fig. 7). However, adhesions components that comprise the clutch do not efficiently transmit all of the force to the ECM, as some of them move in a retrograde direction with the actin but not at the same rate, pointing to a 'slippage' in the actin–adhesion linkage (Huttenlocher and Horwitz, 2011; Parsons et al., 2010). In addition, the strength of connection between the actin and integrins could be weak and slip and a highly pliable ECM could move under contractile forces. This complex feedback loop that connects adhesion, contraction, and ECM pliability led to the notion that a clutch-like mechanism between adhesions and actin is controlling force transmission. When the clutch between adhesions and rearward flowing actin is engaged, rates of forward protrusion of the leading edge increase while the adhesions undergo force-dependent maturation (Heath and Holifield, 1991; Parsons et al., 2010; Pollard and Borisy, 2003).

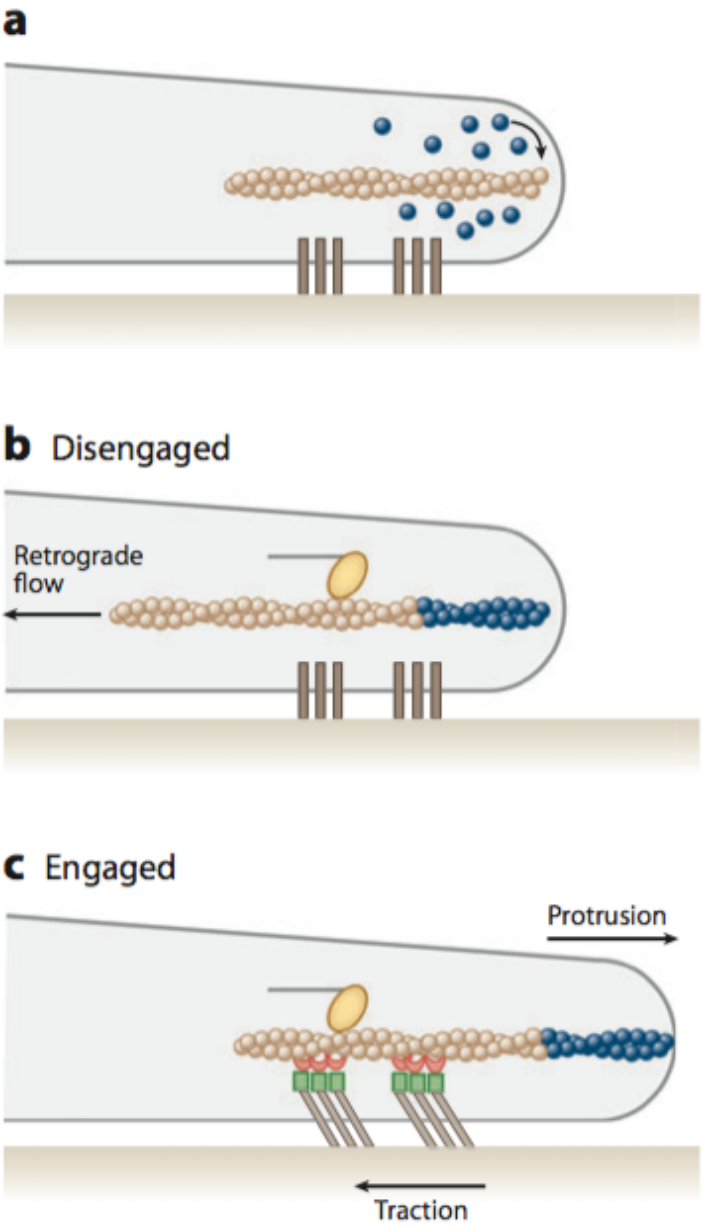

Figure 7. Schematic diagram of the molecular clutch. Focal adhesions act as a molecular clutch in migrating cells. a) At the leading edge, actin monomers (blue spheres) assembles onto the barbed end of the actin filament (arrow). Dark brown lines are integrin transmembrane proteins. (b) When the clutch is disengaged, as actin is assembled (blue spheres), the filament moves away from the leading edge due to the force generated by the polymerization of actin and the action of myosin motors (yellow oval). This leads to retrograde flow of actin. c) When the clutch is engaged, an indirect interaction exists between the actin filament and the ECM through FA proteins (red and green). This restrains the filament allowing new actin polymerization to propel the protrusion of the leading edge and actomyosin forces to be transmitted through the FA into traction on the ECM.

Reprinted from (Gardel, Schneider et al. 2010)

Rho GTPases and cell migration

The Rho family of small GTPases regulates efficient remodeling of the actin cytoskeleton to mediate cell migration (Ridley et al., 2003). Rho GTPases are essential in propagating integrin-mediated responses and, by tightly regulating the dynamics of the actin cytoskeleton, provide a key signaling link through which adhesion, spreading, and migration are controlled (Lawson and Burridge, 2014). The Rho family of GTPases represents a large portion of the Ras superfamily of small GTPases, with an average size of approximately 21 kD (Rossman et al., 2005). There are approximately 25 Rho family GTPases in mammals; however, the majority of these proteins have not been well characterized (Cain and Ridley, 2009). The best-studied ones, Rac1, RhoA and CDC42, together regulate adhesion dynamics by directly controlling the balance between actin-mediated protrusion and myosin II-mediated contraction (Parsons et al., 2010).

These proteins function as molecular switches and exist in two interconvertible forms: the GDP-bound (inactive) and GTP-bound (active) forms (Allende, 1988) (Fig. 8). Active GTPases interact with their specific downstream targets to convert upstream molecular signals into coordinated arrangements of the actin cytoskeleton, whereas GTP-hydrolysis releases the phosphate and inactivates the GTPases (Jaffe and Hall, 2005; Ridley, 2001). The cycling of Rho GTPases between an active and inactive state is regulated by guanine nucleotide exchange factors (GEFs) and GTPase-activating proteins (GAPs). While GEFs facilitate the release of GDP from the GTPases, thus promoting the binding of GTP and the activation of GTPases, GAPs stimulate their intrinsic GTPase activity and convert the GTP-bound form of these proteins to an inactive GDP-bound state.

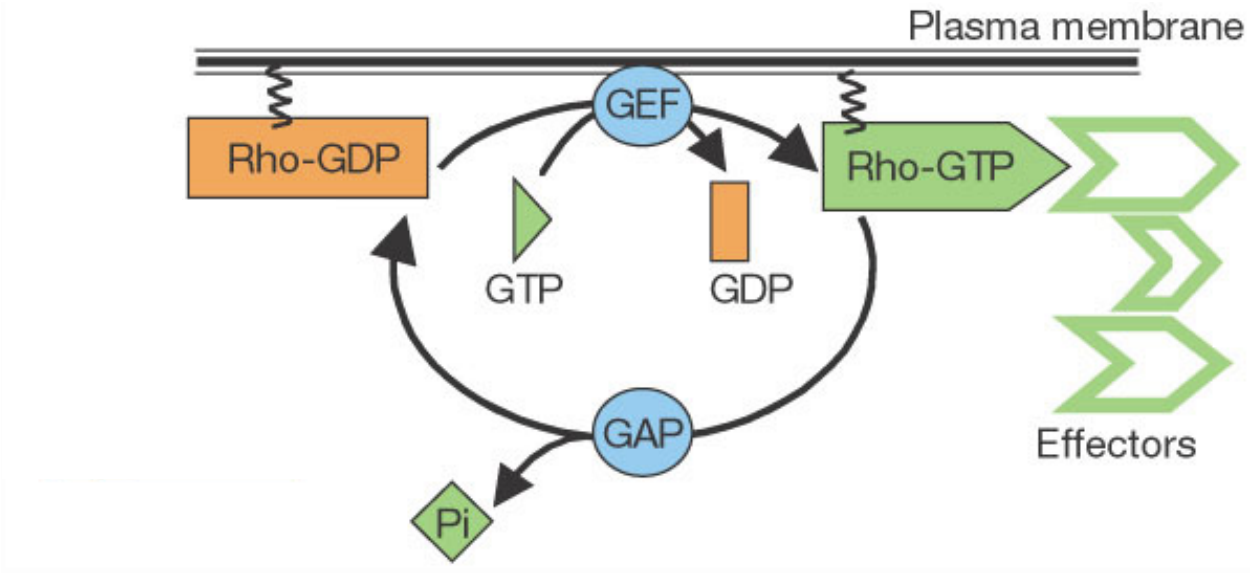

Figure 8. The Rho GTPase cycle. Rho GTPases cycle between the inactive GDP-bound state and active GTP-bound state. Membrane-bound Rho GTPases are activated by guanine nucleotide exchange factors (GEFs), which catalyze the exchange of GDP for GTP. Once activated, the GTPase can activate a host of downstream effector proteins. Inactivation of the GTPase is mediated by GTPase activating proteins (GAPs), which hydrolyze the GTP to produce GDP bound to the GTPase.

Reprinted from Etienne-Manneville and Hall, Nature, 2002

The primary migration-related downstream effectors of the Rho GTPases are molecules that regulate actin polymerization, myosin II contraction and thereby adhesions (Huttenlocher and Horwitz, 2011). Studies have shown that Rac1 affect the phosphorylation of myosin II via its downstream effector, p21-activated kinase (PAK). Downstream of Rac1, PAK has been show to either 1) inhibit myosin light chain kinase, which phosphorylates RLC or 2) phosphorylate RLC directly to activate myosin II (Daniels and Bokoch, 1999; Kiosses et al., 1999). However, the mechanism of how myosin II is regulated by Rac1 in migration has not been established.

While Rac1 and Cdc42 primarily regulate the assembly of protrusive actin-based structures and promote the formation of nascent adhesions near the cell periphery, RhoA mediates the assembly of contractile actomyosin stress fibers (Nobes and Hall, 1995; Ridley and Hall, 1992a). As such, RhoA is thought to stabilize protrusions and to induce the maturation of adhesions (Chrzanowska-Wodnicka and Burridge, 1996; Rottner et al., 1999). To mediate stress fiber formation, RhoA activates the protein-Rho-associated kinase (ROCK), which inactivates the myosin light chain phosphatase and thereby lead to an activated RLC (Kimura et al., 1996). These events activate myosin II, which then associates with actin to form stress fibers (Giuliano and Taylor, 1990).

The polarized migration of cells across the ECM is a dynamic process that is fundamentally linked to the spatially regulated activity of Rho GTPases (Lawson and Burridge, 2014). In migrating cells, Rho GTPases are spatially and temporally regulated, such that active Rac and Cdc42 are localized to the leading edge to induce actin protrusions, while active Rho is present at both the front and the rear of the cell (Machacek et al., 2009; Pertz and Hahn, 2004; Pertz et al., 2006). Rac1 expression gave rise to the branched dendritic network of actin filaments seen in the lamellipodium (Ridley et al., 1992), whereas Cdc42 expression caused an increase in

filopodia along the cell periphery that act as probes for sensing the external environment (Nobes and Hall, 1995). Actin polymerization is stimulated downstream of these two GTPases via downstream effectors such as Wiskott-Aldrich syndrome protein (WASP), WASP-family verprolin homologous protein (WAVE), and PAK. While WAVE and WASP activate the actin nucleating complex Arp2/3, PAK leads to LIM kinase activation, which inhibits cofilin-mediated breakdown of actin filaments (Ridley, 2011). Based on these studies, Rac1 also uses PAK as an effector to modulate actin dynamics. Given the role of RhoA in stimulating actomyosin contractility through its effector ROCK, it is not surprising that this GTPase has been implicated in regulating the retraction of cell tails (Lawson and Burridge, 2014).

This established view of the role of GTPases in polarized migration has however been challenged as a result of data generated using Rho GTPase fluorescence resonance energy transfer (FRET) biosensors (Kurokawa and Matsuda, 2005; Machacek et al., 2009; Pertz and Hahn, 2004; Pertz et al., 2006). Machacek et al. showed that, at the leading edge of mouse embryonic fibroblasts (MEFs), RhoA activation precedes Rac and Cdc42 activation both spatially and temporally. RhoA activity was also strictly associated with the extent of leading edge protrusion, while Rac and Cdc42 are still activated as the protrusion retracts (Machacek et al., 2009). Peak Rac1 activity is observed approximately 40s after peak RhoA activity (Machacek et al., 2009), suggesting that RhoA or RhoA-mediated events may be responsible for initiating Rac1 activity at the leading edge (Lawson and Burridge, 2014).

Based on theses studies, it is clear that Rho GTPases are regulated by an extensive crosstalk so that their signaling is coordinated to facilitate cell migration. Much remains to be learned about the role of Rho GTPases and the crosstalk that exists between them in regulating cell migration. It would be particularly interesting to learn how the GEFs are responsible for

mediating the spatiotemporal activation of Rho and Rac in migrating cells, as well as the mechanisms that regulate the spatial distribution of these components.

Regulators of Rho Family of GTPases

The activation of Rho family GTPases is tightly controlled by GEFs. There are approximately 69 known proteins in humans that belong to the diffuse B cell lymphoma (Dbl) subfamily of Rho GEFs, so named because they share homology with the first identified Rho GEF Dbl (Rossman et al., 2005). All Rho family GEFs mediates nucleotide exchange through the Dbl homology (DH) and a pleckstrin homology (PH) domain (Rossman et al., 2005). The DH domain possesses GEF activity, catalyzing the dissociation of GDP from the GTPases while stabilizing the GTPase's nucleotide-free intermediary conformation (Bos et al., 2007; Cerione and Zheng, 1996). Furthermore, mutations in the DH domains of several other proteins in the Dbl GEF family, of which Asef2 is a member, have been shown to diminish the ability of these GEFs to activate their respective GTPases (Reddy-Alla et al., 2010; Zhu et al., 2000). The PH domain is known for lipid, phosphoinositide, and protein-binding, and is believed to localize the GEF to the plasma membrane(Harlan et al., 1994). In some cases, the PH domain may also affect the activity of the DH domain, since both domains are typically required as the minimum functional unit essential for GEF activity (Jaffe and Hall, 2005; Rameh et al., 1997; Schmidt and Hall, 2002). Furthermore, some Rho GEFs may contain the Src homology (SH2 and SH3) domains, which mediate protein-protein interactions and are commonly found in molecules involved in signal transduction.

The overabundance of GEFs compared to GTPases adds an additional regulatory component to GTPase activity. GEFs contain multiple protein-protein interaction domains that are hypothesized to target the GTPases to specific cellular regions, where they can be activated

by distinct upstream signals (Rossman et al., 2005). While the function of these small GTPases in migration and adhesion dynamics has been studied, the mechanisms by which their specific GEFs function is poorly understood.

The Asef Family of GEFs

One important group of GEFs is the Asef (APC-stimulated guanine nucleotide exchange factor) family, which belongs to the larger Dbl family of Rho GEFs. The three known GEFs in this family are Asef1, Asef2, and collybistin. Whereas Asef1 and Asef2 were initially identified based on their interaction with the tumor suppressor adenomatous polyposis coli (APC) (Hamann et al., 2007; Kawasaki et al., 2007; Kins et al., 2000), collybistin, which does not bind to APC (Kins et al., 2000; Reid et al., 1999), was grouped into the Asef family based on homology (Harvey et al., 2004). Collybistin's most well characterized role has been in neurons as it is almost exclusively expressed in the brain (Hamann et al., 2007; Kneussel et al., 2001; Reid et al., 1999). Thus, this dissertation will not be going into details about collybistin.

Asef1- Asef1 or ARHGEF4, was originally identified in a two-hybrid screening of a human fetal brain library, using the armadillo binding repeat of APC as bait (Kawasaki, 2000). However, Asef1 has a broad expression profile, including brain, colon, and skeletal muscle (Hamann et al., 2007; Kawasaki et al., 2007). This protein contains an APC binding region (ABR), a Src homology 3 (SH3) domain, and a conserved DH, and PH domain (Kawasaki, 2000; Thiesen et al., 2000). Asef1 exist in an autoinhibitory conformation, in which the ABR-SH3 domains interacts with the DH domain, and thereby blocking GTPase binding and sterically hindering binding of APC to Asef1 (Mitin et al., 2007; Murayama et al., 2007; Zhang et al., 2012). Asef1 is thought to be an important regulator of cell migration. Asef1's GEF activity has been shown to promote Rac1 and Cdc42 activation, and its expression increased the phenotype

associated with these important regulators of the actin cytoskeleton actin polymerization, and cell migration (Kawasaki, 2000; Mitin et al., 2007).

Asef2- The Rho Family GEF, Asef2 (or SPATA13), was identified in a database search for molecules with homology to Asef1. Like Asef1, Asef2 activates Cdc42 and Rac1, and comprises the same domain architecture: a DH, PH, and SH3 domain, with an ABR adjacent and N-terminal to the SH3 domain (Hamann et al., 2007; Kawasaki et al., 2007). As a recently identified protein, very little is known about Asef2. With no crystal structure data, Asef2's mechanism of activation is believed to mirror that of Asef1, where the ABR-SH3 domain mediate the release from autoinhibition by binding to APC (Hamann et al., 2007; Kawasaki et al., 2007). This is confirmed as deletion of Asef2's ABR-SH3 region enhances GTPase activation (Hamann et al., 2007; Kawasaki et al., 2007). Asef2 has been implicated in the regulation of cell migration (Bristow et al., 2009), but its function in modulating this process is not well understood. Studies have shown that Asef2 activate both Cdc42 (Bristow et al., 2009; Hamann et al., 2007), and Rac (Bristow et al., 2009; Kawasaki et al., 2007), as well as indirectly reduce Rho activity (Bristow et al., 2009). Furthermore, Asef2 is highly expressed in colorectal tumors, and its deletion in mice resulted in reduction in adenoma growth and the number of associated angiogenic blood vessels (Kawasaki et al., 2009), underscoring its role in the regulation of cancer cell formation.

Because GEFs control the activation of Rho GTPases, they play an active role in regulating cell migration. Although Asef2 has been linked to colorectal cancers and cancer cell migration, much is left to discover about its downstream effectors (i.e. myosin II) and the molecular mechanism by which they regulate cell migration. Both chapter II and chapter III of this thesis, describes a novel role for Asef2-mediated Rac activity in regulating cancer cell

migration and actomyosin contraction.

Hypothesis

Cell migration is a coordinated multistep process that include the extension of an actin-rich protrusion, the formation of cell-matrix adhesions at the leading edge, the forward translocation of the cell body, and the release of adhesions along with retraction of the cell rear. Coordination of these activities to permit cell movement is tightly controlled by members of the Rho family of small GTPases, including Rac, Rho, and Cdc42. While the function of these small GTPases in migration and adhesion dynamics has been studied, the mechanism by which their specific GEFs function is poorly understood. In this thesis, we investigate the role of the recently identified Rho family GEF, Asef2, and its role in regulating cell migration and its underlying processes. As a GEF, Asef2 is known to activate both Rac and Cdc42, and is implicated in promoting cell migration. However, little is know about its effect on downstream effectors, such as MyoII, and the molecular mechanism by which they regulate cell migration. The contractile actomyosin forces mediate adhesion maturation and is essential for rear end retraction. However, whereas most studies have linked RhoA to cell contractility, the role of other Rho GTPases, including Rac, in regulating actomyosin contraction is currently unknown. Since actomyosin contractility is thought to be important for cell migration and Asef2 activates Rac, we hypothesize that Asef2 can regulate cancer cell migration in a process involving the GTPase Rac and MyoII-dependent contractility.

CHAPTER II

ACTIVATION OF RAC BY ASEF2 PROMOTES MYOSIN II-DEPENDENT CONTRACTILITY TO INHIBIT CELL MIGRATION ON TYPE I COLLAGEN

Léolène Jean,[1] Devi Majumdar,[1] Mingjian Shi,[1] Louis E. Hinkle,[1] Nicole L. Diggins,[1] Mingfang Ao,[1] Joshua A. Broussard,[1] J. Corey Evans,[1] David P. Choma,[1,2] and Donna J. Webb[1,3,*]

[1]Department of Biological Sciences and Vanderbilt Kennedy Center for Research on Human Development, Nashville, TN 37203, USA
[2]Department of Nephrology, Vanderbilt University, Nashville, TN 37235, USA
[3]Department of Cancer Biology, Vanderbilt University, Nashville, TN 37235, USA
*Author for correspondence (Email: donna.j.webb@vanderbilt.edu)

This article has been published under the same title in *Journal of Cell Science*. 2013 December 15; 126(24): 5585-5597.

Summary

Non-muscle myosin II (MyoII) contractility is central to the regulation of numerous cellular processes, including migration. Rho is a well-characterized modulator of actomyosin contractility, but the function of other GTPases, such as Rac, in regulating contractility is currently not well understood. Here, we show that activation of Rac by the guanine nucleotide exchange factor Asef2 (also known as SPATA13) impairs migration on type I collagen through a MyoII-dependent mechanism that enhances contractility. Knockdown of endogenous Rac or treatment of cells with a Rac-specific inhibitor decreases the amount of active MyoII, as determined by serine 19 (S19) phosphorylation, and negates the Asef2-promoted increase in contractility. Moreover, treatment of cells with blebbistatin, which inhibits MyoII activity, abolishes the Asef2-mediated effect on migration. In addition, Asef2 slows the turnover of adhesions in protrusive regions of cells by promoting large mature adhesions, which has been linked to actomyosin contractility, with increased amounts of active β1 integrin. Hence, our data reveal a new role for Rac activation, promoted by Asef2, in modulating actomyosin contractility, which is important for regulating cell migration and adhesion dynamics.

Introduction

Cell migration is vital for embryonic development and in maintaining homeostasis in the adult (Vicente-Manzanares and Horwitz, 2011). Migration also plays a central role in pathological disorders, such as atherosclerosis, arthritis and cancer. Therefore, identifying key molecular mechanisms that regulate migration is important for developing new therapeutic approaches for treating these disorders. Cell migration comprises several underlying processes that include establishment of front- back polarity, extension of leading edge protrusions, formation of cell-matrix adhesions, translocation of the cell body and retraction of the cell rear (Lauffenburger and Horwitz, 1996; Vicente-Manzanares et al., 2005). The formation of integrin-based adhesions, which link the actin cytoskeleton to the extracellular matrix (ECM), stabilize leading edge protrusions and generate traction forces on the ECM to propel cell movement (Beningo et al., 2001; Gardel et al., 2008). These nascent adhesions can continue to grow and mature into large focal adhesions, or they can subsequently disassemble to allow for sustained migration (Laukaitis et al., 2001; Webb et al., 2004). The continuous assembly and disassembly of adhesions, termed adhesion turnover, is crucial for cell migration (Webb et al., 2004).

MyoII is an actin motor protein that is emerging as a key modulator of cell migration through its ability to regulate underlying processes. MyoII is important for stabilizing leading edge protrusions and maintaining polarity (Lo et al., 2004). Moreover, MyoII is essential for the maturation of adhesions as well as retraction of the cell rear (Choi et al., 2008; Vicente-Manzanares et al., 2007). Structurally, MyoII is composed of two heavy chains (MHC) as well as two essential (ELC) and two regulatory (RLC) light chains. Each MHC contains an N-terminal head domain, a neck region, and a C-terminal a-helical rod domain (Wang et al., 2011). The head domains, which contain the motor region, bind to actin and allow MyoII to move along

actin filaments by coupling the hydrolysis of ATP to conformational changes. The rod domains can associate with other MyoII rod domains to form bipolar filaments. These bipolar filaments generate contraction by sliding actin filaments relative to one another, which is a major cellular function of MyoII. The activity and function of MyoII is regulated by phosphorylation within the RLC (Adelstein and Conti, 1975; Scholey et al., 1980). Phosphorylation of serine 19 activates the motor domain of MyoII and drives actomyosin contractility (Adelstein and Conti, 1975; Ikebe, 1989). Additional phosphorylation on another residue, threonine 18, further enhances myosin ATPase activity (Ikebe, 1989).

The Rho family of GTPases, which includes Rho, Rac and Cdc42, are molecular switches that exist in two interconvertible forms: a GDP-bound form (inactive) and a GTP-bound form (active) (Ridley et al., 2003). Active GTPases interact with their specific downstream targets to modulate cell migration, actin polymerization, MyoII contraction and adhesion dynamics (Huttenlocher and Horwitz, 2011; Ridley, 2001; Ridley et al., 2003). Rac and Cdc42 regulate the formation of protrusive actin-based structures, lamellipodia and filopodia, respectively, whereas Rho is thought to stabilize lamellipodial protrusions (Nobes and Hall, 1995; Ridley and Hall, 1992b). Rac promotes the assembly of nascent adhesions near the cell periphery, whereas Rho activity induces adhesion maturation (Chrzanowska-Wodnicka and Burridge, 1996; Ridley and Hall, 1992b; Rottner et al., 1999). Rho activity also stimulates the formation of stress fibers, which are contractile F-actin bundles, and promotes actomyosin contractility (Chrzanowska-Wodnicka and Burridge, 1996; Katoh et al., 2001; Ridley and Hall, 1992b). However, little is currently known about the function of the other Rho GTPases, including Rac, in modulating actomyosin contraction.

The activation of Rho GTPases is regulated by guanine nucleotide exchange factors

(GEFs), which facilitate the release of GDP from the GTPases, thus promoting the binding of GTP. Asef2 (also known as SPATA13) is a recently identified GEF known to activate both Rac and Cdc42 (Hamann et al., 2007; Kawasaki et al., 2007). Asef2 comprises four domains, including an N-terminal adenomatous polyposis coli (APC)-binding region (ABR), an adjacent Src homology 3 (SH3) domain, a central Dbl homology (DH) domain that binds GTPases and is necessary for its catalytic function, and a pleckstrin homology (PH) domain, which facilitates membrane targeting (Hamann et al., 2007; Kawasaki et al., 2007). Binding of the tumor suppressor APC to the ABR region has been shown to stimulate the GEF activity of Asef2 by releasing it from an auto-inhibited state, where the C-terminus is bound to the ABR-SH3 domains (Hamann et al., 2007). Asef2 has been implicated in the regulation of cell migration (Bristow et al., 2009; Sagara et al., 2009), but its role in modulating this process is not well understood.

In this study, we demonstrate that Asef2 inhibits cell migration on type I collagen by a Rac- and MyoII-dependent mechanism. Asef2 promotes the activation of Rac, which subsequently stimulates MyoII contractility. In addition, Asef2 slows adhesion turnover and induces large mature adhesions. Therefore, Asef2 modulation of Rac- and MyoII-dependent contractility is likely to regulate cell migration by affecting underlying migratory processes such as adhesion turnover.

Materials and Methods

Reagents

An anti-Asef2 rabbit polyclonal antibody was made as previously described (Bristow et al., 2009). β1 integrin HUTS-4 monoclonal antibody was purchased from Chemicon International (Temecula, CA). AIIB2 β1 integrin antibody was kindly provided by Roy Zent

(Vanderbilt University, Nashville, TN). Phospho-MLC (S19) polyclonal antibody (clone 3671) was obtained from Cell Signaling (Beverly, MA). Phospho-Akt (T308) polyclonal antibody was purchased from Santa Cruz Biotechnology (Santa Cruz, CA). Fibronectin, β-actin monoclonal antibody (clone AC-15) and FLAG-M2 monoclonal antibody were from Sigma-Aldrich (St. Louis, MO). Paxillin monoclonal antibody was purchased from BD Bioscience Pharmingen (San Diego, CA). Alexa-Fluor-555- and Alexa-Fluor-680-conjugated anti-mouse Ig, Alexa-Fluor-647-conjugated anti-rabbit Ig, and FluoSpheres® carboxylate-modified Nile Red microspheres (Cat. No. F-8819) were obtained from Molecular Probes (Eugene, OR). IRDye 800 anti-mouse Ig and 800 anti-rabbit Ig were purchased from Rockland Immunochemicals (Gilbertsville, PA). Rat-tail type I collagen was from BD Biosciences (Bedford, MA). Blebbistatin, NSC23766 and BSA were purchased from EMD Bioscience (La Jolla, CA). Aqua Poly/Mount mounting solution (Cat # 18606) was obtained from Polysciences, Inc. (Warrington, PA).

Plasmids

GFP-Asef2-encoding cDNA was prepared by cloning full-length Asef2 (Spata13) cDNA into pEGFP-C3 vector as previously described (Bristow et al., 2009). mCherry cDNA was a generous gift from Roger Tsien (University of California, San Diego, La Jolla, CA). mCherry-paxillin was kindly provided by Steve Hanks (Vanderbilt University, Nashville, TN). GST-tagged PBD, wild-type Cdc42 and wild-type Rac1 were kind gifts from Alan Hall (Memorial Sloan-Kettering Cancer Center, NY). GST-tagged rhotekin-binding domain and Myc-tagged wild-type RhoA were generously provided by Sarita Sastry (University of Texas Medical Branch, Galveston, TX). shRNA constructs were generated as previously described (Wegner et al., 2008; Zhang and Macara, 2008b) by ligating 64-mer oligonucleotides into GFP-pSUPER vector (Asef2 shRNAs) or pSUPER vector (Rac shRNAs). Both target sequences for Asef2 and

Rac1 have been previously described (Bristow et al., 2009; Chan et al., 2005). A non-targeting shRNA with the sequence 5′-CAGTCGCGTTTGCGACTGG-3′ was used as a control (Saito et al., 2007).

Cell culture

HT1080 cells stably expressing GFP or GFP-Asef2 were generated by retroviral transduction and selected by incubation with 400 µg/ml G418 as previously described (Bristow et al., 2009). Stably expressing GFP and GFP–Asef2 cells were sorted by FACS into populations based on their expression level (Bristow et al., 2009). Experiments for this study were performed with stable cells expressing low levels of GFP or GFP-Asef2, which were the same cells that were used previously (Bristow et al., 2009). Cells were maintained in Dulbecco's modified Eagle's medium (DMEM) (Invitrogen, Carlsbad, CA) supplemented with 10% fetal bovine serum (FBS) (Hyclone, Logan, UT) and penicillin-streptomycin (Invitrogen). Wild-type HT1080 cells were transiently transfected with Lipofectamine™ 2000 (Invitrogen) according to the manufacturer's instructions. MDA-MB-231 cells stably expressing GFP or GFP-Asef2 were prepared by retroviral transduction as described above for HT1080 cells. Stably expressing GFP and GFP-Asef2 MDA-MB-231 cells were maintained in DMEM supplemented with 20% FBS and penicillin-streptomycin.

Microscopy and immunocytochemistry

Cells were plated on glass coverslips, which were coated with 5 µg/ml type I collagen or 2.5 µg/ml fibronectin for 1 hour at 37°C. Following incubation for 2-4 hours at 37°C to permit attachment, cells were fixed for 20 minutes with 2-4% paraformaldehyde and 4% sucrose in phosphate-buffered saline (PBS). In some experiments, cells were fixed by incubation with ice-cold methanol for 10 minutes at -20°C. Cells were permeabilized for 5 minutes at 23°C with

0.2% (v/v) Triton X-100, and incubated with either 20% goat serum or 10% BSA in PBS for 1 hour at 23°C to block non-specific binding. After blocking, cells were incubated with the indicated primary and fluorescently conjugated secondary antibodies, which were diluted in either 5% goat serum or 2% BSA in PBS, for 1 hour at 23°C. Following each step, coverslips were washed three times with PBS. Coverslips were mounted on microscope glass slides (Fisher Scientific, Pittsburgh, PA) with Prolong Gold Antifade reagent (Invitrogen, Carlsbad, CA). Images were acquired with either an inverted Olympus IX71 microscope (Melville, NY) equipped with a Retiga EXi CCD camera (QImaging, Surrey, BC) and a PlanApo 60× OTIRFM objective (NA 1.45) or a Quorum WaveFX spinning disk confocal system with a Nikon Eclipse Ti microscope, a Hamamatsu ImageEM-CCD camera, and a PlanApo 60× TIRF objective (NA 1.49). To visualize GFP, an Endow GFP Bandpass filter cube (excitation HQ470/40, emission HQ525/50, Q495LP dichroic mirror) was used. Alexa Fluor® 555 and mCherry were observed using a TRITC/Cy3 cube (excitation HQ545/30, emission HQ610/75, Q570LP dichroic mirror), and Alexa Fluor® 647 (far-red) was observed with a Cy5™ cube (excitation HQ620/60, emission HQ700/75, Q660LP dichroic mirror). The background-subtracted integrated fluorescent intensity was normalized to cell area (average intensity).

For quantification of phosphorylated (S19) MyoII and total MyoII, the average fluorescence intensity was obtained by normalizing the background-subtracted integrated fluorescence intensity in individual cells to the unit area using MetaMorph software. For quantification of the amount of active and total β1 integrin in adhesions, the average fluorescence intensity was measured by normalizing the background-subtracted integrated fluorescence intensity in individual adhesions to the unit area with MetaMorph software.

In-cell western assay

At total of 10^4 cells were allowed to adhere for 2-4 hours at 37°C to 96-well plates that were coated with 5 μg/ml type I collagen. After attachment, cells were incubated for 20 minutes at 23°C with 4% paraformaldehyde in PBS and permeabilized for 5 minutes at 23°C with 0.2% (v/v) Triton X-100. Cells were then incubated with 5% BSA in PBS (blocking solution) for 1 hour at 23°C to block non-specific binding. Following blocking, cells were incubated with the indicated primary and fluorescently conjugated secondary antibodies in blocking solution for 1 hour at 23°C. Cells were washed three times with PBS after each incubation. After the final wash, 96-well plates were aspirated and inverted to remove the residual wash solution and scanned with a LI-COR® Odyssey® infrared imaging system (LI-COR Biosciences, Lincoln, NE). The background-subtracted mean integrated intensities were obtained using Odyssey® 3.2 ICW module software. Background fluorescence was determined from cells that were incubated with secondary antibodies alone.

Migration assay

Cells were allowed to adhere for 1-2 hours at 37°C to tissue culture dishes that were coated with 5 μg/ml type I collagen or 2.5 μg/ml fibronectin. Phase-contrast images were acquired every 5 minutes for up to 6 hours using MetaMorph software (Molecular Devices, Inc. Sunnyvale, CA), interfaced with a Lambda 10-2 automated controller (Sutter Instruments), and an Olympus IX71 microscope with a 10× objective (NA 0.3). During imaging, cells were maintained in SFM4MAb™ media (Hyclone, Logan, UT) supplemented with 2% FBS (imaging media). In some experiments, cells were pre-treated with 20 μM blebbistatin or DMSO (vehicle control) for 1 hour at 37°C. After pre-incubation, phase contrast images were acquired every 5 minutes for 6 hours. Then, blebbistatin was removed, cells were washed with PBS, fresh imaging

medium was added, and cells were imaged for an additional 6 hours. MetaMorph software was used to track cell movement, and the migration speed was calculated by dividing the total distance that cells moved in microns by the time. Wind-Rose plots were obtained by setting the X-Y coordinates of cell tracks to a common origin.

Analysis of adhesion turnover

Stably expressing GFP and GFP-Asef2 cells were transfected with 1 μg of mCherry-paxillin-encoding cDNA. After 24 hours, cells were plated on microscopy dishes coated with type I collagen and allowed to adhere for 1-2 hours at 37°C. Time-lapse fluorescence images were acquired at 15-second intervals, and $t_{1/2}$ values for adhesion assembly and adhesion disassembly were calculated as previously described (Bristow et al., 2009; Webb et al., 2004).

Rho family GTPase activity assays

GFP and GFP-Asef2 stably expressing cells were transfected with 3 μg cDNA encoding FLAG-Rac1, FLAG-Cdc42 or Myc-RhoA. After 24 hours, cells were lysed and assayed for active Rac, Cdc42 and Rho as previously described (Bristow et al., 2009; Ren et al., 1999). In some experiments, wild-type HT1080 cells were co-transfected with 2 μg FLAG–Rac1 and 2 μg of either Asef2 shRNA 1 or NT shRNA. Three days later, lysates from cells were collected and analyzed as described above.

Traction force measurements

Polyacrylamide (PAA) gels embedded with 1.0 μm FluoSpheres® fluorescent beads were prepared on rectangular glass coverslips as previously described (Sabass et al., 2008). PAA gels were incubated with 140 μg/ml type I collagen for 4 hours at 23°C. The thickness of the PAA gels was ~30 μm, and the Young's modulus of the gels was 15.6 kPa as calculated previously

(Sabass et al., 2008; Yeung et al., 2005). A total of $5x10^3$ GFP or GFP-Asef2 stably expressing cells were incubated with PAA gels coated with type I collagen for 2 hours at 37°C to allow cells to adhere. For each cell of interest, a DIC image of the cell and a fluorescence image of the FluoSpheres® beads with the attached cell were taken. Then, the cell of interest was dissociated from the PAA gel by trypsinization, and a fluorescence image of the FluoSpheres® beads were acquired. Images were acquired using the Quorum WaveFX spinning disk confocal system with a Nikon Eclipse Ti microscope, a Hamamatsu ImageEM-CCD camera, and a Plan Fluor 40X objective (NA 1.3). FluoSpheres® fluorescent beads were imaged using a 561 nm laser and a 593/40 nm BrightLine® single-band bandpass emission filter (Semrock, Rochester, NY). Traction force maps were generated from the acquired images using LIBTRC software (Dembo and Wang, 1999), which was developed by Micah Dembo (Boston University, Boston, MA).

FRET imaging and analysis

Wild-type HT1080 cells were co-transfected with the Raichu-Rac FRET probe (a kind gift from Michiyuki Matsuda, Kyoto University, Kyoto, Japan) and either mCherry-Asef2 or mCherry. After 24 hours, cells were plated on glass coverslips, which were coated with 5 μg/ml type I collagen, for 1 hour at 37°C. Cells were fixed by incubation for 15 minutes at 23°C with a 4% paraformaldehyde (wt/vol) PBS solution containing 0.12 M sucrose. Coverslips were then mounted onto glass slides using Aqua Poly/Mount mounting solution. Images were acquired with a Zeiss LSM 510 Meta inverted confocal microscope using a Plan-Apochromat 63× objective (NA 1.4). CFP, YFP and mCherry fluorophores were excited with a 458, 514 and 543 nm laser, respectively. Images were collected using the following emission filters: CFP, BP 475–525 nm; YFP, LP 530 nm; and mCherry, LP 560 nm. mCherry images were used to identify cells expressing either mCherry–Asef2 or mCherry. CFP and YFP images were acquired both before

and after bleaching YFP (the FRET acceptor) within an ROI. YFP images were taken to confirm that YFP was bleached within the ROI. CFP images were used to calculate the FRET efficiency of the active Rac FRET probe using the following equation: $(CFP_{Post}-CFP_{Pre})/CFP_{Post}\times 100$. CFP_{Post} is the average intensity of CFP in the ROI after bleaching YFP with the 514 nm laser, and CFP_{Pre} is the average intensity of CFP in the ROI before bleaching YFP with the 514 nm laser. The average FRET efficiency of cells expressing mCherry-Asef2 was then compared to cells expressing mCherry using a Student's t-test statistical analysis.

Flow cytometry

GFP and GFP-Asef2 stably expressing cells were cultured on 5 µg/ml dishes coated with type I collagen for 18 hours at 37°C. Cells were then trypsinized (2.5% trypsin without EDTA) and resuspended in ice-cold Opti-MEM (GIBCO) containing 2% FBS (cell-sorting buffer). Cell suspensions (2.5×105 cells) were incubated with primary HUTS-4 antibody (1:500 dilution in cell-sorting buffer) for 30 minutes at 4°C followed by secondary Alexa Fluor® 555 antibody (1:1000 dilution in cell-sorting buffer) for 20 minutes at 4°C. To determine non-specific binding, an equal amount of cell suspension was incubated with secondary antibody alone. Cells were washed three times with ice-cold cell-sorting buffer following each incubation. After the final wash, cells were resuspended in 500 µl of cell-sorting buffer and subjected to flow cytometry. For total β1 integrin staining, cells were incubated with AIIB2 antibody (1:50 dilution) and subjected to flow cytometry as described above. AIIB2 antibody binds to the extracellular domain of β1 integrin. Histograms were generated using FlowJo software.

Collagen gel contraction assay

Type I collagen gel contraction assays were performed as previously described (Tovell et al.; Vernon and Gooden, 2002). Briefly, type I collagen was mixed with DMEM to a final

concentration of 1.5 μg/ml and the pH was adjusted to 7.4 with 1 M NaOH. Cells in DMEM with 10% FBS were added to the type I collagen mixture to a final concentration of 2.5×10^5 cells per gel. This mixture was added to 24-well cell culture plates (Costar, Corning NY) and allowed to solidify by incubation for 1 hour at 37°C. Serum-free DMEM was added to the wells, and the collagen gels were gently detached using a pipette tip. The gels were incubated for 14 hours at 37°C, and then the diameter of the gels were measured. In some experiments, cells were incubated with 100 μM NSC23766 or DMSO as a vehicle control for 14 hours at 37°C.

Results

Asef2 inhibits cell migration on type I collagen

We have previously shown that Asef2 promotes cell migration when cells are plated on fibronectin (Bristow et al., 2009). Indeed, in our previous study, the migration speed of HT1080 cells stably expressing GFP-Asef2 was increased 1.6-fold compared to control cells stably expressing GFP. In this study, to further investigate the role of Asef2 in regulating cell migration, we plated GFP-Asef2 and GFP stably expressing cells on type I collagen. These cells express low levels of GFP-Asef2 (less than 3-fold over endogenous) (Bristow et al., 2009). Intriguingly, GFP-Asef2 cells, plated on type I collagen, migrated significantly more slowly than GFP control cells (Fig. 9A), suggesting that Asef2 impairs migration on type I collagen. Given that these results were surprising, we performed side-by-side migration experiments with GFP and GFP–Asef2 stably expressing cells plated on fibronectin or type I collagen. Consistent with our previous results, GFP-Asef2 promoted migration on fibronectin, but inhibited migration on type I collagen, indicating that Asef2 differentially affects migration on these substrates (Fig. 10A). We continued to probe the function of Asef2 in regulating migration on type I collagen by

transiently transfecting wild-type HT1080 cells with GFP–Asef2 or GFP as a control. As with the stable cells, expression of GFP- Asef2 resulted in a decrease in migration speed as compared to that observed with GFP-expressing cells (Fig. 10B). We then examined the effect of Asef2 on migration on type I collagen in another cell type by generating MDA-MB-231 cells that stably expressed GFP-Asef2 or GFP as a control. As with HT1080 cells, stable expression of GFP-Asef2 in MDA-MB-231 led to a significant reduction in migration speed as compared to that observed with GFP-expressing cells (Fig. 11A), suggesting Asef2 inhibits migration on type I collagen.

We further probed the role of Asef2 in regulating migration on type I collagen by knocking down endogenous expression of the protein using two short hairpin RNA (shRNA) constructs. Although these shRNAs had previously been shown to be effective (Bristow et al., 2009), we confirmed their ability to knockdown Asef2. When wild-type HT1080 cells were transfected with Asef2 shRNA1 or Asef2 shRNA2, endogenous expression of Asef2 was decreased by ~65% compared with empty pSUPER vector or a non-targeting shRNA (NT shRNA) (Fig. 9B). Transfection of HT1080 cells with the two Asef2 shRNAs resulted in a 1.3-fold increase in migration speed compared to that observed with cells transfected with pSUPER or NT shRNA (Fig. 9C), demonstrating that knockdown of endogenous Asef2 enhances migration on type I collagen. Collectively, our results suggest an interesting new role for Asef2 in regulating migration on type I collagen.

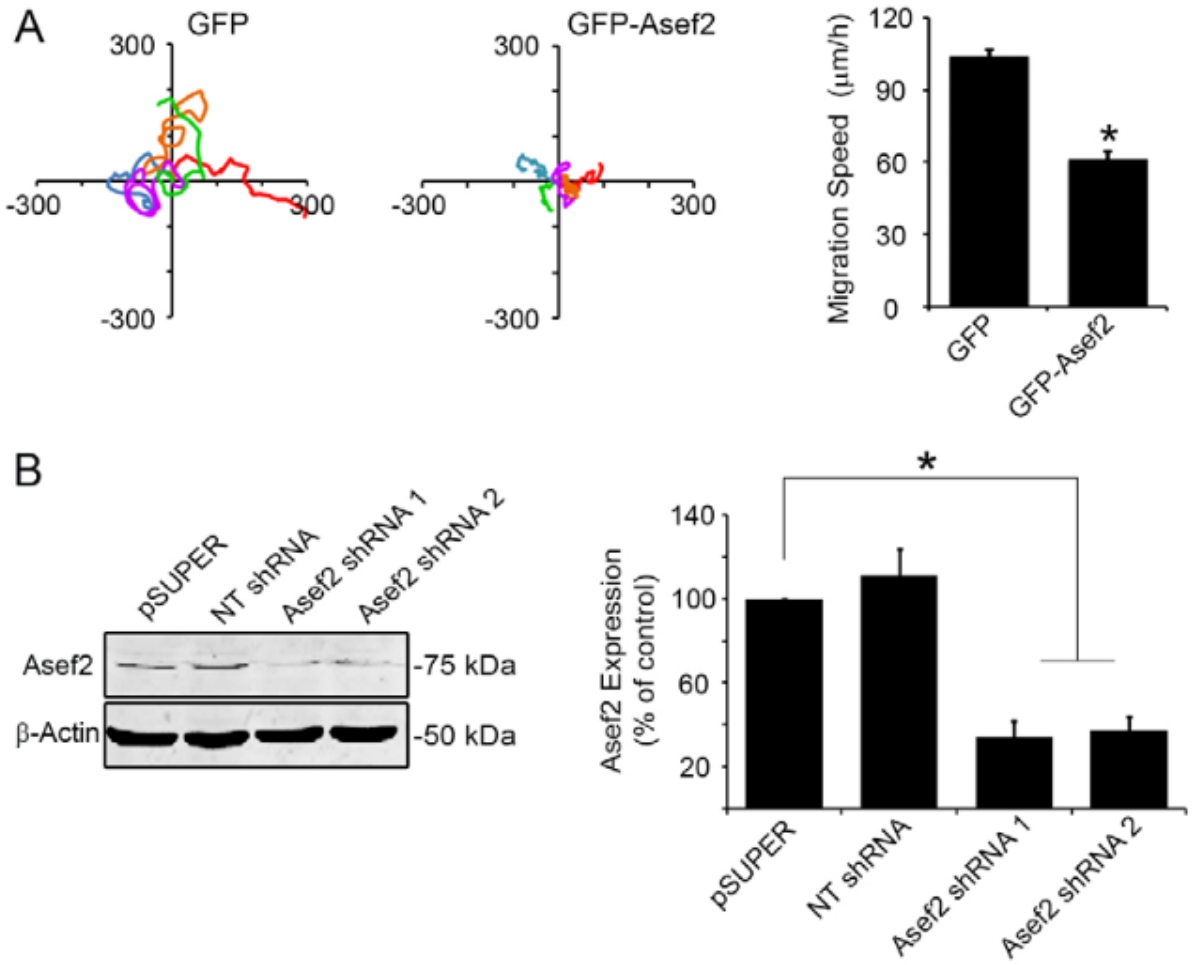

Figure 9. Asef2 impairs cell migration on type I collagen. (A) GFP and GFP–Asef2 stably expressing HT1080 cells were plated on tissue culture dishes coated with type I collagen and imaged using time- lapse microscopy. The migration paths of individual cells were tracked and analyzed. Left, Rose plots of the migration tracks for five cells. Right, quantification of the migration speed for GFP and GFP–Asef2 cells. Error bars represent the s.e.m. for 59–63 cells from three independent experiments. *P<0.0001. (B) Left, wild-type HT1080 cells were transfected with empty pSUPER vector, a non- targeting shRNA (NT shRNA), or Asef2 shRNAs. Cell lysates were immunoblotted for Asef2 to determine endogenous expression of this protein and for b-actin as a loading control. Right, quantification of the amount of endogenous Asef2 in cells transfected with the indicated constructs. Error bars represent the s.e.m. from five independent experiments. *P<0.0001.

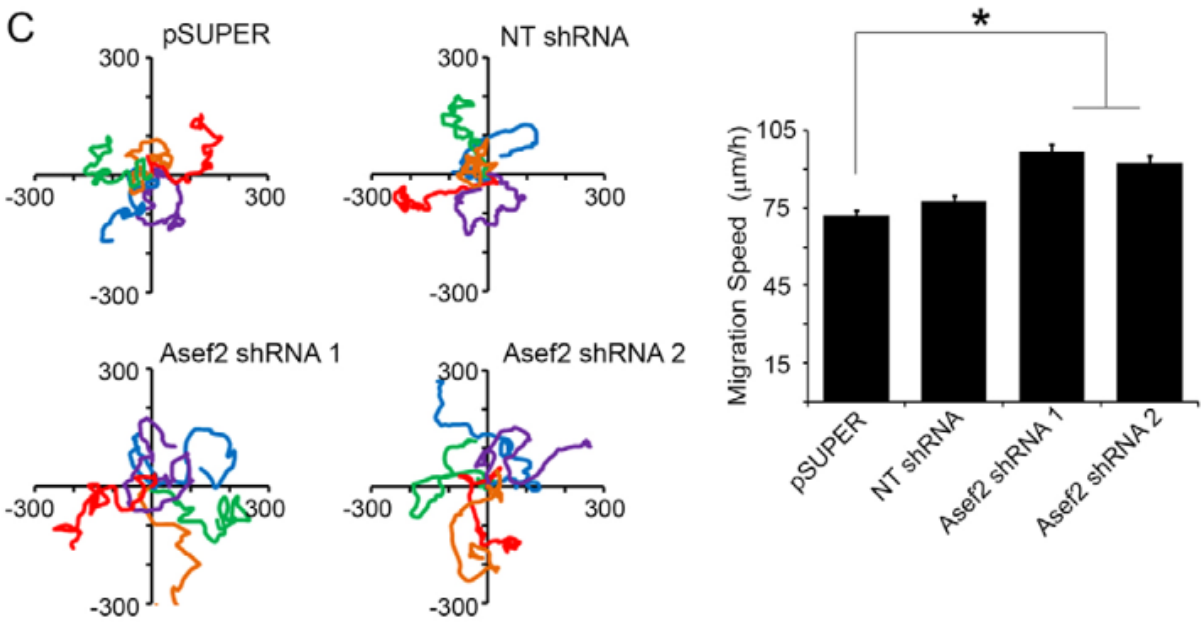

Figure 9 Cont'd. Asef2 impairs cell migration on type I collagen. (C) Wild-type HT1080 cells were transfected with empty pSUPER vector, a NT shRNA or Asef2 shRNAs and used in migration assays 3 days later. Left, Rose plots of migration tracks for cells transfected with these constructs. Right, quantification of the migration speed for cells transfected with empty pSUPER vector, a NT shRNA, or Asef2 shRNAs. Error bars represent the s.e.m. for at least 40 cells from three independent experiments. *P<0.0001.

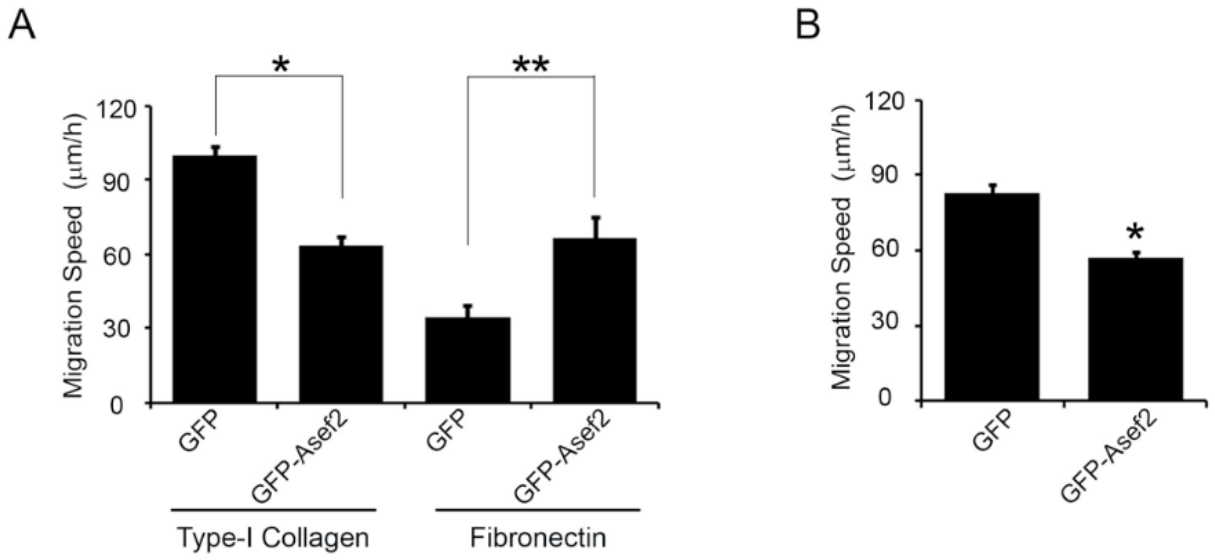

Figure 10. Asef2 regulates migration on fibronectin and type I collagen through distinct molecular mechanisms. (A) GFP and GFP-Asef2 stable HT1080 cells were plated on fibronectin or type I collagen-coated tissue culture dishes and imaged using time-lapse microscopy. The migration of individual cells was tracked and analyzed. Quantification of the migration speed for cells plated on fibronectin and type I collagen is shown. Error bars represent S.E.M. for at least 59 cells from three independent experiments (*$p < 0.0001$, **$p < 0.007$). (B) Wild-type HT1080 cells were transiently transfected with GFP or GFP-Asef2 and used in migration assays. Quantification of the migration speed for GFP and GFP-Asef2 expressing cells is shown. Error bars represent S.E.M. for at least 49 cells from three independent experiments (*$p < 0.0001$).

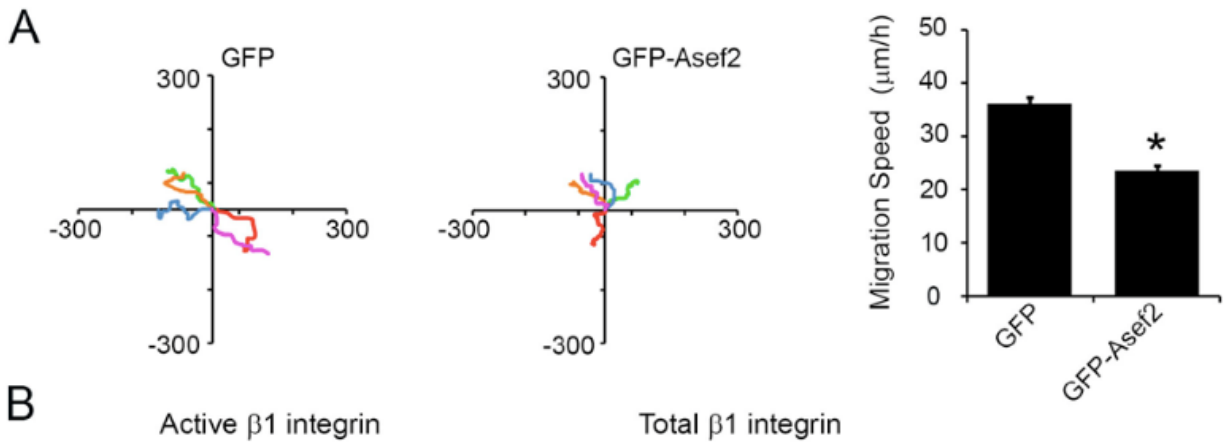

Figure 11. Asef2 impairs cell migration in MDA-MB-231 cells. (A) GFP and GFP-Asef2 stable MDA-MB-231 cells were plated on type I collagen-coated tissue culture dishes and used in migration assays. Left, Rose plots of migration tracks for five GFP and GFP-Asef2 expressing cells are shown. Right, quantification of the migration speed for GFP and GFP-Asef2 cells is shown. Error bars represent S.E.M. for at least 62 cells from three separate experiments (*$p < 0.0001$).

Rac activity is enhanced by Asef2

We next investigated the mechanism by which Asef2 impairs migration on type I collagen. In initial experiments, we examined the effect of Asef2 on the activity of the Rho family GTPases Rac, Cdc42 and Rho using a pulldown assay. In this assay, GFP and GFP–Asef2 cells were plated on type I collagen, and GST- tagged binding domains from effectors were used to detect the active forms of these small GTPases from cell lysates. Interestingly, GFP–Asef2 expression did not significantly affect the level of active Cdc42 or Rho (Fig. 12A). In contrast, the amount of active Rac was increased ~1.8-fold in GFP–Asef2 cells compared to GFP controls (Fig. 12A). Moreover, knockdown of endogenous Asef2 in wild-type HT1080 cells by transfection with Asef2 shRNA 1 caused a decrease in Rac activity compared to that observed with cells transfected with NT shRNA (Fig. 12B). Taken together, these results suggest that Asef2 promotes the activation of Rac, but not Cdc42 and Rho, when cells are plated on type I collagen.

To further demonstrate that Asef2 increases Rac activity, we used a Raichu-Rac fluorescence resonance energy transfer (FRET) probe. Raichu-Rac is composed of yellow fluorescent protein (YFP), the p21-binding domain (PBD) from the Rac effector p21-activated kinase (PAK), Rac, and cyan fluorescent protein (CFP) (Itoh et al., 2002). Upon activation, Rac binds to PBD, which brings YFP and CFP in close enough proximity to undergo FRET (Itoh et al., 2002). To perform acceptor photo-bleaching FRET, we expressed the Raichu-Rac probe and either mCherry–Asef2 or mCherry as a control in HT1080 cells and photo-bleached a region of interest (ROI) with a 514 nm laser. With acceptor photo-bleaching, when YFP (FRET acceptor) is photo-bleached, the intensity of CFP (FRET donor) increases if FRET occurs. YFP images, taken pre- and post- bleaching, demonstrated that YFP was effectively photo- bleached (Fig. 12C). CFP images that were acquired before (pre) and after photo-bleaching YFP (post) showed

an increase in the intensity of CFP emission in Asef2-expressing cells (Fig. 12C), indicating FRET had occurred. Quantification revealed that Asef2 did indeed increase the FRET efficiency of the Raichu-Rac probe (Fig. 12C), showing that Asef2 significantly enhances the level of active Rac in cells.

To determine whether Asef2 inhibition of migration on type I collagen was dependent on Asef2 GEF activity, we generated a GEF deficient mutant. We mutated lysine 382 within the DH domain of Asef2 to alanine (K382A). Mutation of this residue in the related GEF collybistin impaired its GEF activity (Reddy-Alla et al., 2010). In an active Rac pulldown assay, GFP-Asef2 expression significantly enhanced the level of active Rac in HT1080 cells compared to GFP control cells (Fig. 12D). In contrast, expression of the Asef2 GEF mutant (GFP-Asef2- K382A) did not increase the amount of active Rac (Fig. 12D), indicating that the K382A mutation abolished GEF activity in Asef2. The migration speed of cells expressing GFP-Asef2-K382A was comparable to that observed in cells expressing GFP, whereas expression of GFP-Asef2 led to a significant decrease in migration speed (Fig. 12E). Thus, the GEF activity of Asef2 is crucial for the function of Asef2 in impairing migration on type I collagen.

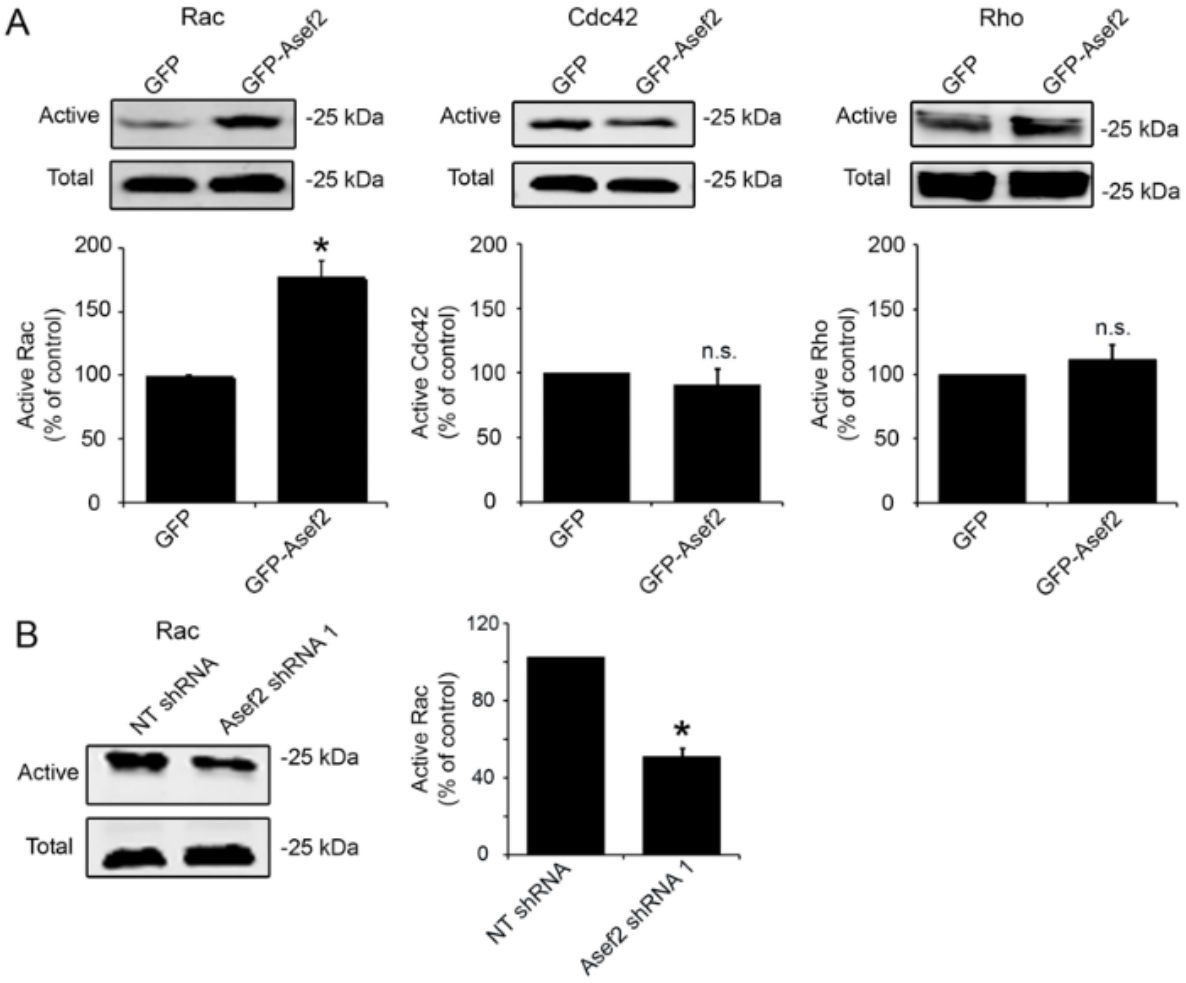

Figure 12. Asef2 enhances activation of Rac and regulates migration through its GEF activity. (A) Upper, the active forms of Rac, Cdc42 and Rho were pulled down from lysates of GFP and GFP–Asef2 cells plated on type I collagen. The total level of these GTPases is shown as a control. Lower, quantification of the amount of active Rac, Cdc42, and Rho from at least three separate experiments. Error bars represent the s.e.m. *P<0.006, n.s. denotes no statistically significant difference. (B) Left, wild-type HT1080 cells were transfected with NT shRNA or Asef2 shRNA 1, and 3 days later, active Rac was pulled down from lysates. The total level of Rac is shown as a control. Right, quantification of the amount of active Rac from three independent experiments. Error bars represent the s.e.m. *P<0.0002.

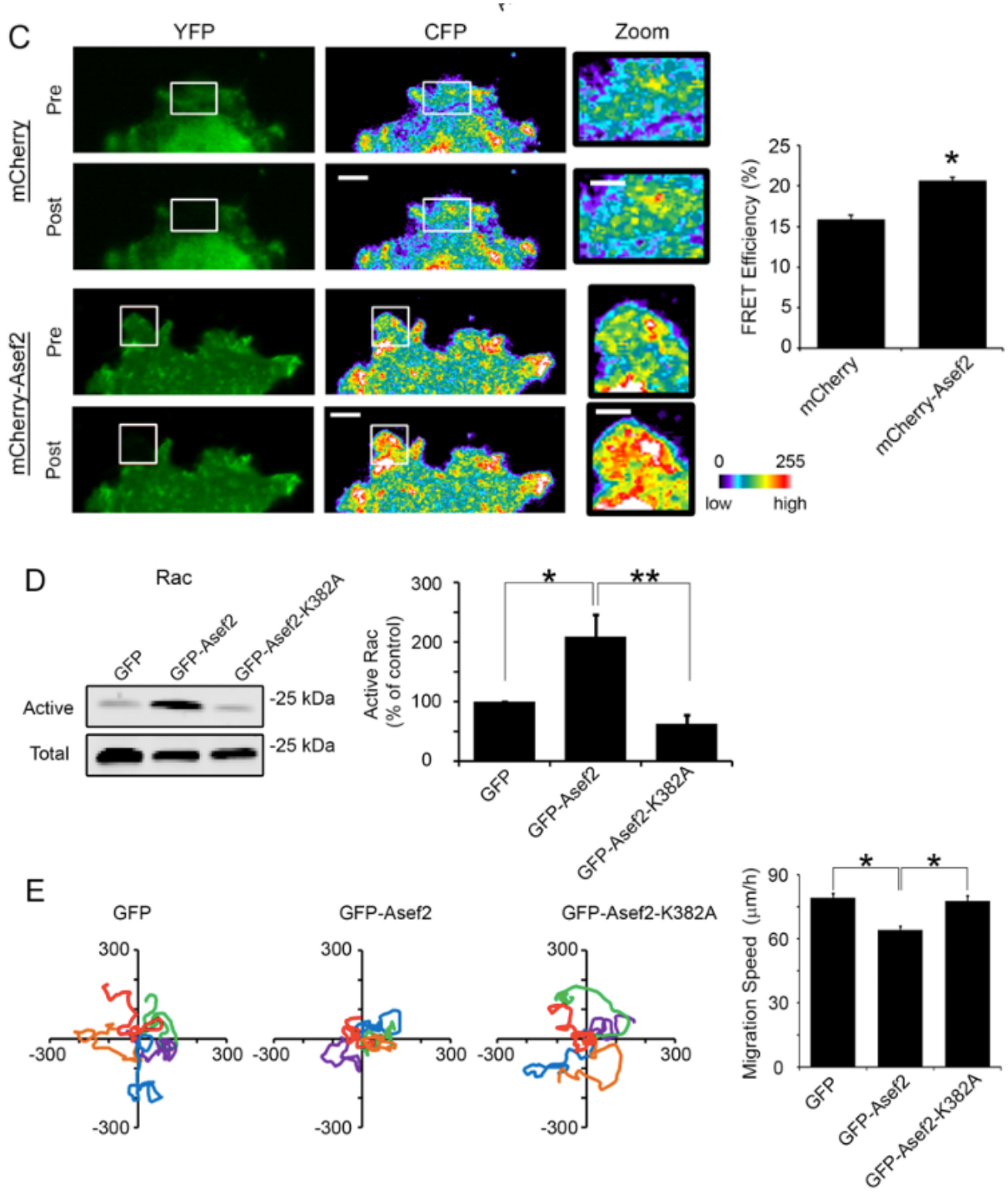

Figure 12 Cont'd. Asef2 enhances activation of Rac and regulates migration through its GEF activity. (C) HT1080 cells co-expressing the Raichu-Rac FRET probe and either mCherry or mCherry–Asef2 were subjected to acceptor photo- bleaching FRET analysis. Left, images of YFP and CFP before (Pre) and after (Post) photo-bleaching YFP with a 514 nm laser. The white square boxes denote the ROI where YFP was bleached. High-magnification images of the CFP

intensity in the bleached ROIs (Zoom). CFP intensities are depicted on a pseudo-color scale in which lower intensity values are displayed in cool colors, whereas higher intensity values are displayed in warm colors. Scale bars: 5 μm (CFP panels), 2 μm ('Zoom' panels). Right, quantification of the average FRET efficiency of the Raichu-Rac FRET probe in mCherry and mCherry–Asef2 expressing cells. Error bars represent s.e.m. for 93–107 cells from three separate experiments. *P<0.0001. (D) Left, the active form of Rac was pulled down from lysates of wild-type HT1080 cells that were co-transfected with FLAG–Rac and either GFP, GFP–Asef2, or GFP–Asef2 in which lysine 382 in the DH domain was mutated to alanine (GFP– Asef2-K382A). Right, quantification of the amount of active Rac from blots from four independent experiments. Error bars represent the s.e.m. *P<0.03, **P<0.01. (E) HT1080 cells were transfected with GFP, GFP–Asef2 or GFP–Asef2-K382A and used in migration assays. Left, Rose plots of migration tracks of transfected cells. Right, quantification of the migration speed of cells transfected with GFP, GFP–Asef2 or GFP–Asef2-K382A. Error bars represent the s.e.m. for at least 70 cells from six independent experiments. *P<0.0001.

Asef2 promotes larger adhesions that turn over slowly on type I collagen

Because adhesion assembly and disassembly (adhesion turnover) at the leading edge of cells is an important process that underlies migration, we hypothesized that the slower migration promoted by Asef2 resulted from impaired adhesion turnover. We began to test this hypothesis by immunostaining GFP and GFP–Asef2 stably expressing HT1080 cells for paxillin, a well-known adhesion marker. In GFP–Asef2 cells, the adhesions appeared larger than those observed in GFP cells, suggesting that adhesion turnover was slower in these cells (Fig. 13A). Indeed, when adhesion turnover was quantified using an assay that we previously developed (Webb et al., 2004), the t1/2 values for adhesion assembly and disassembly were increased by ~2-fold and 1.5-fold, respectively, in GFP–Asef2 cells compared with GFP control cells (Fig. 13B). These results indicate that adhesions are assembling and disassembling significantly more slowly in GFP–Asef2 cells.

Because binding of active (high-affinity state) integrins to the ECM initiates the assembly of adhesions (Hynes, 1992; Welf et al., 2012). Asef2 could affect adhesion turnover by altering the amount of active integrins at the cell membrane. To examine cell surface levels of active β1 integrin, a major integrin that binds to type I collagen, GFP and GFP–Asef2 cells were incubated with HUTS-4 antibody and subjected to flow cytometry. HUTS-4 antibody specifically binds to the activated conformation of β1 integrin (Luque et al., 1996). The amount of cell-surface active β1 integrin was increased ~3-fold in GFP–Asef2 cells compared with GFP controls, whereas the total level of β1 integrin was not significantly different (Fig. 13C). Moreover, as determined by total internal reflection microscopy (TIRF), the level of active β1 integrin in adhesions was significantly higher in GFP–Asef2 cells than in GFP cells, whereas the amount of total β1 integrin was comparable in these cells (Fig. 13D). Interestingly, the Asef2- promoted increase in

the level of active β1 integrin in adhesions was diminished by treatment of GFP–Asef2 cells with the Rac specific inhibitor NSC23766 (Fig. 14). NSC23766 specifically blocks Rac binding and activation by its GEFs (Gao et al., 2004). Furthermore, the amount of active β1 integrin in adhesions was increased in GFP–Asef2 stably expressing MDA-MB-231 cells compared to GFP control cells (Fig. 15). In addition, knockdown of endogenous Asef2 in HT1080 cells with Asef2 shRNA 1 decreased the level of active β1 integrin in adhesions compared to cells transfected with NT shRNA (Fig. 13E). Thus, our data suggest that activation of Rac by Asef2 slows the turnover of adhesions by increasing the level of active β1 integrin in these structures.

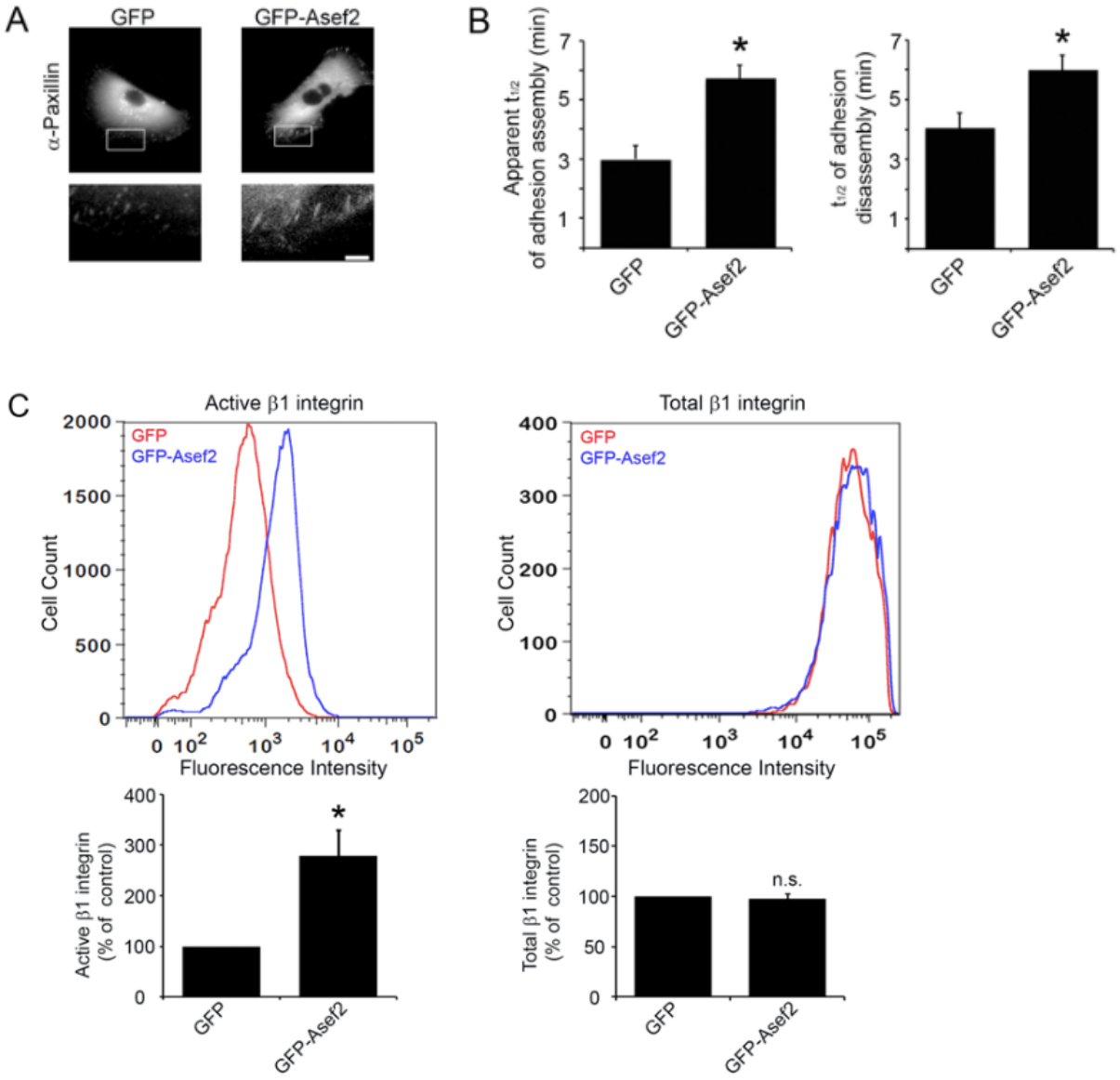

Figure 13. Asef2 increases levels of active β1 integrin in adhesions and slows adhesion turnover. (A) Upper, GFP and GFP–Asef2 cells were immunostained for paxillin, a well-characterized adhesion marker. Lower, higher magnification images of the boxed regions in the upper panels. Scale bar: 5 μm. (B) GFP and GFP–Asef2 cells were transfected with mCherry–paxillin and used in adhesion turnover assays. Quantification of the apparent $t_{1/2}$ for adhesion assembly and the $t_{1/2}$ for adhesion disassembly. Error bars represent the s.e.m. for 20–25 adhesions from four or five cells from three separate experiments. *P<0.0001. (C) Left, GFP and GFP– Asef2 cells were incubated with HUTS-4 antibody, which recognizes active β1 integrin, and fluorescently conjugated secondary antibody. HUTS-4 antibody binding to active β1 integrin on cells was measured using flow cytometry, and histograms are shown. Right, the total level of β1 integrin on GFP and GFP–Asef2 cells were assessed using AIIB2 antibody and flow cytometry. Histograms are shown. Lower, quantification of HUTS-4 (active β1 integrin) and AIIB2 (total β1 integrin) binding to GFP and GFP–Asef2 cells. Error bars represent s.e.m. from three separate experiments. *P,0.0001.

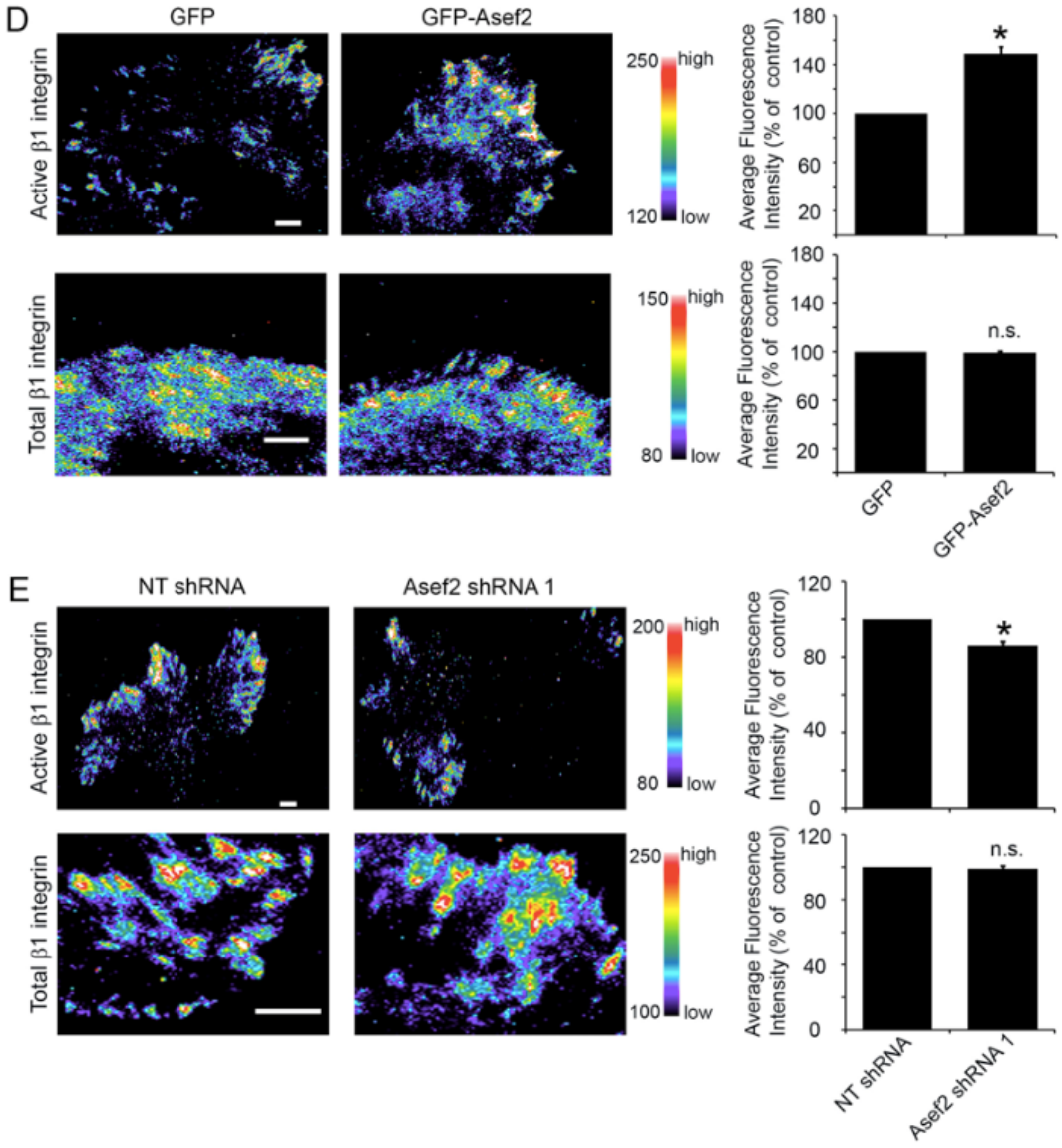

Figure 13 Cont'd. Asef2 increases levels of active β1 integrin in adhesions and slows adhesion turnover. (D) Left, GFP and GFP–Asef2 cells were immunostained for active or total β1 integrin and subjected to TIRF microscopy. Scale bar: 5 μm. Right, quantification of the amount of active β1 integrin (upper panel) and total β1 integrin (lower panel) in adhesions from GFP and GFP–Asef2 cells. Error bars represent s.e.m. from at least 60 adhesions from three separate experiments. *P<0.002. (E) Left, wild-type HT1080 cells were transfected with NT shRNA or Asef2 shRNA 1. After 3 days, cells were immunostained for active or total β1 integrin and subjected to TIRF microscopy. Scale bar: 5 μm. Right, quantification of the amount of active and total β1 integrin in adhesions from NT shRNA and Asef2 shRNA 1 transfected cells. Error bars represent s.e.m. from at least 59 adhesions from three separate experiments. *P<0.0003. For panels D and E, active and total β1 integrin images are shown in pseudo-color coding. For panels C–E, n.s. denotes no statistically significant difference.

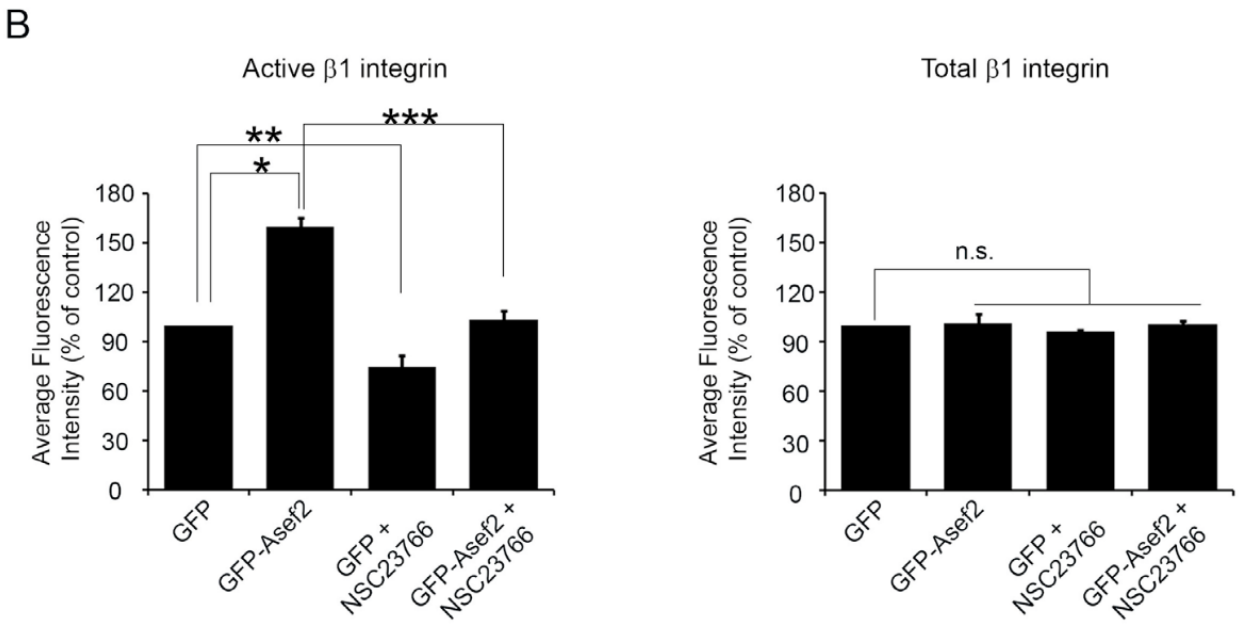

Figure 14. Asef2 regulates the levels of β1 integrin through Rac. (B) GFP and GFP-Asef2 stable HT1080 cells were treated with the Rac inhibitor NSC23766 or DMSO, immunostained for active or total β1 integrin, and imaged with TIRF microscopy. Quantification of the amount of active (left panel) and total (right panel) β1 integrin in adhesions in GFP and GFP-Asef2 cells is shown. Error bars represent S.E.M. from at least 56 adhesions from three separate experiments (*p = 0.0004; **p < 0.03; ***p < 0.003). "n.s." denotes no statistically significant difference.

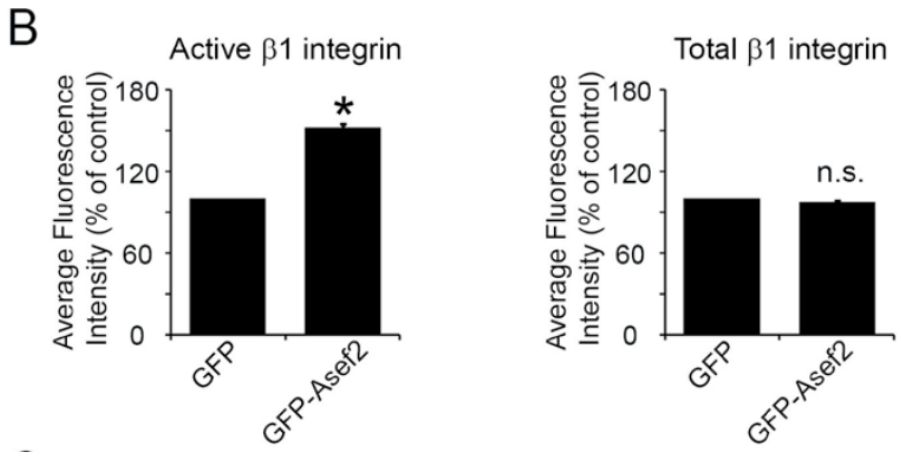

Figure 15. Asef2 increases the amount of active β1 integrin in MDA-MB-231 cells to regulate migration and contractility. (B) GFP and GFP-Asef2 stable MDA-MB-231 cells, plated on type I collagen, were immunostained for active or total β1 integrin and were imaged with TIRF microscopy. Quantification of the amount of active (left panel) and total (right panel) β1 integrin in adhesions in GFP and GFP-Asef2 cells is shown. Error bars represent S.E.M. from at least 83 adhesions from three independent experiments (*$p < 0.0001$).

Traction force and cell contractility are enhanced by Asef2

Because a major role for adhesions is to transmit traction forces to the ECM (Balaban et al., 2001; Beningo et al., 2001), we hypothesized that Asef2 functions by increasing the traction force in cells. Using traction force microscopy, we created vector maps of the traction stresses (force per unit area) that were generated by GFP and GFP–Asef2 stably expressing HT1080 cells. The vector maps showed that the traction stresses were significantly higher in GFP–Asef2 cells compared to GFP controls (Fig. 16A). Relatively high traction stresses were observed throughout GFP– Asef2 cells, but the largest stresses were seen at the cell edge. Quantification revealed that the average traction stress was ~4-fold greater in GFP–Asef2 cells compared with GFP cells. These results demonstrate that Asef2 dramatically enhances traction stresses in cells.

Previous work has shown that actomyosin contractility promotes the maturation of adhesions (Choi et al., 2008; Chrzanowska-Wodnicka and Burridge, 1996). Given that Asef2 induces larger adhesions as well as slowing adhesion turnover, it could function in regulating contractility. To examine the effect of Asef2 on contractility, we used a gel contraction assay (Tovell et al., 2011; Vernon and Gooden, 2002). In this assay, GFP and GFP–Asef2 cells were incubated in type I collagen gels for 14 hours to allow for contraction of the gels by cells. Contractility was assessed by measuring the diameter of gels at the beginning and at the end of the incubation period. At the end of the assay, the diameters of gels that contained GFP–Asef2 cells were significantly reduced compared to those containing GFP cells (Fig. 16B), indicating greater gel contraction by Asef2 cells. When contraction was quantified by expressing the gel diameters at the end of the assay (contracted gels) as a percentage of the original gel diameters, gels containing GFP–Asef2 stable HT1080 cells were decreased by ~40% compared to those containing GFP cells (Fig. 16B). Similar results were observed with GFP–Asef2 stably expressing MDA-MB-231 cells (Fig. 17). In addition, knockdown of endogenous Asef2 in

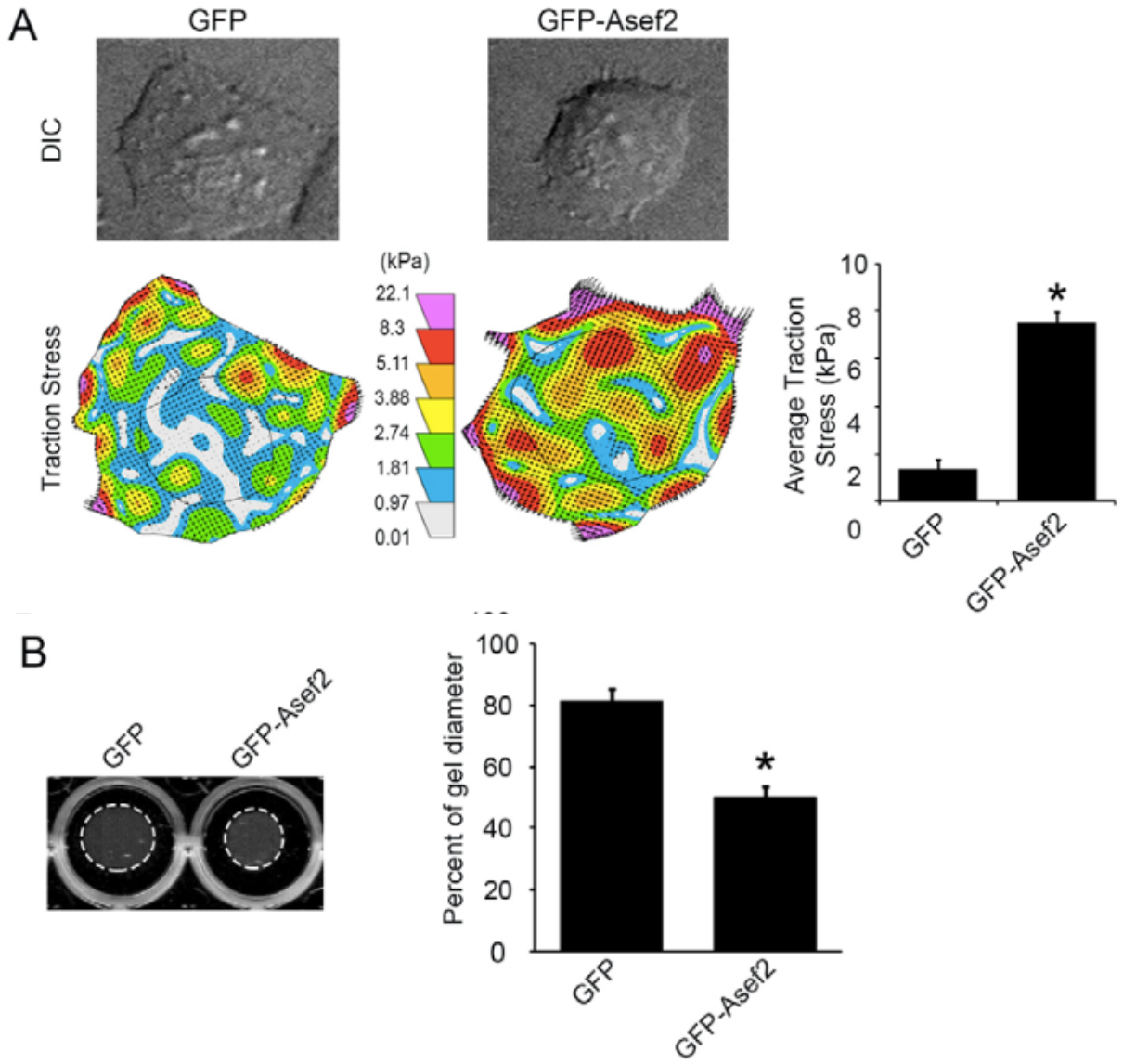

Figure 16. Traction force and cell contractility are significantly increased by Asef2. (A) GFP and GFP–Asef2 stably expressing HT1080 cells were cultured in polyacrylamide (PAA) gels, embedded with FluoSpheresH fluorescent beads, for traction stress measurements. Upper, DIC images of GFP and GFP–Asef2 cells in PAA gels. Lower, color-coded vector maps show traction stresses produced by these cells. In the vector maps, the length and orientation of arrows indicate the magnitude and direction of traction stresses. Right, quantification of average traction stresses generated by GFP and GFP–Asef2 cells. Error bars represent the s.e.m. for 25 cells from at least three individual experiments. *P<0.003. (B) GFP and GFP–Asef2 stable HT1080 cells were embedded in type I collagen gels, and gels were incubated for 14 hours at 37°C to allow for contraction. Left, images of contracted gels with GFP and GFP–Asef2 cells. The gel circumferences are outlined with dotted white lines. Right, at the end of the contraction assay, the diameter of the gels was measured and expressed as a percentage of the original gel diameter (before contraction). Error bars represent s.e.m. from three independent experiments. *P<0.0002.

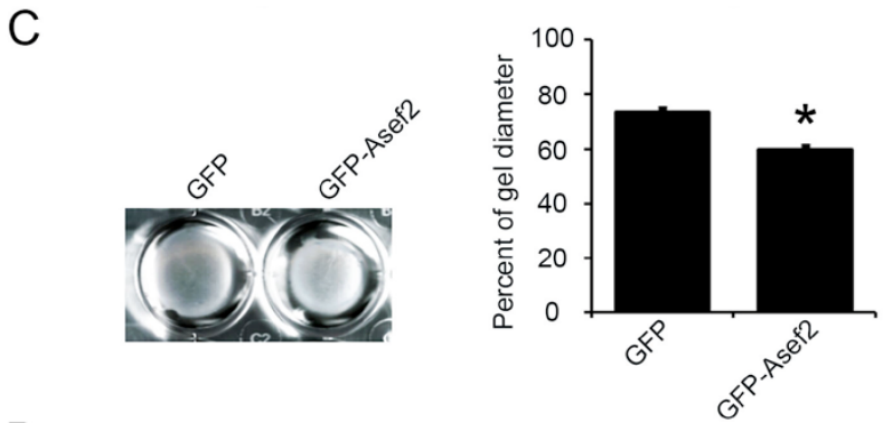

Figure 17. Asef2 leads to increased cell contractility in MDA-MB-231 cells. (C) GFP and GFP-Asef2 stable MDA-MB-231 cells were used in type I collagen gel contraction assays. Left, images of contracted gels with GFP and GFP-Asef2 cells are shown. Right, quantification of gel contraction for GFP and GFP-Asef2 is shown. Error bars represent S.E.M. from three independent experiments (*$p < 0.0009$).

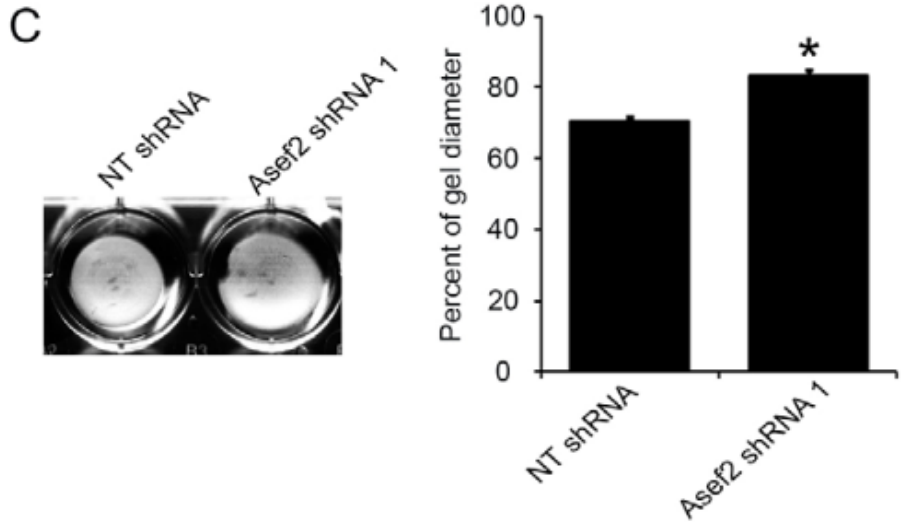

Figure 18. Asef2 knockdown inhibits cell contractility. (C) Wild-type HT1080 cells were transfected with NT shRNA or Asef2 shRNA 1 and used in type I collagen gel contraction assays 3 days later. Left, images of contracted gels with NT shRNA and Asef2 shRNA 1 transfected cells. Right, quantification of gel contraction for cells transfected NT shRNA or Asef2 shRNA 1. Error bars represent s.e.m. from three independent experiments. *$P<0.0005$.

HT1080 cells led to an increase in gel diameters compared to those observed with NT shRNA transfected cells, indicating that Asef2 knockdown reduced gel contraction (Fig. 18). Taken together, these results demonstrate that Asef2 increases contractility in cells.

Asef2 regulates migration by increasing MyoII activity

As our results show that Asef2 increases contractility, and MyoII activity is known to modulate contractility in cells (Adelstein and Conti, 1975; Scholey et al., 1980), we next examined the role of MyoII in mediating Asef2 function. MyoII activity is regulated by phosphorylation of S19 in its RLCs, and thus, the phosphorylation state of this residue can be used to assess MyoII activity (Ikebe, 1989; Matsumura et al., 1998). We determined the level of active MyoII in GFP and GFP–Asef2 stably expressing HT1080 cells by immunostaining with antibody against MyoII phosphorylated at S19 (phospho-S19 MyoII) and imaging with fluorescence microscopy. As shown in Fig. 19A, the amount of phospho-S19 MyoII (p-S19 MyoII; active MyoII) was greater in GFP–Asef2 stably expressing HT1080 cells than in GFP cells. When the fluorescence intensity of active MyoII was quantified for individual cells, the amount of active MyoII was increased ~1.5-fold in GFP–Asef2 cells compared to that observed in GFP cells, whereas the level of total MyoII was not significantly different in these cells (Fig. 19A). Moreover, the amount of active MyoII was increased in GFP–Asef2 stable MDA-MB-231 cells compared with GFP controls (Fig. 20). Conversely, knockdown of endogenous Asef2 in HT1080 cells led to a decrease in the level of active MyoII (Fig. 19B). Thus, these results indicate that Asef2 increases the level of active MyoII in cells.

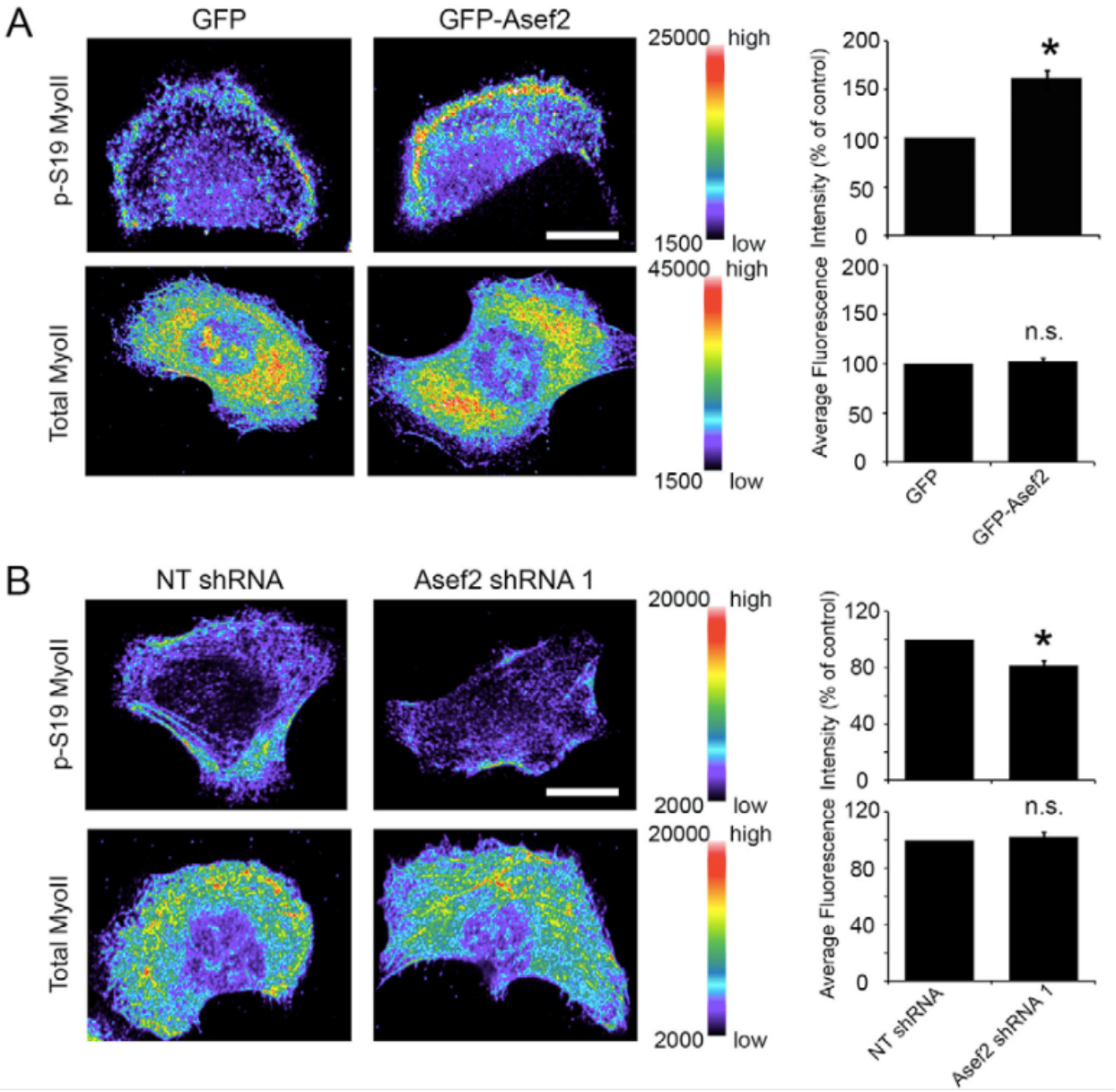

Figure 19. Asef2 increases phosphorylation of MyoII at S19. (A) Left, GFP and GFP–Asef2 stably expressing HT1080 cells were immunostained for MyoII phosphorylated at S19 (p-S19 MyoII) or total MyoII. Scale bar: 15 μm. Right, quantification of the amount of p-S19 MyoII (upper panel) and total MyoII (lower panel) in GFP and GFP-Asef2 cells. Error bars represent the s.e.m. for at least 117 cells from at least six individual experiments. *P<0.002. (B) Left, wild-type HT1080 cells were transfected with NT shRNA or Asef2 shRNA 1. After 3 days, cells were immunostained for S19 phosphorylated MyoII (p-S19 MyoII) or total MyoII. Scale bar: 15 μm. Right, quantification of the amount of p-S19 MyoII and total MyoII in NT shRNA and Asef2 shRNA 1 transfected cells. Error bars represent the s.e.m. for at least 58 cells from at least four individual experiments. *P<0.004.

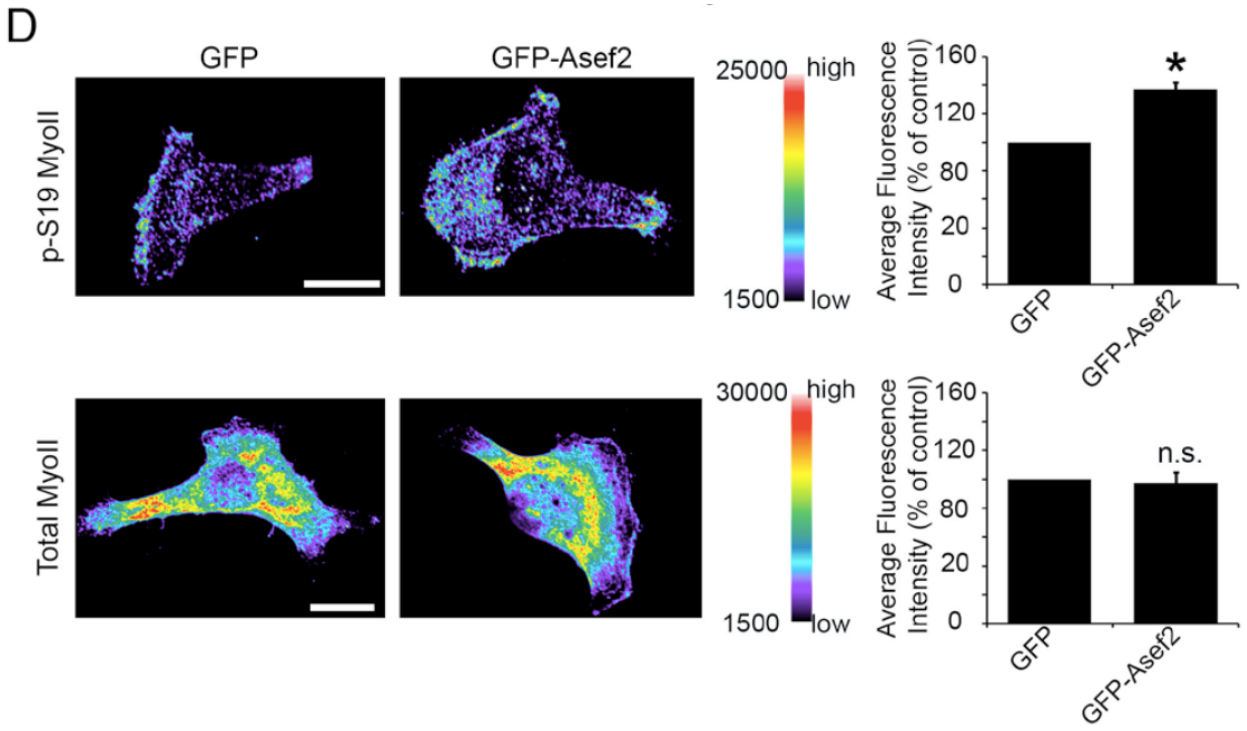

Figure 20. Asef2 increases the levels of active MyoII in MDA-MB-231 cells to regulate contractility. (D) Left, GFP and GFP-Asef2 stable MDA-MB-231 cells were plated on type I collagen-coated coverslips and were immunostained for phospho-S19 MyoII (p-S19 MyoII) or total MyoII. p-S19 MyoII and total MyoII images are shown in pseudo-color coding. Scale bar: 15 μm. Right, quantification of the amount of p-S19 MyoII and total MyoII in GFP and GFP-Asef2 cells is shown. Error bars represent S.E.M. for at least 30 cells from three separate experiments (*p = 0.0002). For panels B and D, "n.s." denotes no statistically significant difference.

To further demonstrate that Asef2 modulates MyoII activity in cells, we performed In-Cell western assays. In this assay, GFP and GFP–Asef2 stably expressing HT1080 cells were allowed to adhere to 96-well culture plates coated with type I collagen and subsequently immunostained for phospho-S19 MyoII or total MyoII followed by fluorescently-conjugated secondary antibody. The background-subtracted integrated fluorescence intensity in each well was then quantified. The amount of active MyoII was ~1.7-fold higher in GFP–Asef2 cells compared to GFP controls, whereas the level of total MyoII was not significantly different in these cells (Fig. 21). Collectively, these results show that Asef2 significantly enhances the amount of active MyoII in cells plated on type I collagen and point to Asef2 as an important regulator of MyoII activity.

Our data also raised the question as to whether Asef2 regulates cell migration on type I collagen through its ability to modulate MyoII activity. To address this question, we inhibited MyoII with blebbistatin, which impairs the ATPase activity of MyoII (Kovacs et al., 2004; Straight et al., 2003), and assessed migration. Treatment of GFP control cells with blebbistatin led to an increase in migration speed (Fig. 22A, B), which is consistent with previous studies (Even-Ram et al., 2007; Liu et al., 2010; Niggli et al., 2006). At the end of the migration assay, we performed washout experiments to show that the effects on migration were due to blebbistatin. In these experiments, blebbistatin-containing medium was removed, cells were washed, fresh medium without blebbistatin was added, and cells were used in migration assays. The migration speed of GFP cells after washout was decreased compared to that observed in GFP cells treated with blebbistatin (Fig. 22A, B). Indeed, the migration speed of GFP cells following washout was similar to that seen in vehicle-treated control cells (Fig. 22A, B). Consistent with our previous results, the migration speed of GFP–Asef2 cells was decreased

when compared to GFP cells. Treatment of GFP–Asef2 cells with blebbistatin resulted in a significant increase in migration speed, and blebbistatin washout negated the increase in migration (Fig. 22A,B), indicating that MyoII activity is crucial for the effect of Asef2 on migration. Collectively, our data suggest that Asef2 regulates migration by modulating MyoII activity and function.

We had previously shown that Asef2 regulates cell migration on fibronectin by a mechanism that is dependent on Rac and the serine/threonine kinase Akt (Bristow et al., 2009). Here, we demonstrate that Asef2 modulates migration on type I collagen by increasing Rac and MyoII activity. This raises the question as to whether Akt also contributes to the regulation of Asef2- mediated migration on type I collagen. To address this question, we plated GFP and GFP–Asef2 stably expressing HT1080 cells on type I collagen and immunostained with antibody against Akt phosphorylated on threonine 308 (phospho-T308 Akt). T308 is one of the key residues that is phosphorylated when Akt is activated; therefore, phospho-T308 Akt antibody can be utilized to detect active Akt (Alessi et al., 1996). Interestingly, the amount of active Akt was similar in GFP and GFP–Asef2 cells plated on type I collagen (Fig. 23C), suggesting that the Asef2-Rac signaling mechanisms are different for cells plated on fibronectin and type I collagen. To further investigate Asef2-Rac signaling on these substrates, we plated GFP and GFP-Asef2 stably expressing HT1080 cells on fibronectin and immunostained for active MyoII with phospho-S19 MyoII antibody. The amount of active MyoII was not significantly different in GFP and GFP-Asef2 cells plated on fibronectin (Fig. 23D). Therefore, our results suggest that Asef2-Rac signaling regulates migration on fibronectin and type I collagen by distinct molecular mechanisms.

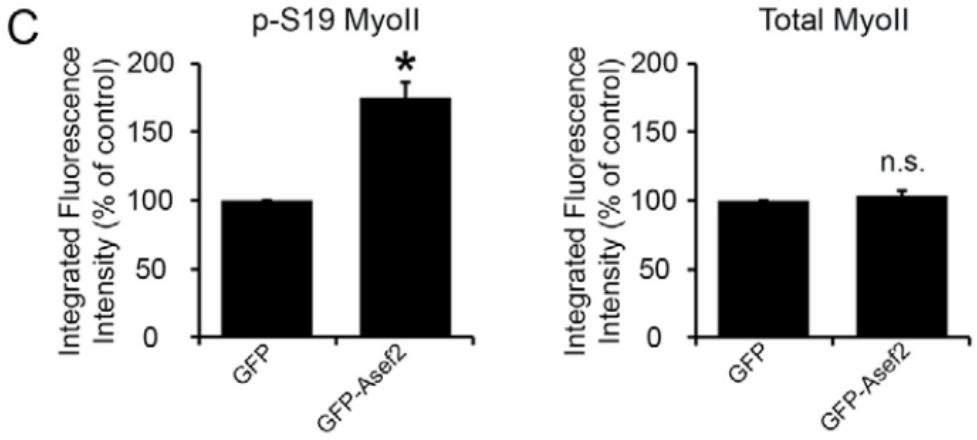

Figure 21. Asef2 increases phosphorylation of MyoII at S19. (C) GFP and GFP–Asef2 cells were subjected to In-Cell western analysis using antibodies against S19 phosphorylated MyoII (p-S19 MyoII) or total MyoII. Left, quantification of the amount of p-S19 MyoII in GFP and GFP-Asef2 cells. Error bars represent s.e.m. from four separate experiments. *P<0.001. Right, quantification of the amount of total MyoII in GFP and GFP–Asef2 cells. Error bars represent the s.e.m. from four separate experiments. n.s. denotes no statistically significant difference.

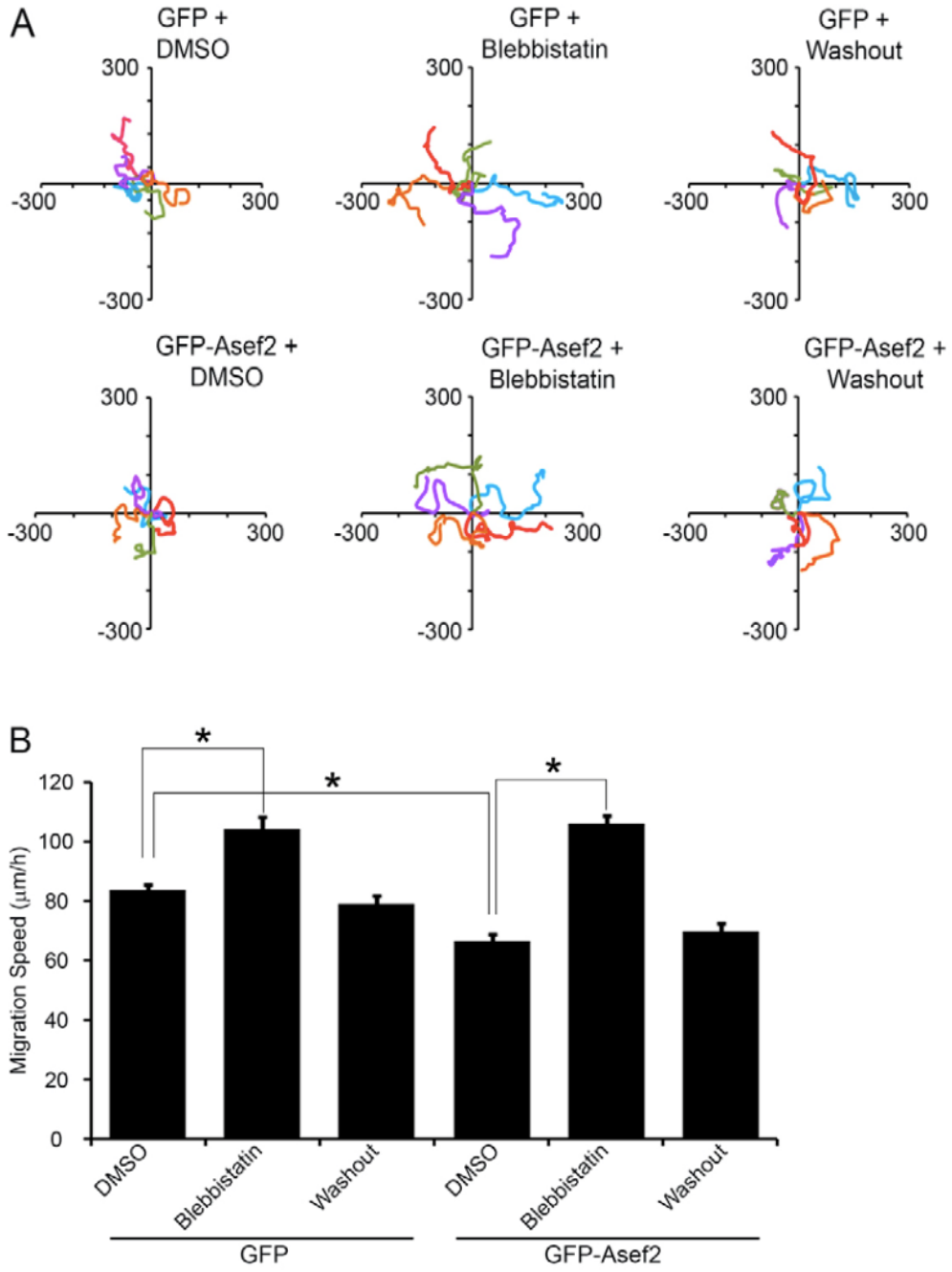

Figure 22. Inhibition of MyoII with blebbistatin enhances basal migration and abolishes the Asef2-mediated decrease in migration on type I collagen. (A) GFP and GFP–Asef2 stably expressing HT1080 cells were pre-treated with 20 μM blebbistatin or vehicle (DMSO) for 1 hour at 37°C and then used in migration assays. After 6 hours, blebbistatin was replaced with fresh imaging medium (Washout), and cells were imaged for an additional 6 hours. Rose plots of the migration tracks for five cells for each treatment are shown. (B) Quantification of the migration speed for GFP and GFP–Asef2 cells with the indicated treatments. Error bars represent s.e.m. for at least 30 cells from three independent experiments. *P<0.0001.

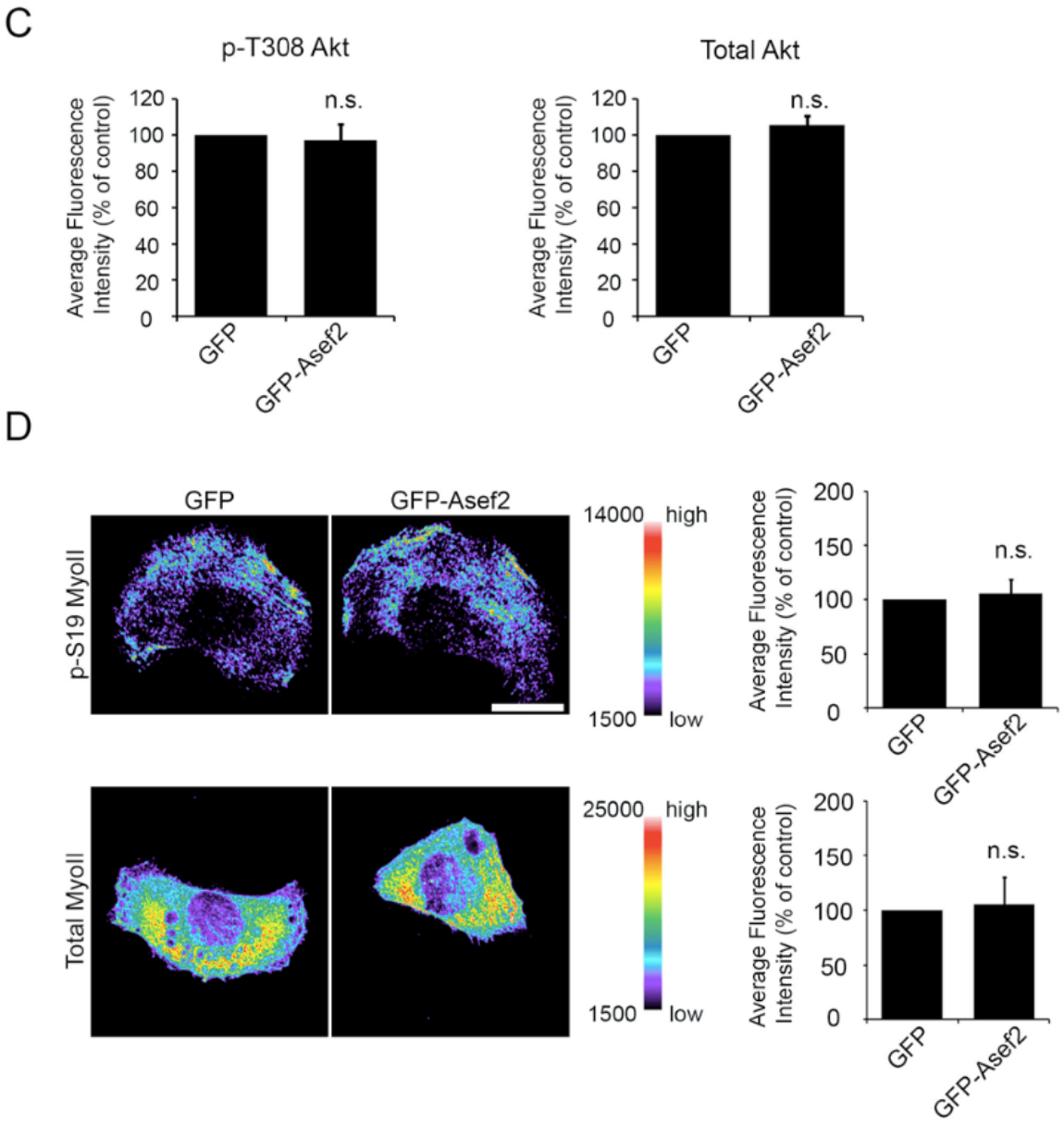

Figure 23. Asef2 regulates migration on fibronectin and type I collagen through distinct molecular mechanisms. (C) GFP and GFP-Asef2 stable HT1080 cells were plated on type I collagen- coated glass coverslips and immunostained for Akt phosphorylated at T308 (p-T308 Akt) or total Akt. Right, quantification of the amount of p-T308 Akt (left panel) and total Akt (right panel) in GFP and GFP-Asef2 cells is shown. Error bars represent S.E.M. for at least 30 cells from at least three separate experiments. (D) Left, GFP and GFP-Asef2 stable HT1080 cells were plated on fibronectin- coated glass coverslips and immunostained for MyoII phosphorylated at S19 (p-S19 MyoII) or total MyoII. p-S19 MyoII and total MyoII images are shown in pseudo-color coding. Scale bar: 15 μm. Right, quantification of the amount of p-S19 MyoII (upper panel) and total MyoII (lower panel) in GFP and GFP-Asef2 cells is shown. Error bars represent S.E.M. for at least 55 cells from three independent experiments. For panels C and D, "n.s." denotes no statistically significant difference.

Activation of Rac by Asef2 regulates MyoII contractility

Because Asef2 increased the amount of active Rac and modulated MyoII activity, we hypothesized that Rac regulates MyoII contractility. To begin to test this hypothesis, we used two shRNA constructs to knockdown endogenous expression of Rac and then assessed MyoII activity by immunostaining with phospho-S19 MyoII antibody. These shRNAs have been previously shown to knockdown endogenous Rac expression in HT1080 cells by ~75% (Bristow et al., 2009). Transfection of GFP stably expressing HT1080 cells with the Rac shRNAs led to an ~2-fold reduction in the amount of active MyoII compared with that observed in cells transfected with pSUPER or NT shRNA (Fig. 24A), indicating that inhibition of basal Rac expression significantly decreased the level of active MyoII. In GFP-Asef2 stably expressing HT1080 cells, the level of active MyoII was significantly increased compared with control cells, and expression of the Rac shRNAs dramatically reduced the amount of active MyoII in these cells (Fig. 24A). Indeed, the level of active MyoII in GFP-Asef2 cells transfected with the Rac shRNAs was similar to that observed in GFP cells transfected with these knockdown constructs (Fig. 24A), indicating that Rac knockdown abrogated the Asef2-mediated effect on MyoII activity. Similar results were obtained when GFP and GFP-Asef2 cells were treated with the Rac inhibitor NSC23766 (supplementary material Fig. 25A). Neither the Rac shRNAs nor NSC23766 affected the level of total MyoII in cells (Fig. 24A; supplementary material Fig. 25A). Taken together, these results suggest that Rac activity regulates the amount of active MyoII in cells, and Asef2 regulates MyoII through Rac.

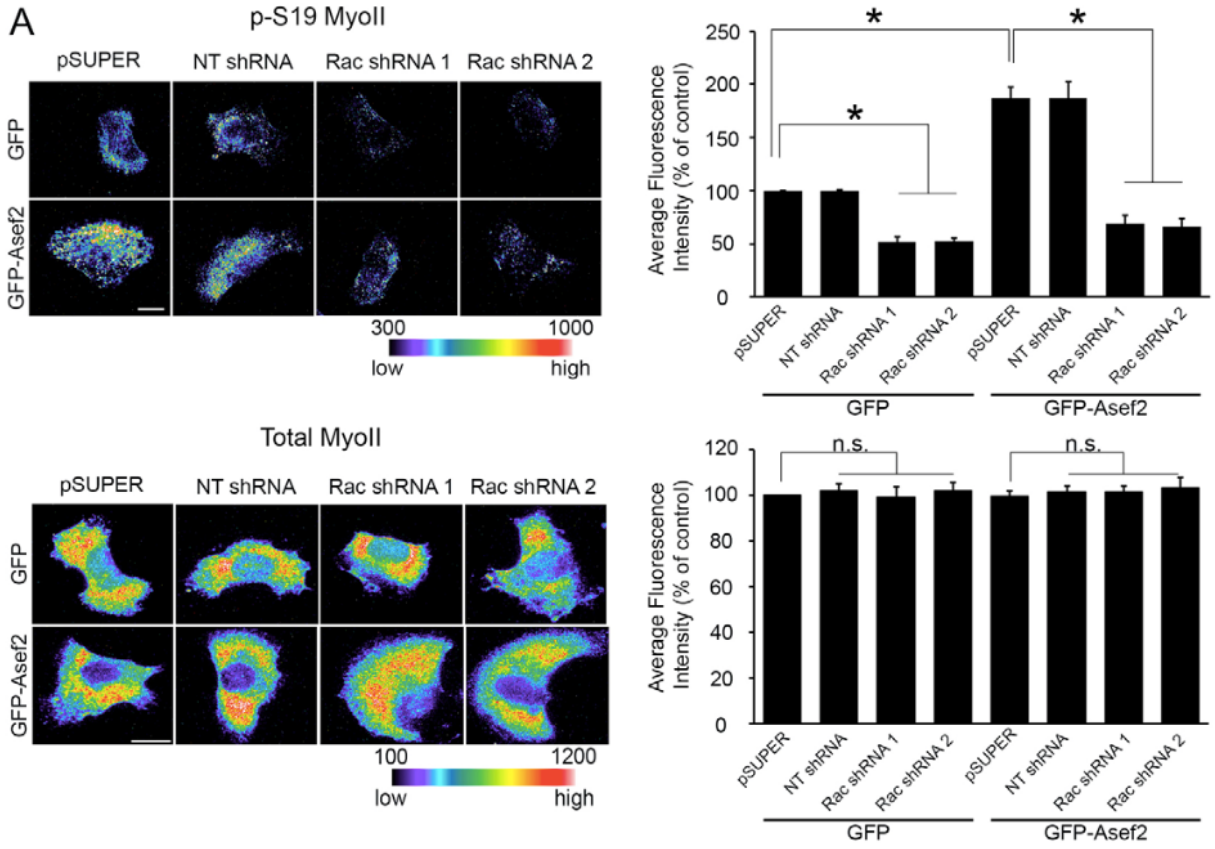

Figure 24. Activation of Rac by Asef2 stimulates active levels of MyoII. (A) Left, GFP and GFP–Asef2 stably expressing HT1080 cells were co- transfected with mCherry and either empty pSUPER vector, a NT shRNA or Rac shRNAs. After 3 days, cells were immunostained with antibodies that recognize S19 phosphorylated MyoII (p-S19 MyoII; upper panels) or total MyoII (lower panels). Scale bar: 15 μm. Right, quantification of the level of p-S19 MyoII (upper panel) and total MyoII (lower panel) in GFP and GFP–Asef2 cells. Error bars represent s.e.m. for 30 cells from three individual experiments. *P<0.002. n.s. denotes no statistically significant difference.

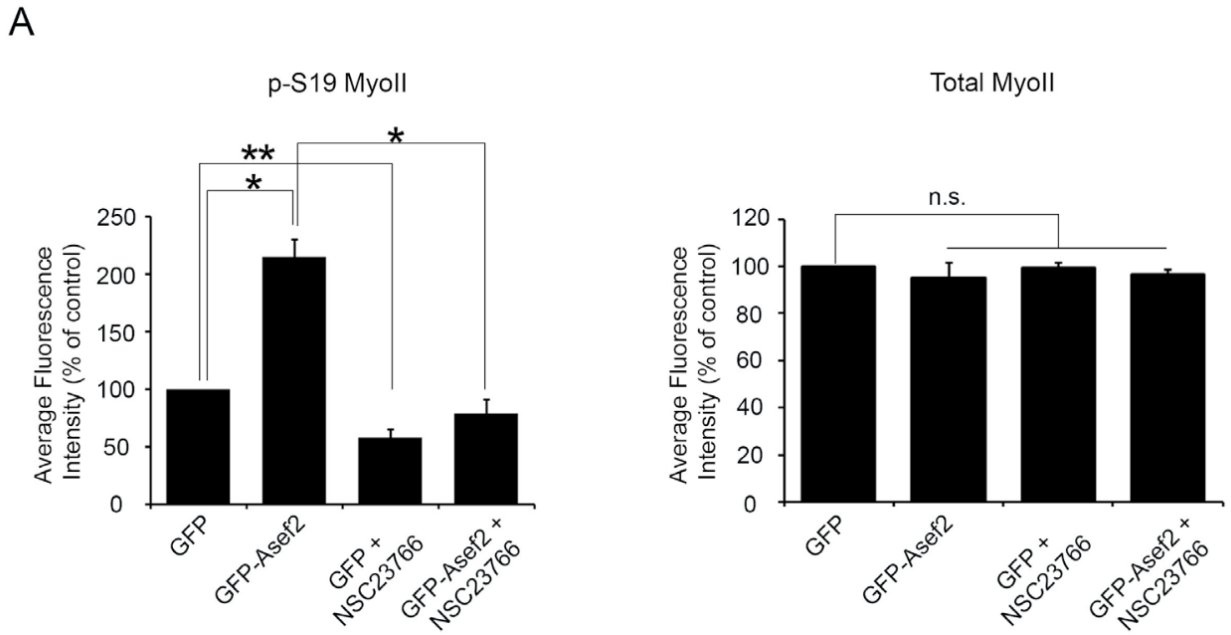

Figure 25. Asef2 regulates the levels of active MyoII through Rac. (A) GFP and GFP-Asef2 stable HT1080 cells were treated with the Rac inhibitor NSC23766 or DMSO and were immunostained with antibodies that recognize S19 phosphorylated MyoII (p-S19 MyoII) or total MyoII. Quantification of the amount of p-S19 MyoII (left panel) and total MyoII (right panel) in GFP and GFP-Asef2 cells is shown. Error bars represent S.E.M. for 40 cells from three individual experiments (*$p < 0.002$; **$p < 0.006$).

Next, we examined the effect of Rac activity on Asef2- mediated contractility by using GFP and GFP–Asef2 cells that were treated with NSC23766 in gel contraction assays. In GFP-Asef2 cells, the gel diameters were significantly reduced compared to those observed in GFP cells (Fig. 26B), demonstrating that Asef2 enhances contractility. Treatment of GFP-Asef2 cells with NSC23766 diminished the increased contractility (Fig. 26B), suggesting that Rac activity induced by Asef2 promotes the enhanced contractility observed with these cells. To further show that Rac modulated contractility, we knocked down Rac in GFP–Asef2 cells using the two Rac shRNAs. Consistent with our previous results, GFP-Asef2 cells transfected with empty pSUPER vector or a NT shRNA showed enhanced contractility, with their gel diameters contracted to less than half of their original diameters (Fig. 26C). Transfection of GFP-Asef2 cells with the Rac shRNAs led to significantly less gel contraction compared to that seen with cells transfected with pSUPER or NT shRNA (Fig. 26C). Collectively, our results show that Asef2 increases gel contraction through Rac, thus, highlighting an important new role for Rac in regulating contractility within cells.

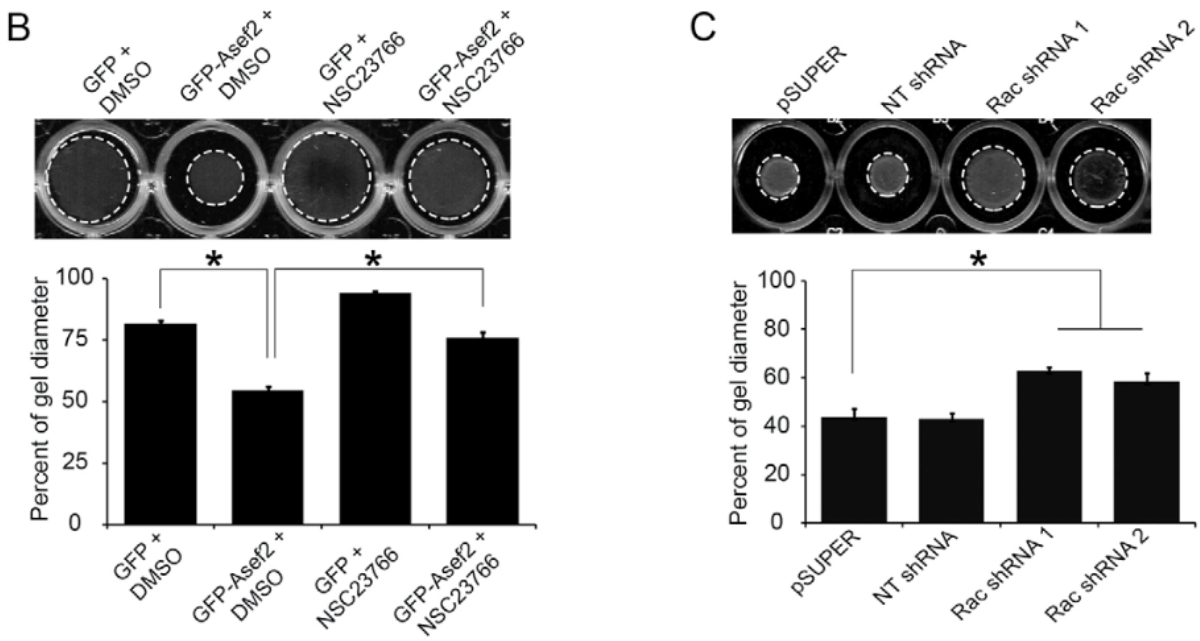

Figure 26. Activation of Rac by Asef2 promotes cell contractility. (B) GFP and GFP-Asef2 stably expressing HT1080 cells were incubated with the Rac inhibitor NSC23766 or DMSO and then used in type I collagen gel contraction assays. Upper, images of contracted gels from GFP and GFP-Asef2 cells treated with DMSO or NSC23766. Lower, quantification of gel contraction for GFP and GFP-Asef2 cells with the indicated treatments. Error bars represent the s.e.m. from three individual experiments. *P<0.0001. (C) GFP-Asef2 stably expressing HT1080 cells were co-transfected with mCherry and empty pSUPER vector, a NT shRNA, or Rac shRNAs and were used in type I collagen gel contraction assays 3 days later. Upper, images of contracted gels from cells transfected with the indicated constructs. Lower, quantification of gel contraction for cells transfected with the indicated constructs. Error bars represent s.e.m. from three individual experiments. *P<0.004. For panels B and C, the gel circumferences are outlined with dotted white lines.

Discussion

Actomyosin contractility plays a crucial role in regulating cell migration through its ability to modulate underlying processes (Clark et al., 2007). Rho is a well-characterized regulator of actomyosin contractility (Wheeler and Ridley, 2004), but the function of other GTPases, such as Rac, in controlling this process is currently poorly understood. Here, we demonstrate that activation of Rac by Asef2 increases MyoII contractility to inhibit cell migration. Knockdown of endogenous Rac using shRNAs or inhibition of Rac activation resulted in a significant decrease in MyoII activity as determined by immunostaining for phosphorylated S19 on MyoII RLCs. In addition, Rac knockdown or inhibition led to a decrease in cell contractility. In contrast, an increase in Rac activity by Asef2 induced MyoII S19 phosphorylation and significantly enhanced cell contractility. Thus, we demonstrate a new function for Rac in regulating actomyosin contractility, which is important for cell migration.

Rac is likely to modulate actomyosin contractility through downstream effectors. One possibility is PAK, which has been shown to phosphorylate RLCs of MyoII on S19 (Chew et al., 1998; Kiosses et al., 1999; Zeng et al., 2000). Moreover, expression of constitutively active Rac led to an increase in S19 phosphorylation of MyoII RLCs, which was mediated, at least in part, through PAK (Brzeska et al., 2004). However, other studies have shown that PAK phosphorylates and inhibits myosin light chain kinase (MLCK), which activates MyoII through phosphorylation of S19 (Goeckeler et al., 2000; Sanders et al., 1999; Wirth et al., 2003). In this case, activation of PAK would decrease MyoII contractility through inhibition of MLCK. Clearly, the effects of PAK on contractility are complex and probably involve the interplay between PAK and other regulators. Therefore, it is entirely possible that other Rac effectors are involved in mediating Rac- induced MyoII-dependent contractility. Identifying the specific Rac

effectors that modulate contractility represents an exciting avenue for future studies.

A known function of MyoII contractility is to promote the maturation of adhesions (Choi et al., 2008; Chrzanowska-Wodnicka and Burridge, 1996). Our results show that Asef2 generates large adhesions that turn over slowly in protrusive regions of cells. Asef2 activation of Rac increases actomyosin contractility, which could serve to induce the maturation of adhesions. As a result, the nascent adhesions that form at the leading edge do not disassemble, but instead continue to grow into large focal adhesions. These large, mature adhesions can impair cell migration given that adhesion turnover at the leading edge is essential for driving rapid migration (Laukaitis et al., 2001; Webb et al., 2004).

In this study, we show that Asef2 activation of Rac inhibits cell migration, when cells are plated on type I collagen, through regulation of actomyosin contractility. We previously demonstrated that Asef2 promotes migration on fibronectin through activation of Rac and the serine/threonine kinase Akt, which subsequently leads to a decrease in Rho activity (Bristow et al., 2009). Interestingly, in both cases, Asef2 modulates cell migration by increasing Rac activity; however, the effects on migration and contractility are quite different. Although the factors that contribute to these differences are currently unknown, it is tempting to speculate that scaffolding proteins are involved. Scaffolding proteins can recruit or bring together various binding partners, through their multiple protein–protein interaction domains, and dictate signaling to various downstream targets (Pawson, 2007). Through the recruitment of Asef2, Rac and particular downstream effectors, scaffolding proteins could provide a mechanism for specificity in Rac signaling. Another Rac GEF, Tiam1, has been shown to associate with different scaffolding proteins to selectively activate distinct downstream Rac effectors (Buchsbaum et al., 2002; Buchsbaum et al., 2003). Scaffolding proteins could also contribute to

the selectivity of the GTPases by recruiting Asef2 and Rac to the complex to enhance Asef2 activation of Rac over other GTPases, such as Cdc42. Interestingly, our results show that Asef2 activates Rac, but not Cdc42, when cells are plated on type I collagen. The interaction of Asef2 and distinct scaffolding proteins could provide a mechanism by which this GEF could selectively activate one GTPase instead of another.

In summary, our study has uncovered an unconventional mechanism by which Rac regulates cell migration. Activation of Rac by Asef2 enhances MyoII contractility, which had been classically thought to be mediated by Rho. Asef2, through Rac, promotes the phosphorylation of S19 in the RLCs of MyoII to increase actomyosin contractility. The increased actomyosin contractility, in turn, might affect underlying migratory processes, such as adhesion dynamics, to modulate cell migration.

CHAPTER III

THE RHO FAMILY GEF ASEF2 REGULATES CELL MIGRATION IN THREE DIMENSIONAL (3D) COLLAGEN MATRICES THROUGH MYOSIN II

Léolène Jean[1], Lijie Yang[2], Devi Majumdar[1], Yandong Gao[2], Mingjian Shi[1], Bryson M. Brewer[2], Deyu Li[2] and Donna J. Webb[1,3*]

[1]Department of Biological Sciences and Vanderbilt Kennedy Center for Research on Human Development, [2] Department of Mechanical Engineering, and [3]Department of Cancer Biology, Vanderbilt University, Nashville, Tennessee 37235
*Author for correspondence (Email: donna.j.webb@vanderbilt.edu)

This article has been published under the same title in *Cell Adhesion and Migration*. 2014 December 17; 8(5): 460-467.

Summary

Cell migration is fundamental to a variety of physiological processes, including tissue development, homeostasis, and regeneration. Migration has been extensively studied with cells on 2-dimensional (2D) substrates, but much less is known about cell migration in 3D environments. Tissues and organs are 3D, which is the native environment of cells in vivo, pointing to a need to understand migration and the mechanisms that regulate it in 3D environments. To investigate cell migration in 3D environments, we developed microfluidic devices that afford a controlled, reproducible platform for generating 3D matrices. Using these devices, we show that the Rho family guanine nucleotide exchange factor (GEF) Asef2 inhibits cell migration in 3D type I collagen (collagen I) matrices. Treatment of cells with the myosin II (MyoII) inhibitor blebbistatin abolished the decrease in migration by Asef2. Moreover, Asef2 enhanced MyoII activity as shown by increased phosphorylation of serine 19 (S19). Furthermore, Asef2 increased activation of Rac, which is a Rho family small GTPase, in 3D collagen I matrices. Inhibition of Rac activity by treatment with the Rac-specific inhibitor NSC23766 abrogated the Asef2-promoted increase in S19 MyoII phosphorylation. Thus, our results indicate that Asef2 regulates cell migration in 3D collagen I matrices through a Rac-MyoII-dependent mechanism.

Introduction

Cell migration is critical to many biological processes, such as tissue morphogenesis, tissue homeostatsis, as well as tissue regeneration and wound repair (Vicente-Manzanares and Horwitz, 2011). Much of our knowledge to date has been obtained from studying cells migrating on 2D substrates. Migration on 2D substrates can be described as a four-step cycle that includes extension of lamellipodia at the leading edge, assembly of cell-extracellular matrix (ECM) adhesions, forward translocation of the cell body, and retraction of the rear of the cell (Lauffenburger and Horwitz, 1996; Vicente-Manzanares et al., 2005). While some aspects of cell migration on 2D substrates are recapitulated in 3D environments, the specific mechanisms and regulation of migration can be dependent on the dimensionality of the matrix (Doyle et al., 2013). Indeed, recent studies with 3D cell culture models, which more closely mimic the microenvironment of tissues, have identified differences in cell morphology and modes of migration when compared with cell migration on 2D substrates (Baker and Chen, 2012; Cukierman et al., 2001; Petrie et al., 2012; Sahai and Marshall, 2003). For example, cells migrating in 3D matrices typically adopt a more elongated morphology and extend dendritic-like protrusions instead of the broad lamellipodia observed with cells migrating on 2D substrates (Cukierman et al., 2001; Petrie et al., 2012). Cells migrating in 3D matrices can interact with the ECM across their entire surfaces, unlike cells on 2D substrates which typically only attach to the ECM at their ventral surfaces. These differences in cell–ECM interfaces as well as ECM topography may be integral to the changes in morphology and modes of cell migration seen in 3D environments.

Although many of the key signaling mechanisms that modulate cell migration on 2D substrates are known, understanding the signaling pathways that regulate 3D migration is only in

its infancy. Available data, however, point to the Rho family of small GTPases, including Rac, Rho, and Cdc42, as having important roles in regulating cell morphology and modes of migration in 3D environments (Petrie et al., 2012; Petrie and Yamada, 2012; Sahai and Marshall, 2003; Sanz-Moreno et al., 2008). For instance, active Rac drives cells toward an elongated, mesenchymal morphology that is important for fibroblast migration in 3D collagen matrices (Petrie et al., 2012; Sanz-Moreno et al., 2008). In contrast, active Rho signaling induces tumor cells to adopt a more rounded morphology that allows for an "amoeboid" mode of migration through 3D matrices (Sahai and Marshall, 2003).

The activity of these Rho GTPases, which is central to their function in migration, is controlled by GEFs and GTPase-activating proteins (GAPs). GEFs facilitate the exchange of GDP for GTP, which serves to activate the GTPases, whereas GAPs stimulate their intrinsic GTPases activity, returning the small GTPases to an inactive state. Active Rho GTPases can interact with downstream effectors to propagate the signal and illicit biological responses. Because Rho GTPase activation is controlled by GEFs, these proteins have been increasingly receiving attention as important regulators of cell migration (Goicoechea et al., 2014). Despite this recent interest, we still have a great deal to learn about the role of GEFs in modulating cell migration, especially their function in regulating cell migration in 3D environments.

Asef2 is a newly identified Rho family GEF that has been shown to regulate migration on 2D substrates (Bristow et al., 2009; Jean et al., 2013; Kawasaki et al., 2007; Sagara et al., 2009). Our previous work demonstrated that Asef2 impairs cell migration on 2D collagen I by increasing activation of Rac, which subsequently enhances MyoII activity (Jean et al., 2013). MyoII is an actin motor protein whose major function in cells is to generate contraction by sliding actin filaments relative to each other. MyoII contractility (activity) is controlled by

phosphorylation within its regulatory light chains (RLC) (Adelstein and Conti, 1975; Scholey et al., 1980). Specifically, phosphorylation of serine 19 (S19) is crucial for activation of the MyoII motor domain, and phosphorylation of threonine 18 further increases MyoII activity (Adelstein and Conti, 1975; Ikebe, 1989). Although MyoII activity is classically thought to be mediated by Rho signaling (Wheeler and Ridley, 2004), our previous data reveal that activation of Rac by Asef2 modulates MyoII activity, and this is an important regulatory mechanism for cell migration on 2D substrates (Jean et al., 2013). However, the role of Asef2 and the contribution of Asef2-Rac-MyoII signaling to cell migration in 3D environments is unknown.

In this study, we demonstrate that Asef2 inhibits HT1080 cell migration in 3D collagen I matrices. Asef2 increases Rac activity, which subsequently enhances S19 MyoII phosphorylation. Inhibition of MyoII activity negates the Asef2-mediated effect on migration, suggesting that Asef2 regulates migration in 3D collagen I matrices via a Rac-MyoII-dependent mechanism.

Materials and Methods

Fabrication and assembly of microfluidic devices

The microfluidic cell culture devices were fabricated using standard soft-lithography techniques with polydimethylsiloxane (PDMS) replica molding (Ellsworth Adhesives, Germantown, WI) as previously described (Gao et al., 2011; Majumdar et al., 2011; McDonald and Whitesides, 2002; Whitesides et al., 2001). To generate the devices, two layers of PDMS with the desired channels and cell chambers were bonded to a microscope coverslip. The bottom PDMS layer consisted of a single large cell culture chamber (5 mm long, 4.6 mm wide, and 500 μm in height) and inlet/outlet media channels that were 500 μm wide and 500 μm in height.

Inlet and outlet holes for three media reservoirs and two gel reservoirs, which were 4 mm and 3.5 mm in diameter, respectively, were punched through the PDMS to facilitate media/gel loading and removal. The large cell culture chamber was connected to the inlet/outlet media channels through vias formed by 1 mm diameter holes that were punched through the bottom PDMS layer. Four separate connecting chambers (100 μm in height) in the top PDMS layer were aligned with the 1 mm holes in the bottom PDMS layer, allowing media to flow through the cell chamber.

The two-layer design with separate inlet/outlet channels for the media and gel mixture allows for direct access of the nutrient media to the cell culture gel without perfusion through the long gel-loading channels filled with polymerized gel. This scheme facilitates a sufficient supply of fresh culture media to the cells in the culture chamber to maintain their long-term health. Note that although media could flow freely in this vertically layered channels, the collagen I gel mixture did not flow backwards through the small vias during loading due to the larger fluidic resistance of the small holes compared with the cell chamber and the loading scheme of using negative pressure to withdraw the gel-cell mixture through the outlet well of the gel-loading channel.

To assemble the device, a pre-polymer PDMS solution was mixed with a curing agent at a ratio of 10:1 and poured over the molds for the bottom layer. After the PDMS polymerized, it was peeled from the mold, and holes were punched through the PDMS for the media wells. The surface of the glass coverslips (No. 1, VWR Vista Vision, Suwanee, GA) as well as the bottom PDMS layer were treated with oxygen plasma and then bonded together. The top PDMS, after oxygen plasma treatment, was subsequently aligned and bonded to the bottom PDMS layer. Pyrex® cloning cylinders (10 mm x 10 mm) (Fisher Scientific, Pittsburg, PA) that served as media reservoirs were glued to the punched holes using the liquid PDMS mixture. The

assembled microfluidic device was placed in an oven at 70°C for 1 h to cure the glue and then sterilized under ultra-violet (UV) light for 1 h.

Reagents and plasmids

Phospho-MLC (S19) polyclonal antibody (clone 3671) and MLC2 polyclonal antibody (clone 3672) were purchased from Cell Signaling (Beverly, MA). FLAG-M2 monoclonal antibody was obtained from Sigma-Aldrich (St. Louis, MO). Asef2 rabbit polyclonal antibody was prepared as previously described (Bristow et al., 2009). Alexa Fluor® 647 anti-rabbit was from Molecular Probes (Eugene, OR). IRDye 680 anti-mouse was obtained from Rockland Immunochemicals (Gilbertsville, PA). Rat tail type I collagen was purchased from BD Biosciences (Bedford, MA). Bovine serum albumin (BSA), blebbistatin, and NSC23766 were from EMD Bioscience (La Jolla, CA). Aqua Poly/Mount mounting solution (Cat # 18606) was purchased from Polysciences, Inc. (Warrington, PA).

GFP-tagged Asef2 cDNA was generated by cloning full-length Asef2 cDNA into pEGFP-C3 vector as previously described (Bristow et al., 2009). Wild-type Rac1 and GST-tagged PBD were kindly provided by Alan Hall (Memorial Sloan-Kettering Cancer Center, NY). Asef2 shRNAs were prepared by ligating 64-mer oligonucleotides into pSUPER vector as previously described (Wegner et al., 2008; Zhang and Macara, 2008a). The target sequences for Asef2 were previously described in Bristow *et al.* (Bristow et al., 2009). The non-target sequence, 5'-CAGTCGCGTTTGCGACTGG-3', was used as a control (Saito et al., 2007).

Cell culture

HT1080 cells stably expressing GFP or GFP-Asef2 were made using retroviral induction as previously described (Bristow et al., 2009). Cells were passaged in Dulbecco's Modified Eagle's Medium (DMEM) (Invitrogen, Carlsbad, CA) supplemented with 10% fetal bovine

serum (FBS) (Hyclone, Logan, UT) and penicillin/streptomycin (Invitrogen) (culture media).

Preparation and loading of 3D collagen I matrices and cells into microfluidic devices

Collagen I was mixed to a final concentration of 1.5 μg/ml in DMEM or PBS and neutralized with 1N NaOH (23 ml x the volume of collagen I solution) on ice. Cells were dissociated and resuspended in culture media (100,000 cells/ml) on ice. Prior to cell loading, microfluidic devices were equilibrated with culture media. Then, 100 ml of collagen I solution was mixed with 100 ml of the cell suspension, loaded into the cell chamber of the microfluidic devices, and incubated for approximately 30 min at 37°C to allow the collagen I gel with embedded cells to solidify. Subsequently, culture media was flowed through the microfluidic devices overnight at 37°C to permit the embedded cells sufficient time to attach and extend protrusions. Cells were then used in either migration assays or for immunocytochemistry. In some experiments, GFP and GFP-Asef2 cells embedded in 3D collagen I matrices were treated with 200 μM NSC23766 or DMSO (vehicle control) for 5 h at 37°C before performing immunocytochemistry.

Microscopy and immunocytochemistry

Cells in 3D matrices were washed by flowing phosphate buffered saline (PBS; Life Technologies, Grand Island, NY) through the microfluidic devices. Cells were then fixed with 4% paraformaldehyde and 4% sucrose for 20 min at 37°C, washed with PBS, and treated with 0.1M glycine in PBS for 30 min. Cells were permeabilized with 0.5% (v/v) Triton X-100 in PBS for 30 min at 23°C and incubated with 2% BSA with 0.3% Triton X-100 in PBS (blocking solution) for 1 h at 23°C to block non-specific antibody binding. Following blocking, cells were incubated overnight at 4°C with primary antibody, washed with 0.3% Triton X-100 in PBS, and subsequently treated with blocking solution for 1 h at 23°C. Fluorescently-conjugated secondary

antibodies, which were diluted in blocking solution, were incubated with cells for 1 h at 23°C. After antibody incubation, cells were washed with 0.3% Triton X-100 in PBS followed by PBS and finally sterile ddH_2O. Three drops of Prolong Gold Antifade reagent (Invitrogen, Carlsbad, CA) were added to the devices before imaging.

Images were collected using a Quorum WaveFX spinning disk confocal system with an inverted Nikon Eclipse Ti microscope, which was equipped with a Hamamatsu ImageEM-CCD camera and a PlanApo 60X TIRF objective (NA 1.49). For excitation of GFP, a 491 nm laser line was used, and GFP was imaged using a 525/50 emission filter (Semrock, Rochester, NY). Alexa Fluor 647 was excited with a 642 nm laser line and imaged using a 700/75 emission filter (Semrock, Rochester, NY). The background-subtracted, average fluorescence intensities (normalized to cell areas) of phosphorylated (S19) MyoII and total MyoII amounts were obtained with MetaMorph software.

Migration in 3D collagen I matrices

Prior to imaging, SFM4MAb™ media (Hyclone, Logan, UT) supplemented with 2-5% FBS was added to the microfluidic devices and flowed through the 3D collagen I matrices. Images were acquired every 5 min for 6 h. At each time point, sequential z-planes images were collected in 5 mm increments, and the z-stack with the best focal plane was selected for each x, y coordinate. Cell migration within the 3D matrices was tracked using MetaMorph software (Molecular Devices, Sunnyvale, CA), and the migration speed was calculated by dividing the total migration distance (mm) by the time. To ensure that the selected cells were embedded in the 3D matrices, the z coordinates where the gels contacted the glass coverslips (bottom of the gels) were determined, and images were collected 50-200 mm above this point. Live-cell imaging in 3D matrices was performed on a Quorum WaveFX spinning disk using a 10X ADL

objective (NA 0.25). Some cells were pre-treated with 50 mM blebbistatin or DMSO (vehicle control) for 3 h at 37°C prior to imaging.

Rac activity assay in 3D Collagen I matrices

Rac activity in cells embedded in 3D collagen I matrices was assessed as previously described (Yamazaki et al., 2009) with some modification. GFP and GFP-Asef2 stable cells were transfected with 8 µg FLAG-Rac1 cDNA (per 100 mm culture dish). Twenty hours later, 5 X 10^6 cells were mixed with DMEM and collagen I (final concentration 1.5 µg/ml). Cell-collagen gel suspensions (600 µl volume) were placed in 12 well plates and incubated overnight at 37°C. The gels were then homogenized in 50 mM Tris, 100 mM NaCl, 2 mM $MgCl_2$, 10% glycerol, 1% NP-40 with a protease inhibitor cocktail, pH 7.5 (lysis buffer) by repeated passage through 1 ml syringes with 26 gauge needles. Active Rac in homogenized samples was determined as previously described for 2D assays (Jean et al., 2013; Knaus et al., 2007). Briefly, a small fraction of each homogenized sample was kept to measure the amount of total Rac. The remaining sample was incubated with GST-PBD, which was attached to glutathione sepharose beads, for 1 h at 4°C with mixing. After washing three times with lysis buffer, bound protein was eluted from the sepharose beads using Laemmli sample buffer and analyzed by Western blot. The amount of active Rac that was pulled down was normalized to total Rac for each sample.

Results and Discussion

Asef2 impairs migration in 3D collagen I matrices via MyoII

The microfluidic devices that we have developed offer a controlled, reproducible platform for generating 3D environments (Fig. 27). Therefore, we used these devices to examine

the migration of HT1080 cells stably expressing GFP or GFP-Asef2 (less than 3-fold over endogenous) (Bristow et al., 2009; Jean et al., 2013) (Fig. 28A) in 3D collagen I matrices. When GFP and GFP-Asef2 cells were mixed with a collagen I solution and loaded into the cell chambers of the microfluidic devices, the cells embedded in 3D matrices adopted an elongated morphology that is characteristic of cells in 3D environments (Cukierman et al., 2001; Cukierman et al., 2002) (Fig. 28B). The migration speeds of GFP-Asef2 cells embedded in 3D collagen I matrices was decreased significantly compared to GFP (control) cells (Fig. 28B). Next, we used two Asef2 short hairpin RNAs (shRNAs) to further demonstrate that Asef2 regulates migration in 3D collagen I matrices. We had previously shown that these Asef2 shRNAs decrease endogenous expression of Asef2 by approximately 65% in HT1080 cells (Bristow et al., 2009; Jean et al., 2013). Transfection of Asef2 shRNA 1 or Asef2 shRNA 2 into HT1080 cells caused a significant increase in the migration speeds of these cells in 3D collagen I matrices compared to that observed with a non-targeting shRNA (NT shRNA) (Fig. 28C), indicating that knockdown of endogenous Asef2 promotes migration in 3D collagen I matrices. These results collectively show that Asef2 inhibits migration in 3D collagen I matrices, which is consistent with our previous observation on 2D collagen I substrates (Jean et al., 2013).

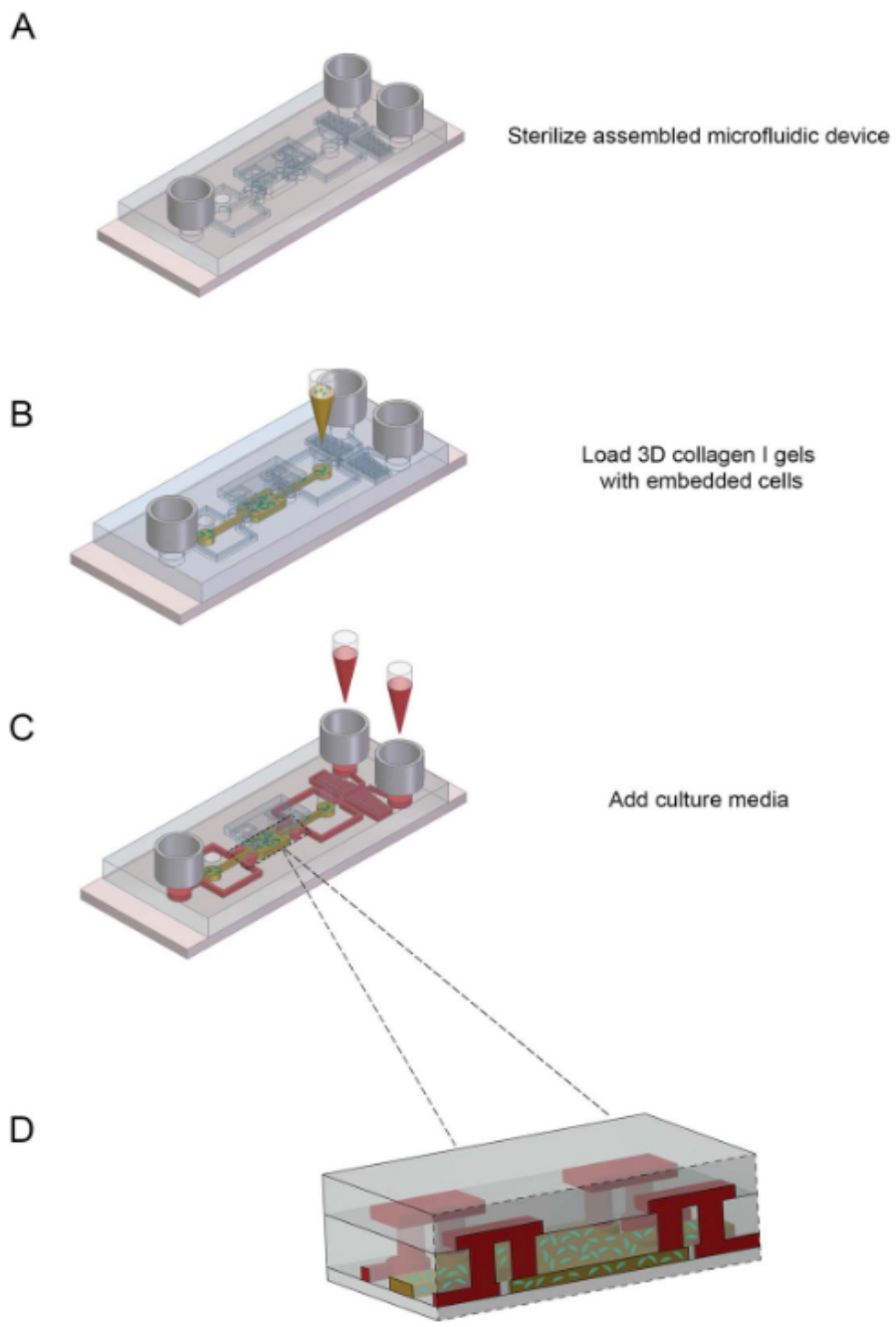

Figure 27. Schematics depicting the loading of 3D matrices with cells into microfluidic devices. (A) Assembled microfluidic devices were sterilized with UV light before loading cells. (B) After sterilization, a solution containing a mixture of collagen I (gold) and embedded cells (blue) was loaded into the cell chamber of microfluidic devices and incubated for 30 min to allow the gel to solidify. (C) Culture media was flowed through the microfluidic devices overnight to allow embedded cells sufficient time to attach and extend protrusions in the 3D matrices. Cells were used the following day in migration assays or for immunocytochemistry. (D) A cross section through the cell chamber shows cells (blue) embedded in a 3D collagen I matrix (gold) and media flow through the cell chamber.

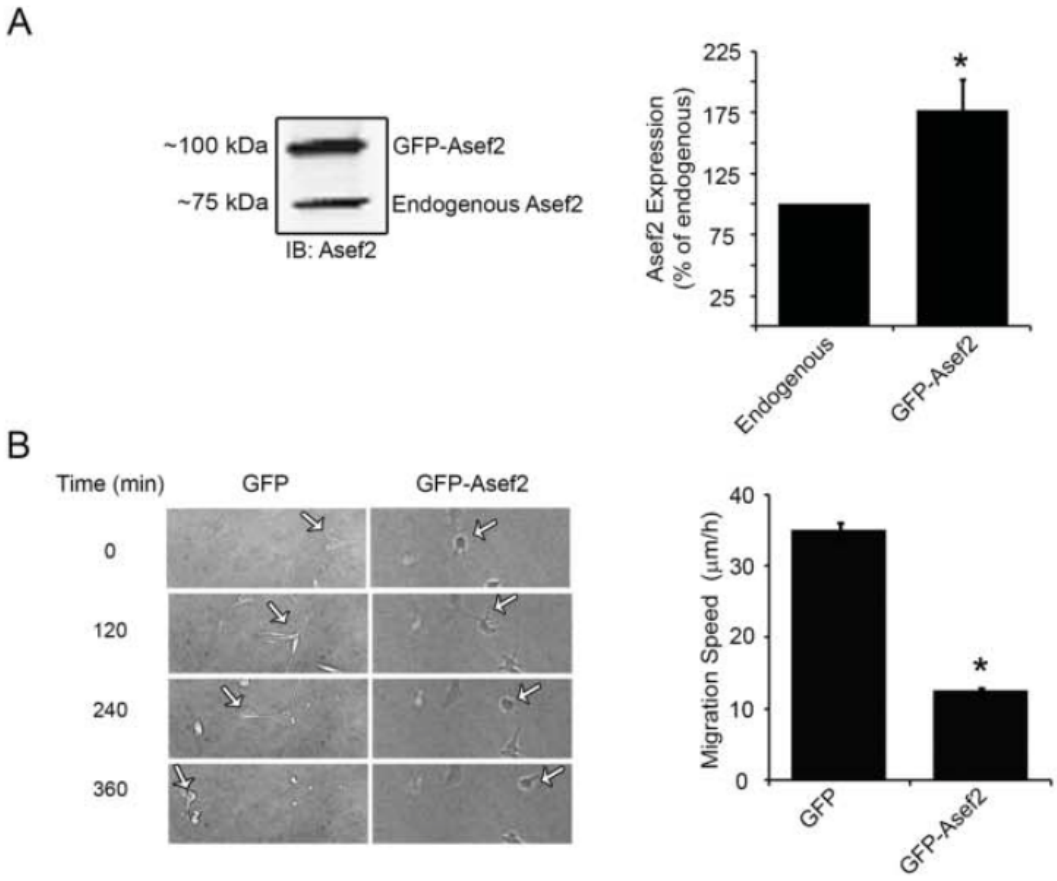

Figure 28. Asef2 hinders migration in 3D collagen I matrices. (A) Left, GFP- Asef2 cells were immunoblotted for Asef2. The ~100 kDa band represents GFP-Asef2, whereas the ~75 kDa band denotes endogenous Asef2. Right, quantification of the amount of Asef2 in GFP-Asef2 cells. Error bars represent SEM from 3 separate experiments (*p =0.04). (B) GFP and GFP-Asef2 cells in 3D collagen I matrices in microfluidic devices were imaged with time-lapse microscopy. Left, time-lapse images show GFP and GFP-Asef2 cells migrating within the 3D matrix (arrows). Right, the migration of individual cells was tracked, and the migration speed was calculated. The average migration speeds for GFP and GFP-Asef2 cells is shown. Error bars represent SEM for 50 cells from 3 independent experiments (*P < 0.0001).

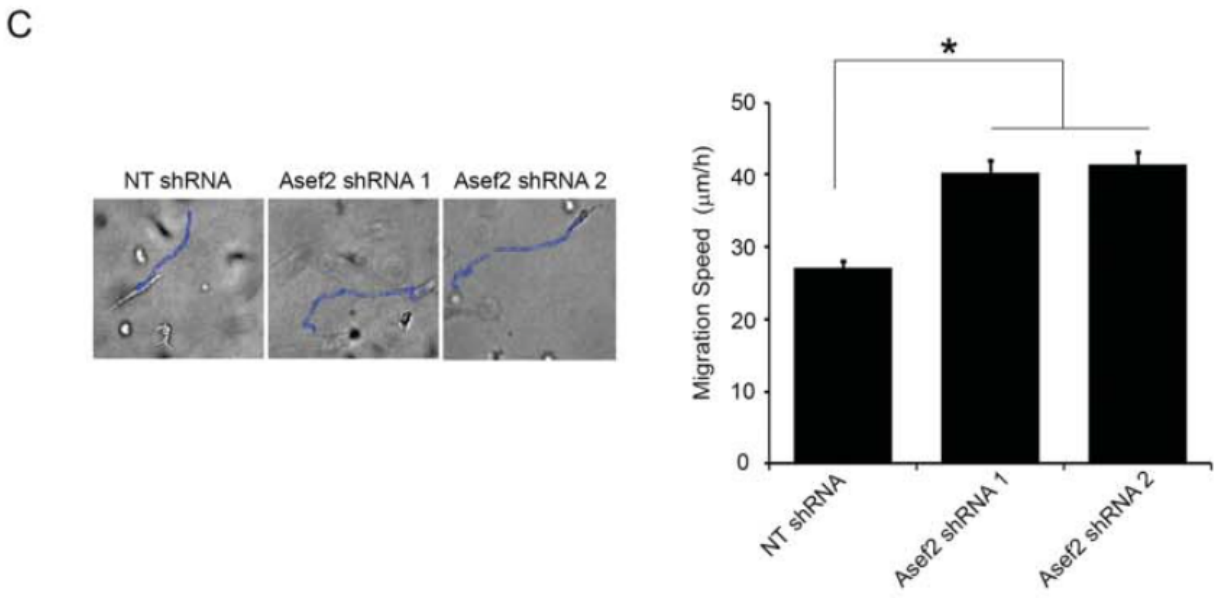

Figure 28 Cont'd. Asef2 hinders migration in 3D collagen I matrices. (C) Left, wild-type HT1080 cells were transfected with a non-targeting shRNA (NT shRNA) or Asef2 shRNAs. Three days later, these cells were used in migration assays. Phase contrast images are shown where the blue line traces the migration path of an individual cell. Right, quantification of the migration speeds for cells transfected NT shRNA or Asef2 shRNAs. Error bars represent SEM for 26– 34 cells from 3 independent experiments (*$p < 0.0001$).

We have previously shown that Asef2 hinders migration on 2D collagen I through a mechanism that is dependent on MyoII (Jean et al., 2013). To determine if Asef2 similarly regulates migration in 3D collagen I matrices, we treated GFP and GFP-Asef2 cells with blebbistatin, an inhibitor of MyoII ATPase (Kovacs et al., 2004; Straight et al., 2003). When GFP cells were incubated with blebbistatin, an increase in migration speed was observed (Fig. 29D). This augmentation of migration by blebbistatin treatment has been previously reported by us as well as by other groups (Even-Ram et al., 2007; Jean et al., 2013; Liu et al., 2010; Niggli et al., 2006). Importantly, the migration speed of GFP-Asef2 cells was significantly decreased compared with that observed with GFP cells, and blebbistatin treatment abolished this Asef2 effect on migration (Fig. 29D). This result suggests that Asef2 regulates migration in 3D collagen I matrices through MyoII.

Asef2 increases Rac activity in 3D collagen I matrices

In our previous study, we showed that Asef2 enhanced Rac activity when cells were plated on 2D collagen I; the augmented active Rac, in turn, increased phosphorylation of MyoII on S19 (Jean et al., 2013). To determine whether Asef2 also increased the amount of Rac in cells in 3D collagen I matrices, we utilized a Rac activity assay. In this assay, the p21-binding domain (PBD), from p21-activated kinase (PAK), is tagged with glutathione-S-transferase (GST) and used to pull down the active form of Rac. PAK is an effector that only binds to the active form of Rac (Knaus et al., 1995; Manser et al., 1994; Martin et al., 1995). When GFP and GFP-Asef2 cells were embedded in collagen I matrices, and Rac activity was assessed, an almost 3-fold increase in the amount of active Rac was seen in GFP-Asef2 cells compared to that observed in GFP cells (Fig. 30). This result indicates that Asef2 induces activation of Rac in 3D collagen I matrices.

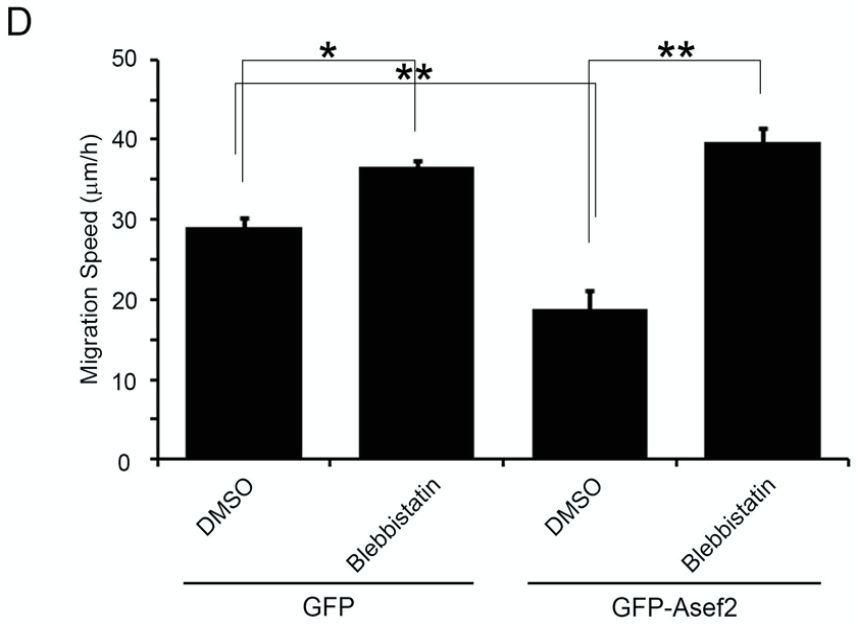

Figure 29. Inhibition of MyoII abolished the Asef2-mediated decrease in migration in 3D collagen I matrices. (**D**) GFP and GFP-Asef2 cells were treated with 50 μM blebbistatin or DMSO (vehicle control) for 3 h at 37°C prior to being used in 3D migration assays. The average migration speed for GFP and GFP-Asef2 cells, subjected to the indicated treatments, was quantified. Error bars represent S.E.M. for 50 cells from three independent experiments (*p = 0.003; **p < 0.0001).

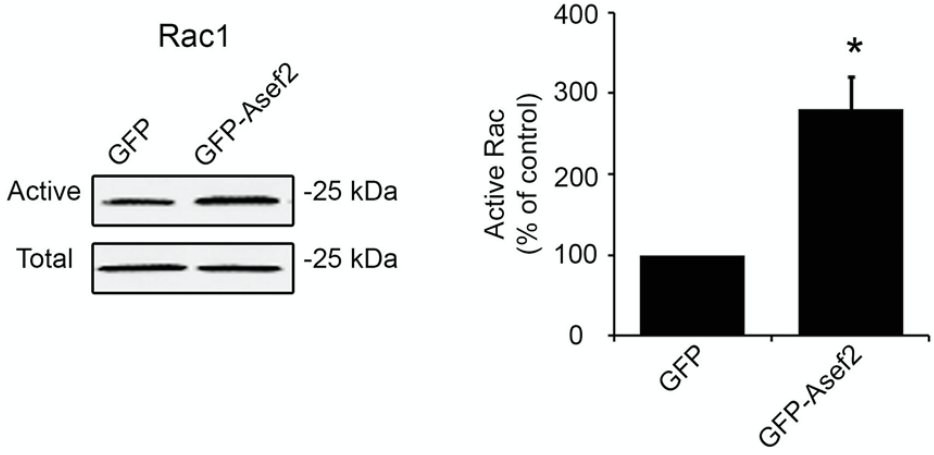

Figure 30. Asef2 augments Rac activity in 3D collagen I matrices. Left, GFP and GFP-Asef2 cells were transfected with FLAG-Rac1 cDNA. Twenty-four hours later, these cells were embedded in 3D collagen I matrices and incubated overnight. Then, the matrices with embedded cells were homogenized, and active Rac was pulled down from homogenized samples. Total Rac is shown as a control. Right, quantification of active Rac levels in homogenized samples of GFP and GFP-Asef2 cells in 3D matrices from at least three separate experiments is shown. Error bars represent S.E.M. (*p < 0.005).

Asef2 promotes S19 phosphorylation of MyoII through Rac

Because our results demonstrate that MyoII activity is important for the Asef2-mediated modulation of cell migration in 3D collagen I matrices (Fig. 29D), we next examined the effect of Asef2 on MyoII S19 phosphorylation. Phosphorylation of S19 within the RLC of MyoII is critical for its activation; therefore, phosphorylation of this amino acid can be utilized to gauge MyoII activity (Ikebe, 1989; Matsumura et al., 1998). GFP and GFP-Asef2 cells were embedded in 3D collagen I matrices and subsequently immunostained with an antibody that recognizes MyoII phosphorylated at S19. The amount of S19 phosphorylated MyoII (p-S19 MyoII) was significantly increased in GFP-Asef2 cells compared to GFP cells (Fig. 31A), whereas the amount of total MyoII was similar in these cells (Fig. 31B). Moreover, we observed a 1.4 ± 0.2-fold (n = 2 separate experiments) increase in the amount of p-S19 MyoII in GFP-Asef2 cells compared to GFP cells, as determined by In-cell Western analysis, which was performed as previously described (Jean et al., 2013). In contrast, the amount of total MyoII was not significantly different in GFP and GFP-Asef2 cells. These results demonstrate that Asef2 enhances the amount of active MyoII in cells in 3D collagen I matrices.

Because we have previously shown that Asef2 increases the level of active MyoII on 2D collagen I via Rac, we investigated the contribution of Rac to the Asef2-promoted increase in MyoII activity. GFP and GFP-Asef2 cells, embedded in 3D collagen I matrices, were treated with the Rac inhibitor NSC23766, and S19 MyoII phosphorylation was assessed. Treatment of GFP cells with NSC23766 resulted in a decrease in S19 phosphorylated MyoII (p-S19 MyoII) (Fig. 31A), suggesting that inhibition of basal Rac activity diminished the amount of active MyoII. Interestingly, treatment of GFP-Asef2 cells with NSC23766 abolished the Asef2-promoted increase in active MyoII (Fig. 31A). The level of total MyoII was similar in GFP and GFP-Asef2 cells and was not affected by NSC23766 treatment (Fig. 31B). These results suggest

that Asef2 enhances MyoII activity through a Rac-dependent mechanism in cells in 3D collagen I matrices.

Our results indicate that Asef2 activates Rac and inhibits the migration of HT1080 cells in 3D collagen I matrices. Others Rac GEFs, including DOCK3 and P-Rex, have also been shown to regulate the migration of tumor cells in 3D environments (Campbell et al., 2013; Sanz-Moreno et al., 2008), pointing to the importance of GEFs in modulating 3D migration. The DOCK3-stimulated activation of Rac promoted an elongated, mesenchymal-like morphology of melanoma cells and suppressed "amoeboid" migration (Sanz-Moreno et al., 2008). We observed a similar elongated morphology with Asef2-expressing HT1080 cells in 3D collagen I matrices. The effect that the Asef2-mediated activation of Rac has on amoeboid movement is currently unknown, but it will most likely depend on the effectors of Asef2-Rac signaling. In this context, Asef2 activation of Rac could recruit and target different effectors to the signaling complex to regulate cell morphology and migration in 3D matrices. Identification of the Asef2-Rac effectors that modulate 3D migration represents an exciting avenue for future study.

In our study, Asef2-Rac signaling increases MyoII activity, which is critical for the impaired migration that we observe in 3D collagen I matrices. Indeed, our data demonstrate that treatment with the MyoII inhibitor blebbistatin abolished this Asef2-mediated effect on migration and resulted in an increase in migration speed. Others have reported that blebbistatin treatment decreases migration in 3D environments (Petrie et al., 2012; Poincloux et al., 2011). The migration speed of human foreskin fibroblasts in cell-derived 3D matrices and human breast adenocarcinoma cells in 3D Matrigel were reduced following blebbistatin treatment (Petrie et al., 2012; Poincloux et al., 2011). Our studies were performed with HT1080 cells migrating in 3D collagen I matrices, whereas the previous experiments were done with other cell types migrating

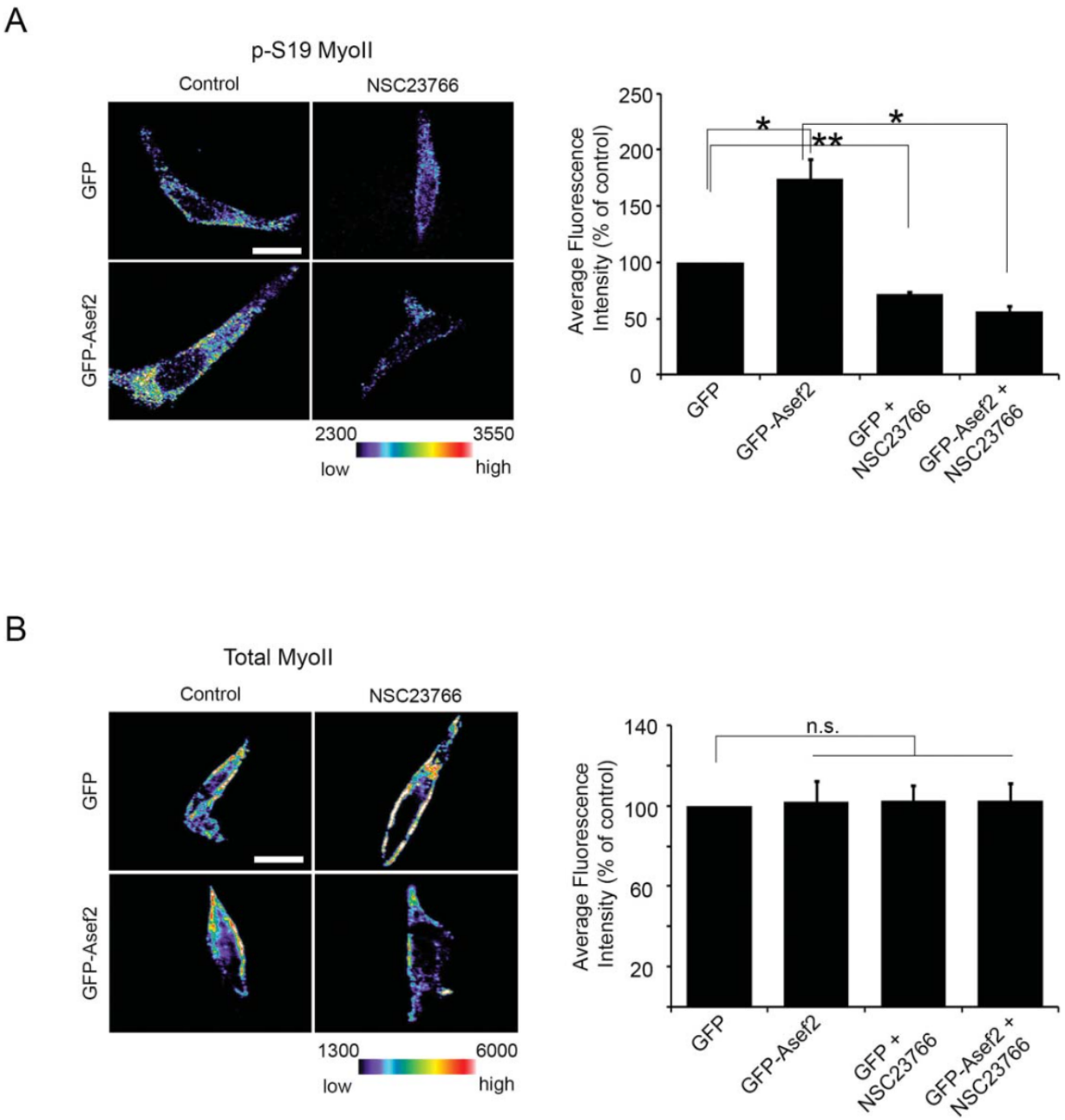

Figure 31. Asef2 promotes S19 phosphorylation of MyoII through Rac. (**A**) Left, GFP and GFP-Asef2 cells embedded in 3D collagen I matrices were incubated with 200 μM NSC23766 or DMSO for 5 h at 37°C and were subsequently immunostained for S19 phosphorylated MyoII (p-S19 MyoII). Scale bar = 15 μm. Right, quantification of p-S19 MyoII levels in these cells is shown. Error bars represent S.E.M. for at least 30 cells from at least three individual experiments (*$p < 0.005$; **$p = 0.0001$). (**B**) Left, GFP and GFP-Asef2 cells embedded in 3D collagen I matrices were treated with NSC23766 or DMSO and immunostained for total myosin. Scale bar = 15 μm. Right, quantification of total MyoII levels in these cells is shown. Error bars represent S.E.M. for at least 39 cells from at least four separate experiments. "n.s." denotes no statistically significance difference.

in 3D cell-derived matrices or 3D Matrigel. Therefore, the differences in matrices as well as cell types could contribute to the differential effect observed on migration with blebbistatin treatment. Future studies will be needed to determine the reasons for this discrepancy.

Conclusions

Our data suggest that Asef2 regulates cell migration in 3D collagen I matrices through Rac and MyoII. Asef2 increased activation of Rac in 3D collagen I matrices, which, in turn, enhanced MyoII activity. MyoII activity was critical for the Asef2 impaired migration in 3D collagen I matrices. Activation of Rac has not been previously demonstrated to induce MyoII activity in 3D matrices; thus, it will be interesting to examine the effect of Rac activation by other GEFs on MyoII. These results are consistent with our previous observations on 2D collagen I (Jean et al., 2013). Therefore, these data point to a common mechanism by which Asef2 modulates migration on 2D collagen I substrates and in 3D matrices.

CHAPTER IV

CONCLUSIONS AND FUTURE DIRECTIONS

The members of the Rho GTPase family are well demonstrated to be important regulators of cell migration. Cell migration is a highly coordinated and spatiotemporally regulated process that has been implicated in diseases such as cancer and atherosclerosis. Although it is well understood that GTPases regulate many aspects of intracellular actin dynamics through their activation by GEFs, very little is known about the specific role these GEFs play in regulating cellular migration. Here, for the first time, we reveal a new role for the GTPase Rac, through Asef2-mediated activation, in modulating actomyosin contractility, and thereby cell migration and adhesion dynamics.

In this study, we show that activation of Rac by Asef2 inhibits cell migration on type I collagen (Col-I), a protein that forms the majority of the connective tissues surrounding tumors (Jean et al., 2013). In live-cell imaging, we observed that the migration speed of fibrosarcoma cells (HT1080) expressing Asef2 is significantly decreased when compared with controls. Additionally, stable expression of GFP-Asef2 in MDA-MB-231 breast cancer cells led to a significant reduction in migration speed as compared to that observed with GFP stable cells (Jean et al., 2013), indicating that the phenotype was not cell type specific. The specificity of Asef2's role in this decreased migration effect was further confirmed with shRNA-mediated knockdown of endogenous Asef2. Asf2 knockdown resulted in a significant increase in migration speed compared to that observed with empty pSUPER vector or a non-targeting (NT) shRNA. We also determined the effect of Asef2 on the activity of the Rho family GTPases Rac, Cdc42, and Rho,

using an active GTPase pulldown assay. Interestingly, while Asef2 expression did not significantly affect the levels of active Cdc42 or Rho, it did increase the amount of active Rac. To investigate local Rac activation, we used the Raichu-Rac fluorescence resonance energy transfer (FRET) probe to further demonstrate that Asef2 increases Rac activity. And, as expected, Asef2 expression did enhance levels of active Rac. Furthermore, our data indicated that the GEF activity of Asef2 is critical for its function in impairing migration on Col-I.

Taken together, the above results suggest that Asef2 promotes the activation of Rac, and not Cdc42 and Rho, when cells are plated on Col-I. Additionally, they show that the Asef2-mediated activation of Rac results in a reduction of migration speed. It would be interesting to examine whether the Asef2-mediated effects on Col-I represent a general mechanism for other Rho family GEFs, especially Rac-specific GEFs. First, we could increase Rac activity in cells by expressing the Rac-specific GEF, Tiam1 (Habets et al., 1994; Habets et al., 1995). We can then assess its effect on cell migration on Col-I. If this pathway is specific to Rac, then Tiam1 will not similarly affect cell migration. However, it is possible that Tiam1 and, potentially, other GEFs are activators of Rac in this pathway which would result in a decrease in cell migration.

As previously mentioned, GTPases are spatially and temporally regulated. Studies have shown active Rac and Cdc42 to be localized to the leading edge of the migrating cell, while active Rho is present at both the front and the rear of the cell (Machacek et al., 2009; Pertz and Hahn, 2004; Pertz et al., 2006). However, GTPases can also regulate each other via an extensive crosstalk to coordinate their own activity to facilitate cell migration (Guilluy et al., 2011). This crosstalk frequently occurs in the form of positive or negative regulation of one GTPase by another. For instance, there are several examples of Rac acting upstream of Rho to stimulate its activation and promote the necessary contractile forces for effective migration (Burridge and

Wennerberg, 2004). Indeed, the protrusive activity of Rac is considered to be a necessary opposing force to the stabilization of stress fiber and contractile forces generated in a Rho-dependent manner. However, other studies indicate that Rac can inactivate Rho, or vice versa (Burridge and Wennerberg, 2004; Sander et al., 1999). Therefore, it is clear that the multiple signaling pathways that result from GTPase crosstalk not only act in compliment to one another, but also are important in regulating migration.

Our lab previously reported Asef2 to promote cell migration on fibronectin through Rac and the serine/threonine kinase Akt, which subsequently leads to a decrease in Rho activity (Bristow et al., 2009). Interestingly, in our current studies investigating the role of Asef2 on Col-I, Asef2 did not change the amount of active Rho. It would therefore be of keen interest to examine the differential effect of Rho inhibition on Rac activation in Asef2-mediated migration. One experiment would be to use FRET biosensors to determine the effect of both Asef2 expression and Rac activation on localized Rho activity when cells are plated on Col-I versus fibronectin.

Our data also indicates a novel role for Rac in regulating Myosin II (MyoII) motor proteins, which bind actin filaments to provide the contractile force needed for translocation. Rho is a well-characterized modulator of actomyosin contractility, but the function of other GTPases, such as Rac, in regulating contractility is currently not well understood. Here we show that activation of Rac by Asef2 increases MyoII contractility to impair cell migration. Cell contractility was assessed using a gel contraction assay, and the diameter of Col-I gels with Asef2-expressing cells were reduced as compared to controls. Levels of active MyoII were also significantly increased by Asef2 expression, as determined by S19 phosphorylation, while knockdown of endogenous Asef2 led to a decrease in active MyoII. In addition, knockdown of

endogenous Rac using shRNAs or treatment of cells with a Rac-specific inhibitor resulted in a significant decrease in the amount of active MyoII, and negated the Asef2-promoted increase in contractility. These results, showing that Rac increases contractility, point to a new role for Rac regulating actomyosin contractility, which is important for cell migration. Furthermore, treatment of cells with blebbistatin, which inhibits MyoII activity, abolishes the Asef2-mediated effect on migration speed. Collectively, these results demonstrate that the Asef2-mediated migration on Col-I is facilitated through Rac and MyoII- dependent cell contractility, which has been classically thought to be mediated by Rho. It would be interesting to determine whether Asef2-mediated migration is mediated only though Rac, specifically looking at the effect of Rho inhibition on levels of active MyoII when cells are plated on Col-I.

Rac most likely modulates actomyosin contractility through downstream effectors (Fig 34). Since p21-activated kinase (PAK) is an effector of Rac and directly phosphorylates MyoII on S19 (Chew et al., 1998; Ramos et al., 1997), PAK may serve as the link between Rac and MyoII. PAK regulates MyoII activity either through direct phosphorylation of the MyoII regulatory light chain (RLC), or indirectly through regulation of the myosin light chain kinase (MLCK) (Chong et al., 2001). Moreover, expression of constitutively active Rac increases S19 phosphorylation of MyoII RLCs, which was mediated, at least in part, through PAK (Brzeska et al., 2004). Preliminary results show that expression of a dominant negative PAK abolishes the Asef2-promoted increase in the level of p-S19 MyoII, and that constitutive activation of PAK mimics the Asef2-mediated decrease in migration speed seen on Col-I (Fig. 32 and 33). These results suggest that PAK links Rac to MyoII in this signaling pathway. However, follow up experiments such as knockdown of endogenous PAK in Asef2-expressing

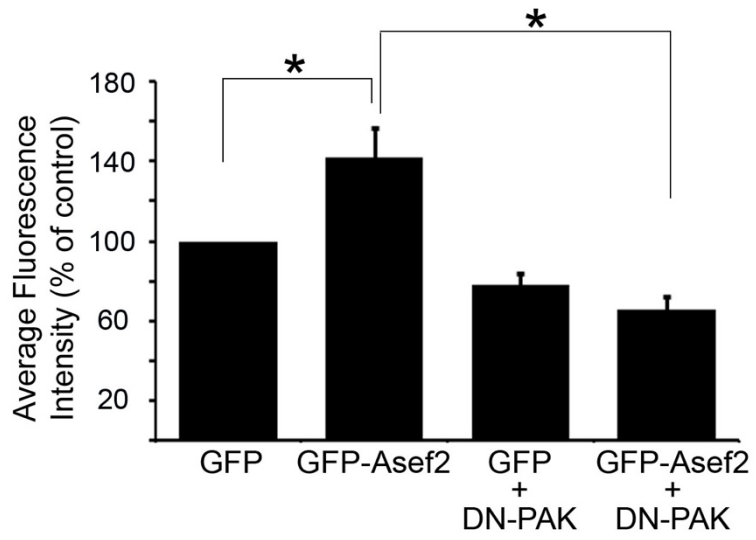

Figure 32. PAK negates the Asef2-promoted increase in MyoII activity. Cells expressing Asef2 were transfected with empty vector or a dominant negative PAK construct and immunostained for p-S19-MyoII. Quantification of average fluorescence intensity as a percent of the GFP is shown. Error bars represent the standard error mean for at least 28 cells from 2 experiments (*p<0.0001; ANOVA-Tukey-Kramer comparison).

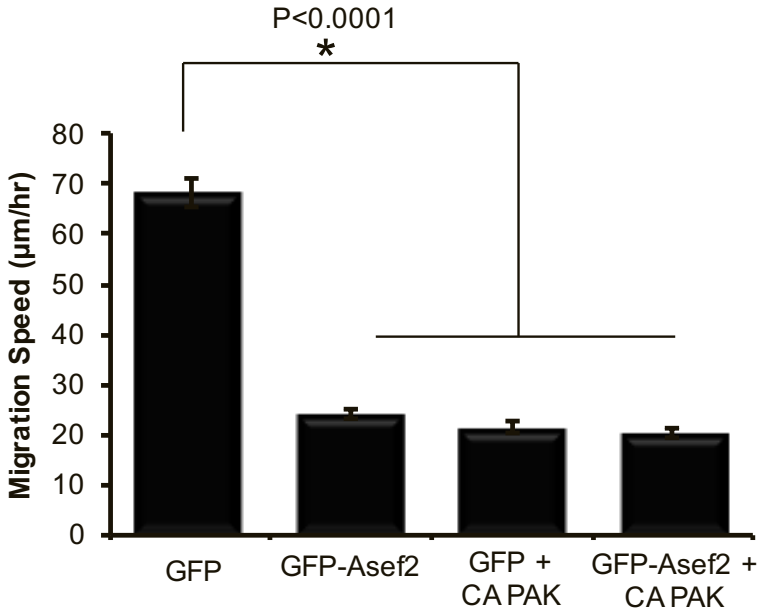

Figure 33. PAK regulates Asef2-mediated decrease in migration. Cells expressing Asef2 were transfected with empty vector or a shRNAs constructs against PAK. Cells were then plated on Col-I and then imaged using time lapse microscopy. Individual cell migrations were tracked and their average speeds are shown. Error bars represent standard error means for at least 38 cells over 3 experiments. (*p<0.0001; ANOVA-Tukey-Kramer comparison).

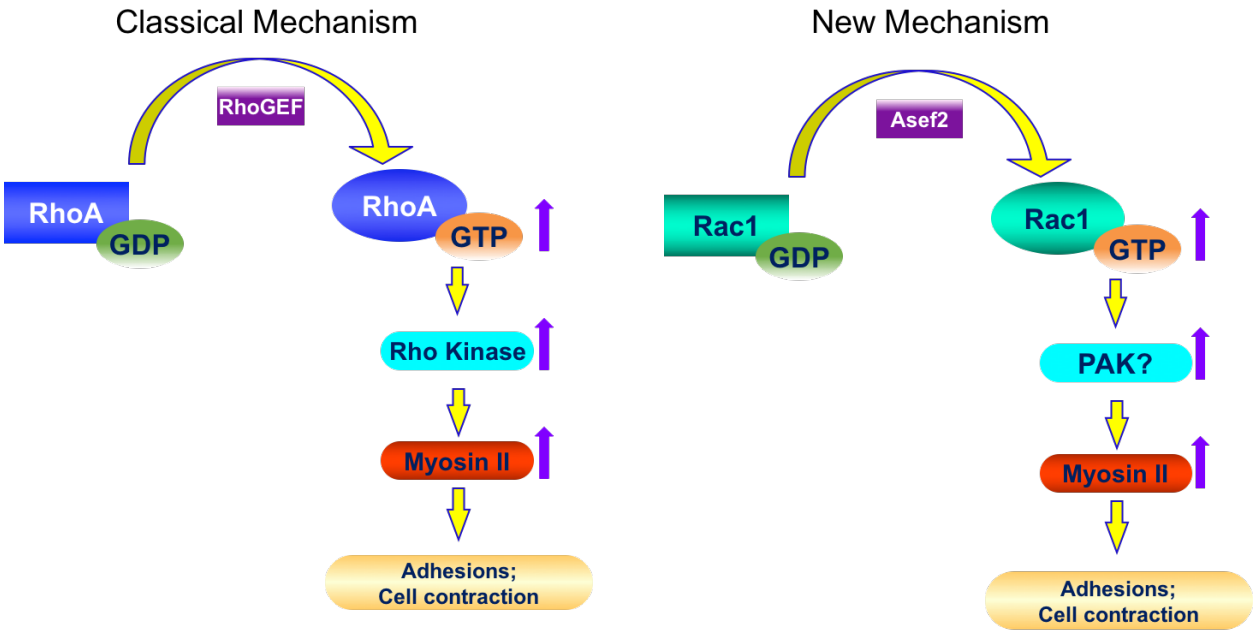

Figure 34. Model of Asef2 regulation of Rac and Myosin II

cells to examine the effect on MyoII activity, contractility, and migration would confirm the role of PAK in Asef2-mediated migration. Still, we could assess whether PAK acts a mediator for Rac-dependent activation of MyoII, and look at the effect of endogenous knockdown of Rac on PAK activity using an antibody that recognizes phosphorylated threonine 423, a key autophosphorylation site for PAK activation (Sells et al., 2000).

Because the growth and stability of cell-matrix adhesions have been linked to actomyosin contractility (Choi et al., 2008; Chrzanowska-Wodnicka and Burridge, 1996), we also examined the effect of Asef2 on adhesions using total internal reflection fluorescence (TIRF) microscopy. Interestingly, Asef2 expression increases active levels of β1 integrin proteins in adhesions, and induces large and mature adhesions that assemble and disassemble (turnover) more slowly compared with controls. However, the Asef2-promoted increase in active β1 integrin in adhesions was diminished by treatment with a Rac inhibitor. Taken together, this data further demonstrated a new role for Rac activation, promoted by Asef2, in modulating actomyosin contractility, which is important for regulating cell migration and adhesion dynamics. According to our results, Asef2 activation of Rac increases actomyosin contractility, which could serve to induce the maturation of adhesions. Nascent adhesions that form at the leading edge of Asef2-expressing cells grow into large focal adhesions instead of undergoing disassembly. In turn, these large mature adhesions serve to inhibit cell migration given that adhesion turnover at the leading edge is essential for driving rapid migration (Laukaitis et al., 2001; Webb et al., 2004).

We could further show that the Rac-mediated increase in active MyoII is important for the regulation of adhesion dynamics by Asef2 by investigating the effect of MyoII inhibition on adhesion size and adhesion turnover using the MyoII inhibitors and mutants. Since MyoII promotes adhesion maturation by contracting F-actin (Choi et al., 2008; Vicente-Manzanares et

al., 2007), we anticipate that MyoII inhibition will result in smaller, "immature" adhesions in Asef2-expressing cells. Additionally, inhibition of MyoII induce faster adhesion assembly and disassembly rates in Asef2-expressing cells, allowing these cells to move faster. Another experiment would be to use a Rac inhibitor and Rac shRNAs and examine the effect of decreased Rac activity and expression on the Asef2-mediated regulation of adhesion size and turnover. We expect that knockdown of Rac would lead to similar results as those obtained with MyoII inhibition on adhesion size and adhesion turnover. Moreover, future studies can also be carried out to determine whether the effects of Rac and MyoII on adhesion turnover are mediated through PAK using a similar approach.

Because three-dimensional (3D) matrices more closely mimic the physiologic environment of cells (Cukierman et al., 2002), it is important to test observations obtained from cultured cells in a more *in vivo*-like environment. Thus, we investigated the role of Asef2 in regulating migration and MyoII activity in 3D *in vivo*-like environments. We used microfluidic devices that afford a controlled reproducible platform for generating 3D Col-I matrices (Jean et al., 2014). Using these devices, we have shown that Asef2 inhibits cell migration in 3D Col-I matrices, and that treatment of these cells with blebbistatin abolishes the Asef2-mediated decrease in migration. Moreover, Asef2 enhances MyoII activity and treatment with a Rac inhibitor abolishes the Asef2-promoted increase in active MyoII. Collectively, these results indicate that Asef2-mediated Rac activation is critical for modulating MyoII activity and cancer cell migration in both 2D and 3D environments.

The data from this dissertation puts forth new findings in the field of cell migration and adhesion dynamics, in that Rac activation has not previously been linked to a reduction in migration (Bristow et al., 2009), and Rho has been classically shown to regulate MyoII

contractility (Chrzanowska-Wodnicka and Burridge, 1996; Wheeler and Ridley, 2004). Interestingly, it seems that though Asef2 modulates cell migration by increasing Rac activity, the effects on migration and contractility are quite different depending on the given ECM (i.e. Col-I vs fibronectin) (Bristow et al., 2009; Jean et al., 2013). These differential effects on migration may be attributed to different combinations of scaffolding proteins downstream of ECM engagement. Scaffolding proteins can recruit or bring together various binding partners through their multiple protein-protein interaction domains, and dictate signaling to various downstream targets (Pawson, 2007). And as such, the recruitment of Asef2, Rac and other downstream effectors upon ECM engagement may assemble different scaffolding proteins and provide a mechanism for specificity in Rac signaling (Fig. 34). This hypothesis is further confirmed with studies on another Rac GEF, Tiam1, which has been shown to associate with different scaffolding proteins to selectively activate distinct downstream Rac effectors (Buchsbaum et al., 2002; Buchsbaum et al., 2003).

In addition, scaffolding proteins could also promote the selectivity of GTPases by amplifying the recruitment of Asef2 and Rac to the signaling complex, and thus enhance Asef2 activation of Rac over other GTPases, such as Cdc42. Interestingly, although Asef2 is a Rac and Cdc42 GEF, our results show that Asef2 preferentially activates Rac on Col-I. The interaction of Asef2 and distinct scaffolding proteins seems to provide a mechanism by which this GEF is selectively activating one GTPase over another. Thus, investigating the upstream mechanisms that regulate Asef2 activation would shed light on the sequence of events in Asef2-mediated signaling. The overabundance of GEFs compared to GTPases adds an additional regulatory component to GTPase activity as most GEFs contain multiple protein-protein interaction domains that are hypothesized to target the GTPases to specific cellular regions, where they can

be activated by distinct upstream signals (Rossman et al. 2005). It would be interesting to determine the effect of upstream signaling of various growth factors, such as epidermal growth factor (EGF) on the formation of the different protein complexes on Col-I and fibronectin, and on Asef2's localization within migrating cells. Another approach would be to identify Asef2's binding partners on Col-I and fibronectin using high-resolution mass spectrometry.

Asef2 is aberrantly expressed in colorectal tumors, and its expression has been shown to be necessary for intestinal adenoma metastasis and progression (Kawasaki et al., 2009). This aberrant regulation of Asef2 in colorectal tumor cells is believed to result from its interaction with the mutated form of the tumor suppressor adenomatous polyposis coli (APC) typically found in colorectal tumor cells (Kawasaki et al., 2013; Kawasaki et al., 2009). Genetic deletion of Asef2 in mice led to a reduction in adenoma number and size in an $APC^{Min/+}$ background (Kawasaki et al., 2009), which is a common model of colorectal cancer (Su et al., 1992). Furthermore, deletion of Asef2 reduced the number of angiogenic blood vessels, indicating that Asef2 is required for tumor angiogenesis (Kawasaki et al., 2009). These studies show that Asef2 contribute to adenoma formation, as well as to tumor progression in mice, via histology and immunohistochemistry. In contrast, because our result on Col-I suggests that Asef2 is reducing migration, it is possible that APC is not the activator in Asef2-mediated migration on Col-I. The metastasis phenotype seen on the APC background mice might be due to the fact that upstream activators of Asef2 specify the downstream signaling of Asef2 on different ECM. Additionally, our lab has observed Asef2 differentially inhibiting migration on Col-I and increasing migration on fibronectin by two different mechanisms. This suggest a strong role for the tumor microenvironment in dictating cancer cell metastasis. Further investigation of metastatic cancer types, and surrounding tissue may offer some insight into the localized regulation of Asef2.

Moreover, since aberrant cell migration is implicated in tumor cell metastasis, it would be interesting to address the potential role Asef2 in the regulation of metastasis *in vivo* using a viable system.

Asef2: A promising target for cancer therapeutics

Our data point to an important role for Asef2 in regulating cancer cell migration and its underlying processes. By investigating the function of Asef2 in cell migration, we should gain significant insight into the molecular mechanisms that regulate this process, which could lead to new therapeutic treatments for various diseases. We are optimistic that Asef2, or other effectors which regulate its activity, could be a direct molecular target for controlling cancer metastasis.

REFERENCES

Adelstein, R.S., and M.A. Conti. 1975. Phosphorylation of platelet myosin increases actin-activated myosin ATPase activity. *Nature*. 256:597-598.

Aguilar-Cuenca, R., A. Juanes-Garcia, and M. Vicente-Manzanares. 2014. Myosin II in mechanotransduction: master and commander of cell migration, morphogenesis, and cancer. *Cell Mol Life Sci*. 71:479-492.

Alessi, D.R., M. Andjelkovic, B. Caudwell, P. Cron, N. Morrice, P. Cohen, and B.A. Hemmings. 1996. Mechanism of activation of protein kinase B by insulin and IGF-1. *Embo J*. 15:6541-6551.

Alexandrova, A.Y., K. Arnold, S. Schaub, J.M. Vasiliev, J.J. Meister, A.D. Bershadsky, and A.B. Verkhovsky. 2008. Comparative dynamics of retrograde actin flow and focal adhesions: formation of nascent adhesions triggers transition from fast to slow flow. *PloS one*. 3:e3234.

Allende, J.E. 1988. GTP-mediated macromolecular interactions: the common features of different systems. *FASEB journal : official publication of the Federation of American Societies for Experimental Biology*. 2:2356-2367.

Amano, M., K. Chihara, K. Kimura, Y. Fukata, N. Nakamura, Y. Matsuura, and K. Kaibuchi. 1997. Formation of actin stress fibers and focal adhesions enhanced by Rho-kinase. *Science*. 275:1308-1311.

Anderson, K.I., Y.L. Wang, and J.V. Small. 1996. Coordination of protrusion and translocation of the keratocyte involves rolling of the cell body. *J Cell Biol*. 134:1209-1218.

Baker, B.M., and C.S. Chen. 2012. Deconstructing the third dimension: how 3D culture microenvironments alter cellular cues. *Journal of cell science*. 125:3015-3024.

Balaban, N.Q., U.S. Schwarz, D. Riveline, P. Goichberg, G. Tzur, I. Sabanay, D. Mahalu, S. Safran, A. Bershadsky, L. Addadi, and B. Geiger. 2001. Force and focal adhesion assembly: a close relationship studied using elastic micropatterned substrates. *Nat Cell Biol*. 3:466-472.

Ballestrem, C., B. Hinz, B.A. Imhof, and B. Wehrle-Haller. 2001. Marching at the front and dragging behind: differential alphaVbeta3-integrin turnover regulates focal adhesion behavior. *J Cell Biol*. 155:1319-1332.

Beningo, K.A., M. Dembo, I. Kaverina, J.V. Small, and Y.-L. Wang. 2001. Nascent focal adhesions are responsible for the generation of strong propulsive forces in migrating fibroblasts. *J. Cell Biol.* 153:881-888.

Bershadsky, A.D., N.Q. Balaban, and B. Geiger. 2003. Adhesion-dependent cell mechanosensitivity. *Annu Rev Cell Dev Biol*. 19:677-695.

Bershadsky, A.D., C. Ballestrem, L. Carramusa, Y. Zilberman, B. Gilquin, S. Khochbin, A.Y. Alexandrova, A.B. Verkhovsky, T. Shemesh, and M.M. Kozlov. 2006. Assembly and mechanosensory function of focal adhesions: experiments and models. *Eur J Cell Biol*. 85:165-173.

Bhatt, A., I. Kaverina, C. Otey, and A. Huttenlocher. 2002. Regulation of focal complex composition and disassembly by the calcium-dependent protease calpain. *J Cell Sci*. 115:3415-3425.

Borisy, G.G., and T.M. Svitkina. 2000. Actin machinery: pushing the envelope. *Curr. Opin. Cell Biol.* 12:104-112.

Bos, J.L., H. Rehmann, and A. Wittinghofer. 2007. GEFs and GAPs: critical elements in the control of small G proteins. *Cell*. 129:865-877.

Bristow, J.M., M.H. Sellers, D. Majumdar, B. Anderson, L. Hu, and D.J. Webb. 2009. The Rho-family GEF Asef2 activates Rac to modulate adhesion and actin dynamics and thereby regulate cell migration. *Journal of cell science*. 122:4535-4546.

Broussard, J.A., D.J. Webb, and I. Kaverina. 2008. Asymmetric focal adhesion disassembly in motile cells. *Curr Opin Cell Biol*. 20:85-90.

Brown, M.C., and C.E. Turner. 2004. Paxillin: adapting to change. *Physiol Rev*. 84:1315-1339.

Brzeska, H., J. Szczepanowska, F. Matsumura, and E.D. Korn. 2004. Rac-induced increase of phosphorylation of myosin regulatory light chain in HeLa cells. *Cell Motil Cytoskeleton*. 58:186-199.

Buchsbaum, R.J., B.A. Connolly, and L.A. Feig. 2002. Interaction of Rac exchange factors Tiam1 and Ras-GRF1 with a scaffold for the p38 mitogen-activated protein kinase cascade. *Molecular and cellular biology*. 22:4073-4085.

Buchsbaum, R.J., B.A. Connolly, and L.A. Feig. 2003. Regulation of p70 S6 kinase by complex formation between the Rac guanine nucleotide exchange factor (Rac-GEF) Tiam1 and the scaffold spinophilin. *J Biol Chem*. 278:18833-18841.

Burridge, K., and M. Chrzanowska-Wodnicka. 1996. Focal adhesions, contractility, and signaling. *Annu. Rev. Cell. Dev. Biol.* 12:463-518.

Burridge, K., K. Fath, T. Kelly, G. Nuckolls, and C. Turner. 1988. Focal adhesions: transmembrane junctions between the extracellular matrix and the cytoskeleton. *Annu Rev Cell Biol*. 4:487-525.

Burridge, K., and K. Wennerberg. 2004. Rho and Rac take center stage. *Cell*. 116:167-179.

Cain, R.J., and A.J. Ridley. 2009. Phosphoinositide 3-kinases in cell migration. *Biol. Cell*. 101:13-29.

Campbell, A.D., S. Lawn, L.C. McGarry, H.C. Welch, B.W. Ozanne, and J.C. Norman. 2013. P-Rex1 cooperates with PDGFRbeta to drive cellular migration in 3D microenvironments. *PloS one*. 8:e53982.

Campbell, I.D., and M.H. Ginsberg. 2004. The talin-tail interaction places integrin activation on FERM ground. *Trends in biochemical sciences*. 29:429-435.

Carragher, N.O., M.A. Westhoff, V.J. Fincham, M.D. Schaller, and M.C. Frame. 2003. A novel role for FAK as a protease-targeting adaptor protein: regulation by p42 ERK and Src. *Curr Biol*. 13:1442-1450.

Carson, M., A. Weber, and S.H. Zigmond. 1986. An actin-nucleating activity in polymorphonuclear leukocytes is modulated by chemotactic peptides. *J. Cell Biol.* 103:2707-2714.

Cerione, R.A., and Y. Zheng. 1996. The Dbl family of oncogenes. *Curr Opin Cell Biol*. 8:216-222.

Chan, A.Y., S.J. Coniglio, Y.-y. Chuang, D. Michaelson, U.G. Knaus, M.R. Philips, and M. Symons. 2005. Roles of the Rac1 and Rac3 GTPases in human tumor cell invasion. *Oncogene*. 24:7821-7829.

Chan, K.T., D.A. Bennin, and A. Huttenlocher. 2010. Regulation of adhesion dynamics by calpain-mediated proteolysis of focal adhesion kinase (FAK). *J Biol Chem*. 285:11418-11426.

Chew, T.L., R.A. Masaracchia, Z.M. Goeckeler, and R.B. Wysolmerski. 1998. Phosphorylation of non-muscle myosin II regulatory light chain by p21-activated kinase (gamma-PAK). *J Muscle Res Cell Motil*. 19:839-854.

Choi, C.K., M. Vicente-Manzanares, J. Zareno, L.A. Whitmore, A. Mogilner, and A.R. Horwitz. 2008. Actin and alpha-actinin orchestrate the assembly and maturation of nascent adhesions in a myosin II motor-independent manner. *Nat Cell Biol*. 10:1039-1050.

Chong, C., L. Tan, L. Lim, and E. Manser. 2001. The mechanism of PAK activation. Autophosphorylation events in both regulatory and kinase domains control activity. *J Biol Chem*. 276:17347-17353.

Chrzanowska-Wodnicka, M., and K. Burridge. 1996. Rho-stimulated contractility drives the formation of stress fibers and focal adhesions. *J Cell Biol*. 133:1403-1415.

Clark, K., M. Langeslag, C.G. Figdor, and F.N. van Leeuwen. 2007. Myosin II and mechanotransduction: a balancing act. *Trends Cell Biol*. 17:178-186.

Cortesio, C.L., L.R. Boateng, T.M. Piazza, D.A. Bennin, and A. Huttenlocher. 2011. Calpain-mediated proteolysis of paxillin negatively regulates focal adhesion dynamics and cell migration. *J Biol Chem*. 286:9998-10006.

Crowley, E., and A.F. Horwitz. 1995. Tyrosine phosphorylation and cytoskeletal tension regulate the release of fibroblast adhesions. *J Cell Biol*. 131:525-537.

Cukierman, E., R. Pankov, D.R. Stevens, and K.M. Yamada. 2001. Taking cell-matrix adhesions to the third dimension. *Science*. 294:1708-1712.

Cukierman, E., R. Pankov, and K.M. Yamada. 2002. Cell interactions with three-dimensional matrices. *Current opinion in cell biology*. 14:633–639.

Daniels, R.H., and G.M. Bokoch. 1999. p21-activated protein kinase: a crucial component of morphological signaling? *Trends in biochemical sciences*. 24:350-355.

De Wever, O., P. Demetter, M. Mareel, and M. Bracke. 2008. Stromal myofibroblasts are drivers of invasive cancer growth. *Int J Cancer*. 123:2229-2238.

Defilippi, P., P. Di Stefano, and S. Cabodi. 2006. p130Cas: a versatile scaffold in signaling networks. *Trends Cell Biol*. 16:257-263.

del Rio, A., R. Perez-Jimenez, R. Liu, P. Roca-Cusachs, J.M. Fernandez, and M.P. Sheetz. 2009. Stretching single talin rod molecules activates vinculin binding. *Science*. 323:638-641.

Digman, M.A., C.M. Brown, A.R. Horwitz, W.W. Mantulin, and E. Gratton. 2008. Paxillin dynamics measured during adhesion assembly and disassembly by correlation spectroscopy. *Biophys J*. 94:2819-2831.

Doyle, A.D., R.J. Petrie, M.L. Kutys, and K.M. Yamada. 2013. Dimensions in cell migration. *Curr Opin Cell Biol*. 25:642-649.

Even-Ram, S., A.D. Doyle, M.A. Conti, K. Matsumoto, R.S. Adelstein, and K.M. Yamada. 2007. Myosin IIA regulates cell motility and actomyosin-microtubule crosstalk. *Nature cell biology*. 9:299-309.

Ezratty, E.J., C. Bertaux, E.E. Marcantonio, and G.G. Gundersen. 2009. Clathrin mediates integrin endocytosis for focal adhesion disassembly in migrating cells. *J Cell Biol*. 187:733-747.

Ezratty, E.J., M.A. Partridge, and G.G. Gundersen. 2005. Microtubule-induced focal adhesion disassembly is mediated by dynamin and focal adhesion kinase. *Nat Cell Biol*. 7:581-590.

Fincham, V.J., and M.C. Frame. 1998. The catalytic activity of Src is dispensable for translocation to focal adhesions but controls the turnover of these structures during cell motility. *EMBO J*. 17:81-92.

Franco, S.J., and A. Huttenlocher. 2005. Regulating cell migration: calpains make the cut. *J Cell Sci*. 118:3829-3838.

Franco, S.J., M.A. Rodgers, B.J. Perrin, J. Han, D.A. Bennin, D.R. Critchley, and A. Huttenlocher. 2004. Calpain-mediated proteolysis of talin regulates adhesion dynamics. *Nat Cell Biol*. 6:977-983.

Frantz, C., K.M. Stewart, and V.M. Weaver. 2010. The extracellular matrix at a glance. *J Cell Sci*. 123:4195-4200.

Friedland, J.C., M.H. Lee, and D. Boettiger. 2009. Mechanically activated integrin switch controls alpha5beta1 function. *Science*. 323:642-644.

Galbraith, C.G., and M.P. Sheetz. 1997. A micromachined device provides a new bend on fibroblast traction forces. *Proc. Natl. Acad. Sci. U S A*. 94:9114-9118.

Gao, Y., J.B. Dickerson, F. Guo, J. Zheng, and Y. Zheng. 2004. Rational design and characterization of a Rac GTPase-specific small molecule inhibitor. *Proc Natl Acad Sci U S A*. 101:7618-7623.

Gao, Y., D. Majumdar, B. Jovanovic, C. Shaifer, P.C. Lin, A. Zijlstra, D.J. Webb, and D. Li. 2011. A versatile valve-enabled microfluidic cell co-culture platform and demonstration of its applications to neurobiology and cancer biology. *Biomedical microdevices*. 13:539-548.

Gardel, M.L., B. Sabass, L. Ji, G. Danuser, U.S. Schwarz, and C.M. Waterman. 2008. Traction stress in focal adhesions correlates biphasically with actin retrograde flow speed. *J Cell Biol*. 183:999-1005.

Gardel, M.L., I.C. Schneider, Y. Aratyn-Schaus, and C.M. Waterman. 2010. Mechanical integration of actin and adhesion dynamics in cell migration. *Annu Rev Cell Dev Biol*. 26:315-333.

Geiger, B., A. Bershadsky, R. Pankov, and K.M. Yamada. 2001. Transmembrane crosstalk between the extracellular matrix--cytoskeleton crosstalk. *Nat Rev Mol Cell Biol*. 2:793-805.

Geiger, B., J.P. Spatz, and A.D. Bershadsky. 2009. Environmental sensing through focal adhesions. *Nat Rev Mol Cell Biol*. 10:21-33.

Geiger, B., and K.M. Yamada. 2011. Molecular architecture and function of matrix adhesions. *Cold Spring Harbor perspectives in biology*. 3.

Giuliano, K.A., and D.L. Taylor. 1990. Formation, transport, contraction, and disassembly of stress fibers in fibroblasts. *Cell Motil Cytoskeleton*. 16:14-21.

Goeckeler, Z.M., R.A. Masaracchia, Q. Zeng, T.L. Chew, P. Gallagher, and R.B. Wysolmerski. 2000. Phosphorylation of myosin light chain kinase by p21-activated kinase PAK2. *J Biol Chem*. 275:18366-18374.

Goicoechea, S.M., S. Awadia, and R. Garcia-Mata. 2014. I'm coming to GEF you: Regulation of RhoGEFs during cell migration. *Cell adhesion & migration*. 8.

Guilluy, C., R. Garcia-Mata, and K. Burridge. 2011. Rho protein crosstalk: another social network? *Trends Cell Biol*. 21:718-726.

Habets, G.G., E.H. Scholtes, D. Zuydgeest, R.A. van der Kammen, J.C. Stam, A. Berns, and J.G. Collard. 1994. Identification of an invasion-inducing gene, Tiam-1, that encodes a protein with homology to GDP-GTP exchangers for Rho-like proteins. *Cell*. 77:537-549.

Habets, G.G., R.A. van der Kammen, N.A. Jenkins, D.J. Gilbert, N.G. Copeland, A. Hagemeijer, and J.G. Collard. 1995. The invasion-inducing TIAM1 gene maps to human chromosome band 21q22 and mouse chromosome 16. *Cytogenet Cell Genet*. 70:48-51.

Hamann, M.J., C.M. Lubking, D.N. Luchini, and D.D. Billadeau. 2007. Asef2 functions as a Cdc42 exchange factor and is stimulated by the release of an autoinhibitory module from a concealed C-terminal activation element. *Mol Cell Biol*. 27:1380-1393.

Harlan, J.E., P.J. Hajduk, H.S. Yoon, and S.W. Fesik. 1994. Pleckstrin homology domains bind to phosphatidylinositol-4,5-bisphosphate. *Nature*. 371:168-170.

Harvey, K., I.C. Duguid, M.J. Alldred, S.E. Beatty, H. Ward, N.H. Keep, S.E. Lingenfelter, B.R. Pearce, J. Lundgren, M.J. Owen, T.G. Smart, B. Luscher, M.I. Rees, and R.J. Harvey. 2004. The GDP-GTP exchange factor collybistin: an essential determinant of neuronal gephyrin clustering. *J Neurosci*. 24:5816-5826.

Heath, J.P., and B.F. Holifield. 1991. Cell locomotion: new research tests old ideas on membrane and cytoskeletal flow. *Cell Motil Cytoskeleton*. 18:245-257.

Humphries, J.D., P. Wang, C. Streuli, B. Geiger, M.J. Humphries, and C. Ballestrem. 2007. Vinculin controls focal adhesion formation by direct interactions with talin and actin. *J Cell Biol*. 179:1043-1057.

Huttenlocher, A., and A.R. Horwitz. 2011. Integrins in cell migration. *Cold Spring Harbor perspectives in biology*. 3:a005074.

Huttenlocher, A., S.P. Palecek, Q. Lu, W. Zhang, R.L. Mellgren, D.A. Lauffenburger, M.H. Ginsberg, and A.F. Horwitz. 1997. Regulation of cell migration by the calcium-dependent protease calpain. *J Biol Chem*. 272:32719-32722.

Hynes, R.O. 1992. Integrins: versatility, modulation, and signaling in cell adhesion. *Cell*. 69:11-25.

Hynes, R.O. 2002. Integrins: bidirectional, allosteric signaling machines. *Cell*. 110:673-687.

Hynes, R.O. 2009. The extracellular matrix: not just pretty fibrils. *Science*. 326:1216-1219.

Ikebe, M. 1989. Phosphorylation of a second site for myosin light chain kinase on platelet myosin. *Biochemistry*. 28:8750-8755.

Ilic, D., Y. Furuta, S. Kanazawa, N. Takeda, K. Sobue, N. Nakatsuji, S. Nomura, J. Fujimoto, M. Okada, and T. Yamamoto. 1995. Reduced cell motility and enhanced focal adhesion contact formation in cells from FAK-deficient mice. *Nature*. 377:539-544.

Itoh, R.E., K. Kurokawa, Y. Ohba, H. Yoshizaki, N. Mochizuki, and M. Matsuda. 2002. Activation of rac and cdc42 video imaged by fluorescent resonance energy transfer-based single-molecule probes in the membrane of living cells. *Mol Cell Biol*. 22:6582-6591.

Jaffe, A.B., and A. Hall. 2005. Rho GTPases: biochemistry and biology. *Annu Rev Cell Dev Biol*. 21:247-269.

Jean, L., D. Majumdar, M. Shi, L.E. Hinkle, N.L. Diggins, M. Ao, J.A. Broussard, J.C. Evans, D.P. Choma, and D.J. Webb. 2013. Activation of Rac by Asef2 promotes myosin II-dependent contractility to inhibit cell migration on type I collagen. *Journal of cell science*.

Jean, L., L. Yang, D. Majumdar, Y. Gao, M. Shi, B.M. Brewer, D. Li, and D.J. Webb. 2014. The Rho family GEF Asef2 regulates cell migration in three dimensional (3D) collagen matrices through myosin II. *Cell adhesion & migration*. 8:460-467.

Jiang, G., G. Giannone, D.R. Critchley, E. Fukumoto, and M.P. Sheetz. 2003. Two-piconewton slip bond between fibronectin and the cytoskeleton depends on talin. *Nature*. 424:334-337.

Kanchanawong, P., G. Shtengel, A.M. Pasapera, E.B. Ramko, M.W. Davidson, H.F. Hess, and C.M. Waterman. 2010. Nanoscale architecture of integrin-based cell adhesions. *Nature*. 468:580-584.

Katoh, K., Y. Kano, M. Amano, H. Onishi, K. Kaibuchi, and K. Fujiwara. 2001. Rho-kinase--mediated contraction of isolated stress fibers. *J Cell Biol*. 153:569-584.

Kaverina, I., O. Krylyshkina, and J.V. Small. 1999. Microtubule targeting of substrate contacts promotes their relaxation and dissociation. *J Cell Biol*. 146:1033-1044.

Kawasaki, Y. 2000. Asef, a Link Between the Tumor Suppressor APC and G-Protein Signaling. *Science*. 289:1194-1197.

Kawasaki, Y., S. Furukawa, R. Sato, and T. Akiyama. 2013. Differences in the localization of the adenomatous polyposis coli-Asef/Asef2 complex between adenomatous polyposis coli wild-type and mutant cells. *Cancer Sci*. 104:1135-1138.

Kawasaki, Y., M. Sagara, Y. Shibata, M. Shirouzu, S. Yokoyama, and T. Akiyama. 2007. Identification and characterization of Asef2, a guanine-nucleotide exchange factor specific for Rac1 and Cdc42. *Oncogene*. 26:7620-7267.

Kawasaki, Y., S. Tsuji, K. Muroya, S. Furukawa, Y. Shibata, M. Okuno, S. Ohwada, and T. Akiyama. 2009. The adenomatous polyposis coli-associated exchange factors Asef and Asef2 are required for adenoma formation in Apc(Min/+)mice. *EMBO reports*. 10:1355-1362.

Kimura, K., M. Ito, M. Amano, K. Chihara, Y. Fukata, M. Nakafuku, B. Yamamori, J. Feng, T. Nakano, K. Okawa, A. Iwamatsu, and K. Kaibuchi. 1996. Regulation of myosin phosphatase by Rho and Rho-associated kinase (Rho-kinase). *Science*. 273:245-248.

Kins, S., H. Betz, and J. Kirsch. 2000. Collybistin, a newly identified brain-specific GEF, induces submembrane clustering of gephyrin. *Nature neuroscience*. 3:22-29.

Kiosses, W.B., R.H. Daniels, C. Otey, G.M. Bokoch, and M.A. Schwartz. 1999. A role for p21-activated kinase in endothelial cell migration. *J Cell Biol*. 147:831-844.

Klinghoffer, R.A., C. Sachsenmaier, J.A. Cooper, and P. Soriano. 1999. Src family kinases are required for integrin but not PDGFR signal transduction. *EMBO J*. 18:2459-2471.

Knaus, U.G., A. Bamberg, and G.M. Bokoch. 2007. Rac and Rap GTPase activation assays. *Methods in molecular biology*. 412:59-67.

Knaus, U.G., S. Morris, H.J. Dong, J. Chernoff, and G.M. Bokoch. 1995. Regulation of human leukocyte p21-activated kinases through G protein--coupled receptors. *Science*. 269:221-223.

Kneussel, M., D. Engelkamp, and H. Betz. 2001. Distribution of transcripts for the brain-specific GDP/GTP exchange factor collybistin in the developing mouse brain. *Eur J Neurosci*. 13:487-492.

Kovacs, M., J. Toth, C. Hetenyi, A. Malnasi-Csizmadia, and J.R. Sellers. 2004. Mechanism of blebbistatin inhibition of myosin II. *J Biol Chem*. 279:35557-35563.

Kurokawa, K., and M. Matsuda. 2005. Localized RhoA activation as a requirement for the induction of membrane ruffling. *Mol Biol Cell*. 16:4294-4303.

Lauffenburger, D.A., and A.F. Horwitz. 1996. Cell migration : a physically integrated molecular process. *Cell*. 84:359-369.

Laukaitis, C.M., D.J. Webb, K. Donais, and A.F. Horwitz. 2001. Differential dynamics of alpha 5 integrin, paxillin, and alpha-actinin during formation and disassembly of adhesions in migrating cells. *J. Cell Biol.* 153:1427-1440.

Lawson, C.D., and K. Burridge. 2014. The on-off relationship of Rho and Rac during integrin-mediated adhesion and cell migration. *Small GTPases*. 5:e27958.

Lee, J., A. Ishihara, J.A. Theriot, and K. Jacobson. 1993. Principles of locomotion for simple-shaped cells. *Nature*. 362:167-171.

Lee, J., M. Leonard, T. Oliver, A. Ishihara, and K. Jacobson. 1994. Traction forces generated by locomoting keratocytes. *J. Cell Biol.* 127:1957-1964.

Liu, Z., L.A. van Grunsven, E. Van Rossen, B. Schroyen, J.P. Timmermans, A. Geerts, and H. Reynaert. 2010. Blebbistatin inhibits contraction and accelerates migration in mouse hepatic stellate cells. *Br J Pharmacol*. 159:304-315.

Lo, C.M., D.B. Buxton, G.C. Chua, M. Dembo, R.S. Adelstein, and Y.L. Wang. 2004. Nonmuscle myosin IIb is involved in the guidance of fibroblast migration. *Mol Biol Cell*. 15:982-989.

Luque, A., M. Gomez, W. Puzon, Y. Takada, F. Sanchez-Madrid, and C. Cabanas. 1996. Activated conformations of very late activation integrins detected by a group of antibodies (HUTS) specific for a novel regulatory region (355-425) of the common beta 1 chain. *J Biol Chem*. 271:11067-11075.

Machacek, M., L. Hodgson, C. Welch, H. Elliott, O. Pertz, P. Nalbant, A. Abell, G.L. Johnson, K.M. Hahn, and G. Danuser. 2009. Coordination of Rho GTPase activities during cell protrusion. *Nature*. 461:99-103.

Majumdar, D., Y. Gao, D. Li, and D.J. Webb. 2011. Co-culture of neurons and glia in a novel microfluidic platform. *J Neurosci Methods*. 196:38-44.

Manser, E., T. Leung, H. Salihuddin, Z.S. Zhao, and L. Lim. 1994. A brain serine/threonine protein kinase activated by Cdc42 and Rac1. *Nature*. 367:40-46.

Martin, G.A., G. Bollag, F. McCormick, and A. Abo. 1995. A novel serine kinase activated by rac1/CDC42Hs-dependent autophosphorylation is related to PAK65 and STE20. *The EMBO journal*. 14:4385.

Matsumura, F., S. Ono, Y. Yamakita, G. Totsukawa, and S. Yamashiro. 1998. Specific localization of serine 19 phosphorylated myosin II during cell locomotion and mitosis of cultured cells. *J Cell Biol*. 140:119-129.

Mattila, P.K., and P. Lappalainen. 2008. Filopodia: molecular architecture and cellular functions. *Nat Rev Mol Cell Biol*. 9:446-454.

McDonald, J.C., and G.M. Whitesides. 2002. Poly(dimethylsiloxane) as a material for fabricating microfluidic devices. *Accounts of chemical research*. 35:491-499.

Mitchison, T.J., and L.P. Cramer. 1996. Actin-based cell motility and cell locomotion. *Cell*. 84:371-379.

Mitin, N., L. Betts, M.E. Yohe, C.J. Der, J. Sondek, and K.L. Rossman. 2007. Release of autoinhibition of ASEF by APC leads to CDC42 activation and tumor suppression. *Nat Struct Mol Biol*. 14:814-823.

Mitra, S.K., and D.D. Schlaepfer. 2006. Integrin-regulated FAK-Src signaling in normal and cancer cells. *Curr Opin Cell Biol*. 18:516-523.

Miyamoto, S., S.K. Akiyama, and K.M. Yamada. 1995a. Synergistic roles for receptor occupancy and aggregation in integrin transmembrane function. *Science*. 267:883-885.

Miyamoto, S., H. Teramoto, O.A. Coso, J.S. Gutkind, P.D. Burvbelo, S.K. Akiyama, and K.M. Yamada. 1995b. Integrin function: molecular hierarchies of cytoskeletal and signaling molecules. *J. Cell Biol.* 131:791-805.

Murayama, K., M. Shirouzu, Y. Kawasaki, M. Kato-Murayama, K. Hanawa-Suetsugu, A. Sakamoto, Y. Katsura, A. Suenaga, M. Toyama, T. Terada, M. Taiji, T. Akiyama, and S. Yokoyama. 2007. Crystal structure of the rac activator, Asef, reveals its autoinhibitory mechanism. *J Biol Chem*. 282:4238-4242.

Niggli, V., M. Schmid, and A. Nievergelt. 2006. Differential roles of Rho-kinase and myosin light chain kinase in regulating shape, adhesion, and migration of HT1080 fibrosarcoma cells. *Biochem Biophys Res Commun*. 343:602-608.

Nobes, C.D., and A. Hall. 1995. Rho, rac, and cdc42 GTPases regulate the assembly of multimolecular focal complexes associated with actin stress fibers, lamellipodia, and filopodia. *Cell*. 81:53-62.

Oser, M., and J. Condeelis. 2009. The cofilin activity cycle in lamellipodia and invadopodia. *J Cell Biochem*. 108:1252-1262.

Otey, C.A., and O. Carpen. 2004. Alpha-actinin revisited: a fresh look at an old player. *Cell Motil Cytoskeleton*. 58:104-111.

Palecek, S.P., A. Huttenlocher, A.F. Horwitz, and D.A. Lauffenburger. 1998. Physical and biochemical regulation of integrin release during rear detachment of migrating cells. *J Cell Sci*. 111 (Pt 7):929-940.

Palecek, S.P., J.C. Loftus, M.H. Ginsberg, D.A. Lauffenburger, and A.F. Horwitz. 1997. Integrin-ligand binding properties govern cell migration speed through cell-substratum adhesiveness. *Nature*. 385:537-540.

Parsons, J.T. 2003. Focal adhesion kinase: the first ten years. *J Cell Sci*. 116:1409-1416.

Parsons, J.T., A.R. Horwitz, and M.A. Schwartz. 2010. Cell adhesion: integrating cytoskeletal dynamics and cellular tension. *Nat Rev Mol Cell Biol*. 11:633-643.

Pawson, T. 2007. Dynamic control of signaling by modular adaptor proteins. *Curr Opin Cell Biol*. 19:112-116.

Peacock, J.G., A.L. Miller, W.D. Bradley, O.C. Rodriguez, D.J. Webb, and A.J. Koleske. 2007. The Abl-related gene tyrosine kinase acts through p190RhoGAP to inhibit actomyosin contractility and regulate focal adhesion dynamics upon adhesion to fibronectin. *Mol Biol Cell*. 18:3860-3872.

Pertz, O., and K.M. Hahn. 2004. Designing biosensors for Rho family proteins--deciphering the dynamics of Rho family GTPase activation in living cells. *J Cell Sci*. 117:1313-1318.

Pertz, O., L. Hodgson, R.L. Klemke, and K.M. Hahn. 2006. Spatiotemporal dynamics of RhoA activity in migrating cells. *Nature*. 440:1069-1072.

Petrie, R.J., N. Gavara, R.S. Chadwick, and K.M. Yamada. 2012. Nonpolarized signaling reveals two distinct modes of 3D cell migration. *The Journal of cell biology*. 197:439-455.

Petrie, R.J., and K.M. Yamada. 2012. At the leading edge of three-dimensional cell migration. *J Cell Sci*. 125:5917-5926.

Poincloux, R., O. Collin, F. Lizarraga, M. Romao, M. Debray, M. Piel, and P. Chavrier. 2011. Contractility of the cell rear drives invasion of breast tumor cells in 3D Matrigel. *Proceedings of the National Academy of Sciences of the United States of America*. 108:1943-1948.

Pollard, T.D., and G.G. Borisy. 2003. Cellular motility driven by assembly and disassembly of actin filaments. *Cell*. 112:453-465.

Ponti, A., M. Machacek, S.L. Gupton, C.M. Waterman-Storer, and G. Danuser. 2004. Two distinct actin networks drive the protrusion of migrating cells. *Science*. 305:1782-1786.

Rameh, L.E., A. Arvidsson, K.L. Carraway, 3rd, A.D. Couvillon, G. Rathbun, A. Crompton, B. VanRenterghem, M.P. Czech, K.S. Ravichandran, S.J. Burakoff, D.S. Wang, C.S. Chen, and L.C. Cantley. 1997. A comparative analysis of the phosphoinositide binding specificity of pleckstrin homology domains. *J Biol Chem*. 272:22059-22066.

Ramos, E., R.B. Wysolmerski, and R.A. Masaracchia. 1997. Myosin phosphorylation by human cdc42-dependent S6/H4 kinase/gammaPAK from placenta and lymphoid cells. *Recept Signal Transduct*. 7:99-110.

Reddy-Alla, S., B. Schmitt, J. Birkenfeld, V. Eulenburg, S. Dutertre, C. Bohringer, M. Gotz, H. Betz, and T. Papadopoulos. 2010. PH-domain-driven targeting of collybistin but not Cdc42 activation is required for synaptic gephyrin clustering. *Eur J Neurosci*. 31:1173-1184.

Regen, C.M., and A.F. Horwitz. 1992. Dynamics of beta 1 integrin-mediated adhesive contacts in motile fibroblasts. *J Cell Biol*. 119:1347-1359.

Reid, T., A. Bathoorn, M.R. Ahmadian, and J.G. Collard. 1999. Identification and characterization of hPEM-2, a guanine nucleotide exchange factor specific for Cdc42. *J Biol Chem*. 274:33587-33593.

Ren, X.D., W.B. Kiosses, and M.A. Schwartz. 1999. Regulation of the small GTP-binding protein Rho by cell adhesion and the cytoskeleton. *Embo J*. 18:578-585.

Rid, R., N. Schiefermeier, I. Grigoriev, J.V. Small, and I. Kaverina. 2005. The last but not the least: the origin and significance of trailing adhesions in fibroblastic cells. *Cell Motil Cytoskeleton*. 61:161-171.

Ridley, A.J. 2001. Rho GTPases and cell migration. *J Cell Sci*. 114:2713-2722.

Ridley, A.J. 2011. Life at the leading edge. *Cell*. 145:1012-1022.

Ridley, A.J., and A. Hall. 1992a. The small GTP-binding protein rho regulates the assembly of focal adhesions and actin stress fibers in response to growth factors. *Cell*. 70:389-399.

Ridley, A.J., and A. Hall. 1992b. The small GTP-binding protein rho regulates the assembly of focal adhesions and actin stress fibers in response to growth factors. *Cell*. 70:389-399.

Ridley, A.J., H.F. Paterson, C.L. Johnston, D. Diekmann, and A. Hall. 1992. The small GTP-binding protein rac regulates growth factor-induced membrane ruffling. *Cell*. 70:401-410.

Ridley, A.J., M.A. Schwartz, K. Burridge, R.A. Firtel, M.H. Ginsberg, G. Borisy, J.T. Parsons, and A.R. Horwitz. 2003. Cell migration: integrating signals from front to back. *Science*. 302:1704–1709.

Roca-Cusachs, P., T. Iskratsch, and M.P. Sheetz. 2012. Finding the weakest link: exploring integrin-mediated mechanical molecular pathways. *J Cell Sci*. 125:3025-3038.

Rossman, K.L., C.J. Der, and J. Sondek. 2005. GEF means go: turning on RHO GTPases with guanine nucleotide-exchange factors. *Nat Rev Mol Cell Biol*. 6:167-180.

Rottner, K., A. Hall, and J.V. Small. 1999. Interplay between Rac and Rho in the control of substrate contact dynamics. *Curr Biol*. 9:640-648.

Rozario, T., and D.W. DeSimone. 2010. The extracellular matrix in development and morphogenesis: a dynamic view. *Dev Biol*. 341:126-140.

Sabass, B., M.L. Gardel, C.M. Waterman, and U.S. Schwarz. 2008. High resolution traction force microscopy based on experimental and computational advances. *Biophys J*. 94:207-220.

Sagara, M., Y. Kawasaki, S.I. Iemura, T. Natsume, Y. Takai, and T. Akiyama. 2009. Asef2 and Neurabin2 cooperatively regulate actin cytoskeletal organization and are involved in HGF-induced cell migration. *Oncogene*. 28:1357-1365.

Sahai, E., and C.J. Marshall. 2003. Differing modes of tumour cell invasion have distinct requirements for Rho/ROCK signalling and extracellular proteolysis. *Nature cell biology*. 5:711-719.

Saito, T., C.C. Jones, S. Huang, M.P. Czech, and P.F. Pilch. 2007. The Interaction of Akt with APPL1 Is Required for Insulin-stimulated Glut4 Translocation. *J. Biol. Chem.* 282:32280-32287.

Sander, E.E., J.P. ten Klooster, S. van Delft, R.A. van der Kammen, and J.G. Collard. 1999. Rac downregulates Rho activity: reciprocal balance between both GTPases determines cellular morphology and migratory behavior. *J Cell Biol*. 147:1009-1022.

Sanders, L.C., F. Matsumura, G.M. Bokoch, and P. de Lanerolle. 1999. Inhibition of myosin light chain kinase by p21-activated kinase. *Science*. 283:2083-2085.

Sanz-Moreno, V., G. Gadea, J. Ahn, H. Paterson, P. Marra, S. Pinner, E. Sahai, and C.J. Marshall. 2008. Rac activation and inactivation control plasticity of tumor cell movement. *Cell*. 135:510-523.

Sawada, Y., M. Tamada, B.J. Dubin-Thaler, O. Cherniavskaya, R. Sakai, S. Tanaka, and M.P. Sheetz. 2006. Force sensing by mechanical extension of the Src family kinase substrate p130Cas. *Cell*. 127:1015-1026.

Schmidt, A., and A. Hall. 2002. Guanine nucleotide exchange factors for Rho GTPases: turning on the switch. *Genes & development*. 16:1587-1609.

Schoenwaelder, S.M., and K. Burridge. 1999. Bidirectional signaling between the cytoskeleton and integrins. *Curr. Opin. Cell Biol.* 11:274-286.

Scholey, J.M., K.A. Taylor, and J. Kendrick-Jones. 1980. Regulation of non-muscle myosin assembly by calmodulin-dependent light chain kinase. *Nature*. 287:233-235.

Schwartz, M.A., and D.W. DeSimone. 2008. Cell adhesion receptors in mechanotransduction. *Curr Opin Cell Biol*. 20:551-556.

Sells, M.A., A. Pfaff, and J. Chernoff. 2000. Temporal and spatial distribution of activated Pak1 in fibroblasts. *J Cell Biol*. 151:1449-1458.

Sheetz, M.P. 1994. Cell migration by graded attachment to substrates and contraction. *Semin. Cell Biol.* 5:149-155.

Small, J.V. 1988. The actin cytoskeleton. *Electron Microsc Rev*. 1:155-174.

Smilenov, L.B., A. Mikhailov, R.J. Pelham, E.E. Marcantonio, and G.G. Gundersen. 1999. Focal adhesion motility revealed in stationary fibroblasts. *Science*. 286:1172-1174.

Straight, A.F., A. Cheung, J. Limouze, I. Chen, N.J. Westwood, J.R. Sellers, and T.J. Mitchison. 2003. Dissecting temporal and spatial control of cytokinesis with a myosin II Inhibitor. *Science*. 299:1743-1747.

Su, L.K., K.W. Kinzler, B. Vogelstein, A.C. Preisinger, A.R. Moser, C. Luongo, K.A. Gould, and W.F. Dove. 1992. Multiple intestinal neoplasia caused by a mutation in the murine homolog of the APC gene. *Science*. 256:668-670.

Svitkina, T.M., A.B. Verkhovsky, K.M. McQuade, and G.G. Borisy. 1997. Analysis of the actin-myosin II system in fish epidermal keratocytes: mechanism of cell body translocation. *J Cell Biol*. 139:397-415.

Thiesen, S., S. Kubart, H.H. Ropers, and H.G. Nothwang. 2000. Isolation of two novel human RhoGEFs, ARHGEF3 and ARHGEF4, in 3p13-21 and 2q22. *Biochem Biophys Res Commun*. 273:364-369.

Tilghman, R.W., J.K. Slack-Davis, N. Sergina, K.H. Martin, M. Iwanicki, E.D. Hershey, H.E. Beggs, L.F. Reichardt, and J.T. Parsons. 2005. Focal adhesion kinase is required for the spatial organization of the leading edge in migrating cells. *J Cell Sci*. 118:2613-2623.

To, W.S., and K.S. Midwood. 2011. Plasma and cellular fibronectin: distinct and independent functions during tissue repair. *Fibrogenesis Tissue Repair*. 4:21.

Tomar, A., and D.D. Schlaepfer. 2009. Focal adhesion kinase: switching between GAPs and GEFs in the regulation of cell motility. *Curr Opin Cell Biol*. 21:676-683.

Tovell, V.E., A.H. Dahlmann-Noor, P.T. Khaw, and M. Bailly. 2011. Advancing the treatment of conjunctival scarring: a novel ex vivo model. *Arch Ophthalmol*. 129:619-627.

Umemoto, S., A.R. Bengur, and J.R. Sellers. 1989. Effect of multiple phosphorylations of smooth muscle and cytoplasmic myosins on movement in an in vitro motility assay. *J Biol Chem*. 264:1431-1436.

Vernon, R.B., and M.D. Gooden. 2002. An improved method for the collagen gel contraction assay. *In Vitro Cell Dev Biol Anim*. 38:97-101.

Vicente-Manzanares, M., C.K. Choi, and A.R. Horwitz. 2009a. Integrins in cell migration--the actin connection. *J Cell Sci*. 122:199-206.

Vicente-Manzanares, M., and A.R. Horwitz. 2011. Cell migration: an overview. *Methods Mol Biol*. 769:1-24.

Vicente-Manzanares, M., M.A. Koach, L. Whitmore, M.L. Lamers, and A.F. Horwitz. 2008. Segregation and activation of myosin IIB creates a rear in migrating cells. *J Cell Biol*. 183:543-554.

Vicente-Manzanares, M., X. Ma, R.S. Adelstein, and A.R. Horwitz. 2009b. Non-muscle myosin II takes centre stage in cell adhesion and migration. *Nat Rev Mol Cell Biol*. 10:778-790.

Vicente-Manzanares, M., K. Newell-Litwa, A.I. Bachir, L.A. Whitmore, and A.R. Horwitz. 2011. Myosin IIA/IIB restrict adhesive and protrusive signaling to generate front-back polarity in migrating cells. *J Cell Biol*. 193:381-396.

Vicente-Manzanares, M., D.J. Webb, and A.R. Horwitz. 2005. Cell migration at a glance. *Journal of cell science*. 118:4917-4919.

Vicente-Manzanares, M., J. Zareno, L. Whitmore, C.K. Choi, and A.F. Horwitz. 2007. Regulation of protrusion, adhesion dynamics, and polarity by myosins IIA and IIB in migrating cells. *J Cell Biol*. 176:573-580.

Wang, A., X. Ma, M.A. Conti, and R.S. Adelstein. 2011. Distinct and redundant roles of the non-muscle myosin II isoforms and functional domains. *Biochem Soc Trans*. 39:1131-1135.

Wang, Y.-L. 1985. Exchange of actin subunits at the leading edge of living fibroblasts: possible role of treadmilling. *J. Cell Biol.* 101:597-602.

Webb, D.J., K. Donais, L.A. Whitmore, S.M. Thomas, C.E. Turner, J.T. Parsons, and A.F. Horwitz. 2004. FAK-Src signalling through paxillin, ERK and MLCK regulates adhesion disassembly. *Nat. Cell Biol.* 6:154-161.

Webb, D.J., J.T. Parsons, and A.F. Horwitz. 2002. Adhesion assembly, disassembly and turnover in migrating cells -- over and over and over again. *Nat Cell Biol*. 4:E97-100.

Wegner, A.M., C.A. Nebhan, L. Hu, D. Majumdar, K.M. Meier, A.M. Weaver, and D.J. Webb. 2008. N-WASP and the Arp2/3 Complex Are Critical Regulators of Actin in the Development of Dendritic Spines and Synapses. *J. Biol. Chem.* 283:15912-15920.

Welf, E.S., U.P. Naik, and B.A. Ogunnaike. 2012. A Spatial Model for Integrin Clustering as a Result of Feedback between Integrin Activation and Integrin Binding. *Biophys J*. 103:1379-1389.

Wheeler, A.P., and A.J. Ridley. 2004. Why three Rho proteins? RhoA, RhoB, RhoC, and cell motility. *Exp Cell Res*. 301:43-49.

Whitesides, G.M., E. Ostuni, S. Takayama, X. Jiang, and D.E. Ingber. 2001. Soft lithography in biology and biochemistry. *Annual review of biomedical engineering*. 3:335-373.

Wirth, A., M. Schroeter, C. Kock-Hauser, E. Manser, J.M. Chalovich, P. De Lanerolle, and G. Pfitzer. 2003. Inhibition of contraction and myosin light chain phosphorylation in guinea-pig smooth muscle by p21-activated kinase 1. *J Physiol*. 549:489-500.

Worthylake, R.A., S. Lemoine, J.M. Watson, and K. Burridge. 2001. RhoA is required for monocyte tail retraction during transendothelial migration. *J Cell Biol*. 154:147-160.

Yamada, K.M., and S. Miyamoto. 1995. Integrin transmembrane signaling and cytoskeletal control. *Curr. Opin. Cell Biol.* 7:681-689.

Yamazaki, D., S. Kurisu, and T. Takenawa. 2009. Involvement of Rac and Rho signaling in cancer cell motility in 3D substrates. *Oncogene*. 28:1570-1583.

Yeung, T., P.C. Georges, L.A. Flanagan, B. Marg, M. Ortiz, M. Funaki, N. Zahir, W. Ming, V. Weaver, and P.A. Janmey. 2005. Effects of substrate stiffness on cell morphology, cytoskeletal structure, and adhesion. *Cell Motil Cytoskeleton*. 60:24-34.

Zaidel-Bar, R., C. Ballestrem, Z. Kam, and B. Geiger. 2003. Early molecular events in the assembly of matrix adhesions at the leading edge of migrating cells. *J. Cell Sci.* 116:4605-4613.

Zaidel-Bar, R., M. Cohen, L. Addadi, and B. Geiger. 2004. Hierarchical assembly of cell-matrix adhesion complexes. *Biochem. Soc. Trans.* 32:416-420.

Zaidel-Bar, R., R. Milo, Z. Kam, and B. Geiger. 2007. A paxillin tyrosine phosphorylation switch regulates the assembly and form of cell-matrix adhesions. *J Cell Sci*. 120:137-148.

Zamir, E., M. Katz, Y. Posen, N. Erez, K.M. Yamada, B.Z. Katz, S. Lin, D.C. Lin, A. Bershadsky, Z. Kam, and B. Geiger. 2000. Dynamics and segregation of cell-matrix adhesions in cultured fibroblasts. *Nat Cell Biol*. 2:191-196.

Zeng, Q., D. Lagunoff, R. Masaracchia, Z. Goeckeler, G. Cote, and R. Wysolmerski. 2000. Endothelial cell retraction is induced by PAK2 monophosphorylation of myosin II. *J Cell Sci*. 113 (Pt 3):471-482.

Zhang, H., and I.G. Macara. 2008a. The PAR-6 Polarity Protein Regulates Dendritic Spine Morphogenesis through p190 RhoGAP and the Rho GTPase. *Dev Cell*. 14:216-226.

Zhang, H., and I.G. Macara. 2008b. The PAR-6 Polarity Protein Regulates Dendritic Spine Morphogenesis through p190 RhoGAP and the Rho GTPase. *Developmental Cell*. 14:216-226.

Zhang, Z., L. Chen, L. Gao, K. Lin, L. Zhu, Y. Lu, X. Shi, Y. Gao, J. Zhou, P. Xu, J. Zhang, and G. Wu. 2012. Structural basis for the recognition of Asef by adenomatous polyposis coli. *Cell research*. 22:372-386.

Zhu, K., B. Debreceni, R. Li, and Y. Zheng. 2000. Identification of Rho GTPase-dependent sites in the Dbl homology domain of oncogenic Dbl that are required for transformation. *J Biol Chem*. 275:25993-26001.

Ziegler, W.H., R.C. Liddington, and D.R. Critchley. 2006. The structure and regulation of vinculin. *Trends Cell Biol*. 16:453-460.

Zimerman, B., T. Volberg, and B. Geiger. 2004. Early molecular events in the assembly of the focal adhesion-stress fiber complex during fibroblast spreading. *Cell Motil Cytoskeleton*. 58:143-159.